Probing the IGM/Galaxy Connection IV: The LCO/WFCCD Galaxy Survey of 20 Fields Surrounding UV Bright Quasars

J. Xavier Prochaska[1], B. Weiner[2], H.-W. Chen[3], K.L. Cooksey[4], J.S. Mulchaey[5],

ABSTRACT

We publish the survey for galaxies in 20 fields containing ultraviolet bright quasars (with $z_{\rm em} \approx 0.1$ to 0.5) that can be used to study the association between galaxies and absorption systems from the low-z intergalactic medium (IGM). The survey is magnitude limited ($R \approx 19.5$ mag) and highly complete out to $10'$ from the quasar in each field. It was designed to detect dwarf galaxies ($L \approx 0.1L^*$) at an impact parameter $\rho \approx 1$ Mpc ($z = 0.1$) from a quasar. The complete sample (all 20 fields) includes R-band photometry for 84718 sources and confirmed redshifts for 2800 sources. This includes 1198 galaxies with $0.005 < z < (z_{\rm em} - 0.01)$ at a median redshift of 0.18, which may associated with IGM absorption lines. All of the imaging was acquired with cameras on the Swope $40''$ telescope and the spectra were obtained via slitmask observations using the WFCCD spectrograph on the Dupont $100''$ telescope at Las Campanas Observatory (LCO). This paper describes the data reduction, imaging analysis, photometry, and spectral analysis of the survey. We tabulate the principal measurements for all sources in each field and provide the spectroscopic dataset online.

Subject headings: IGM : metals, O VI, galaxies—techniques

---

[1]Department of Astronomy and Astrophysics & UCO/Lick Observatory, University of California, 1156 High Street, Santa Cruz, CA 95064; xavier@ucolick.org

[2]Steward Observatory, University of Arizona, 933 N. Cherry Ave., Tucson, AZ 85721; bjw@as.arizona.edu

[3]Department of Astronomy; University of Chicago; 5640 S. Ellis Ave., Chicago, IL 60637; hchen@oddjob.uchicago.edu

[4]NSF Astronomy & Astrophysics Postdoctoral Fellow, MIT Kavli Institute for Astrophysics & Space Research, 77 Massachusetts Avenue, 37-611, Cambridge, MA 02139, USA; kcooksey@space.mit.edu

[5]Carnegie Observatories; 213 Santa Barbara St., Pasadena, CA 91101; mulchaey@obs.carnegiescience.edu

1. Introduction

The intergalactic medium (IGM) is the gas and dust which permeates the space between galaxies in our universe. The IGM is inferred to be the dominant repository of baryons in our universe; it provides the fuel for galaxies and serves as a 'sink' for the metals they expel. The IGM is almost exclusively observed through absorption-line techniques in the spectra of distant objects, e.g. quasars, gamma-ray bursts. The so-called Lyα forest, for example, is the thicket of H I absorption lines which trace modest overdensities in the universe.

Despite its name, which suggests a disconnect from galaxies, the IGM exhibits several characteristics which connect it to them. Chief among these is the presence of metals, generally in the form of highly-ionized species like C IV, Si IV, and O VI absorption. The medium is too diffuse and ionized to support *in situ* star-formation, therefore it is expected that these metals were produced within galaxies and transported by one or more mechanisms to the IGM (e.g. galactic-scale winds, tidal stripping). Identifying the timing, the processes, and the precise interplay between galaxies and the IGM remains a very active area of current astrophysical research (e.g. Scannapieco et al. 2006; Oppenheimer & Davé 2009; Wiersma et al. 2010).

For several decades now, researchers have surveyed the fields surrounding bright quasars with the goal of connecting galaxies that they discover to specific characteristics of the IGM (as revealed by rest-frame UV spectroscopy of the quasars). These include surveys to explore the association of galaxies to the Lyα forest (Morris et al. 1993; Lanzetta et al. 1995; Stocke et al. 1995; Shull et al. 1996; Bowen et al. 2002; Chen et al. 2005; Shone et al. 2010); searches for galaxies related to strong Mg II lines (Bergeron & Boisse 1991; Steidel 1993; Barton & Cooke 2009; Chen et al. 2010); and studies of the structures giving rise to O VI absorption (Tripp & Savage 2000; Bowen et al. 2001; Savage et al. 2002; Sembach et al. 2004; Tumlinson et al. 2005; Prochaska et al. 2006; Stocke et al. 2006; Tripp et al. 2006; Cooksey et al. 2008; Chen & Mulchaey 2009; Wakker & Savage 2009). The latter ion has received considerable attention because it has been proposed to trace the $T \approx 10^{5-7}$ K phase of the IGM, termed the warm-hot intergalactic medium (WHIM). Although the WHIM is a generic prediction of cosmological simulations (Cen & Ostriker 1999; Davé et al. 2001; Fang & Bryan 2001), its low density and modest temperature make it especially elusive to empirical detection. The O VI doublet, however, has been extensively surveyed and owing to its high ionization state may track a portion of the WHIM.

Motivated by the analysis of O VI and its relation to galaxies and the WHIM, we initiated a program to survey galaxies in the fields surrounding UV-bright, $z_{\rm em} \gtrsim 0.1$ quasars that were targeted (or likely to be targeted) by the *Far Ultraviolet Spectroscopic Explorer (FUSE)* and/or the *Hubble Space Telescope (HST)*. Prior to the commissioning of the Cosmic

Origins Spectrograph (COS), there were only a small set of known quasars that were bright enough for such observations. The sources are widely separated across the sky such that existing, ongoing, and/or planned galaxy surveys (e.g. SDSS, 2dF) do not cover the fields or are often too shallow for studying $L > L^*$ galaxies beyond $z \approx 0.05$. Therefore, we designed a survey with two main observational goals: (1) achieve high completeness for galaxies as faint as $\approx 0.1L^*$ at $z = 0.1$; and (2) survey an area corresponding to at least 1 Mpc at $z = 0.1$. Technically, this implied a magnitude limit of $R \approx 19.5$ mag and a field-of-view (FOV) of roughly $10'$ radius around each quasar. These requirements were well-suited to the WFCCD spectrograph on the $100''$ Dupont Telescope at Las Campanas Observatory (LCO). Over the course of several years, we targeted 20 fields at equatorial and Southern declinations (Table 1). Early results from this survey have been used to explore the IGM/galaxy connection for O VI absorbers (Prochaska et al. 2006; Cooksey et al. 2008), the Lyα forest (Chen et al. 2005), and a Lyman limit absorber (Lehner et al. 2009).

With this paper, we provide the full data release of the LCO/WFCCD survey. This stands, for now, as the largest dataset for exploring the association between the IGM and galaxies and their large-scale structures at $z \sim 0.1$. This manuscript comments on galaxies derived only from our own LCO/WFCCD survey and we emphasize that other datasets (e.g. SDSS) and publications do provide complementary coverage for about half of the fields. In future (and previous) papers, we analyze the IGM/galaxy connection with this dataset. We organize the paper as follows: § 2 describes the observations, data reduction, and spectral analysis for redshift determinations; we present our survey of the fields in § 3; and offer a brief summary in § 4. Unless otherwise specified, we adopt the 5yr WMAP cosmology (Dunkley et al. 2009): $\Omega_\Lambda = 0.74, \Omega_m = 0.26, H_0 = 72\,\mathrm{km\,s^{-1}\,Mpc^{-1}}$. Furthermore, all distances are quoted in proper units unless otherwise denoted.

2. Observations and Data Reduction

We selected 20 fields accessible from Las Campanas Observatory (declination $\delta < 25$ deg) surrounding UV bright quasars with emission redshifts $z_{\rm em} > 0.05$. These quasars had existing UV spectroscopy from the *HST* or *FUSE* telescopes, had planned UV spectroscopic observations with one of these telescopes, and/or have sufficiently high UV flux to permit UV spectroscopic observations with one of these facilities. The quasars were also chosen to have a wide range of right ascension, to enable a year-round observing campaign. The quasars and their UV spectroscopic datasets are summarized in Table 1.

All of the fields in our survey were imaged with the Swope $40''$ telescope using a direct imaging camera. The majority were taken with the SITe1 CCD which has $0.6964''$ pixels in

a 2048×2048 array. The remainder were observed with the SITe3 CCD which has $0.435''$ pixels in a 2048×3150 array. All of the fields were imaged through an R-band filter and most also had contemporaneous B-band images taken. The data were obtained in a series of dithered exposures intended to map at least a $20' \times 20'$ field-of-view (FOV). This was designed to enable a survey to approximately a 1 Mpc impact parameter ρ at $z \approx 0.1$. Most of the imaging data were obtained under photometric conditions; Table 2 summarizes the weather and provides a log of the observations. Most of the data were acquired in good seeing conditions, i.e. FWHM $\approx 1''$.

The imaging data were reduced with standard IRAF routines to overscan subtract and flat-field the images. We used custom routines to determine integer offsets between the dithered images and combined the frames after weighting by a global measure of the inverse variance. We derived a photometric solution for each night from analysis of Landoldt standard stars (Landolt 1992) that were observed at a range of airmass. We solved for the zeropoint, airmass and $(B-R)$ color terms. We estimate the systematic uncertainty related to the photometric solution to be approximately 0.05 mag.

Each combined R-band image was analyzed with the SExtractor (v2.0 Bertin & Arnouts 1996) package. The parameters were set to require a minimum detection area of 6 pixels and a detection threshold of 1.5σ above the RMS of the sky background. For each object detected, SExtractor reports a star-galaxy (S/G) classifier with values ranging from 0 to 1 where unity indicates a point-spread-function consistent with a point source (i.e. a likely star). Finally, we produced a segmentation map of each field and calculated B and R magnitudes by summing the flux in the pixels assigned to each object. There are no corrections made for flux that falls below our detection threshold. The true galaxy magnitudes, therefore, may be up to a few tenths magnitude brighter especially for low-surface brightness galaxies.

Proper astrometry for each field was applied with the publicly- available Image World Coordinate Setting Program *imwcs*[1] version 3.6.8. First, several World Coordinate System (WCS) keywords were added to the reduced and combined image header in order to define its estimated pointing and plate scale ($0.6964''\,\mathrm{pix}^{-1}$ for the SITe1 CCD and $0.4349''\,\mathrm{pix}^{-1}$ for SITe3). Next, we used *imwcs* to fit a plane-tangent projection, using stars in the image that *imwcs* identified and stars from a reference catalog, namely, the US Naval Observatory astrometric catalog USNO-A2.0.[2] The *imwcs* algorithm typically matched a dozen or more stars and converged in six iterations, with a mean arcsec offset of $0.15''$ in any given image. Finally, all astrometized images were visually compared to the USNO-A2.0 sample to verify

[1]http://tdc-www.harvard.edu/software/wcstools/imwcs/index.html.

[2]http://tdc-www.harvard.edu/software/catalogs/ua2.html.

that the solution held across the whole field (e.g., no systematic rotation was obvious towards the outskirts of the image).

Based on our SExtractor analysis of the images, we designed a set of slit masks for each field to be used with the WFCCD instrument on the Dupont 100″ telescope. Targets were identified as follows. First, we examined the isophotal area versus R magnitude from the imaging of a given field. In all cases, stars trace out a well-defined locus for $R < 19.5$ mag (see Fig. 1 of Prochaska et al. 2006, for an example). We traced this locus and discarded all objects that fall within the stellar region or fall just outside the locus and have a S/G value greater than 0.98. We also did not target the few, very bright ($R < 15$ mag) and very large (angular diameter $> 10''$) galaxies that exist in the survey fields. Most of these have previously published redshifts and/or lie at too low redshift ($z < 0.01$) for our main scientific program. For those that remained, we targeted all objects with $R \leq R_{\rm max}$ and $\theta < \theta_{\rm max}$ of the QSO. We set $R_{\rm max} \geq 19.5$ mag, adopting fainter values for fields with a lower surface density of targets on the sky or where we had particular scientific interest in the field (see Table 1). For all but two of the fields, $\theta_{\rm max} = 10'$. The two exceptions are PKS0312−770 and PKS0405−123, where we expanded the survey to cover $\theta_{\rm max} \approx 15'$ and $\approx 20'$ respectively.

We performed multi-slit spectroscopy on each field with the WFCCD spectrometer using the blue grism and the Tek#5 CCD. This affords a spectral resolution FWHM ≈ 375km s^{-1}, a dispersion of ≈ 2Å per pixel, and a nominal wavelength coverage $\lambda \approx 3800$–9000Å. Our standard integration was a pair of 1800s exposures, and most of the data were obtained under clear conditions. Longer total exposure times were used for the faintest fields or in worse conditions. These exposure times generally achieved a signal-to-noise S/N > 3 per pixel for even the faintest objects. Table 3 shows a log of the WFCCD observations.

All of these WFCCD data were reduced with a custom IDL software package[3] (see Prochaska et al. 2006, for a full description). The extracted and coadded 1D spectra were analyzed with a modified version of the SDSS pipeline task *zfind* to establish the object's redshift. This routine fits PCA templates derived from the SDSS dataset (Early Data Release; Stoughton et al. 2002) to the emission and/or absorption lines in the object spectrum. In general, these redshift values have uncertainties of $\sigma_z \approx 10^{-4}$ (i.e. $\sigma_v \approx 30$km s^{-1}). Each of the fits was inspected, and, when necessary, the redshift was modified to account for an obvious failure. With few exceptions, we determined an unambiguous redshift for every object on a given mask. The exceptions include rare cases where slit design or fabrication failed (e.g. significant portions of one slit overlapped another) and also faint sources that had no obvious spectral features. This PCA analysis yields eigenvalues for the four galaxy

[3]http://www.ucolick.org/∼xavier/WFCCD/index.html

eigenspectra fitted to our data. As in Prochaska et al. (2006), we define E_C to be the eigenvalue for the first eigenfunction (which is dominated by early-type spectral features) and L_C is the the second eigenvalue minus the sum of the third and fourth coefficients. All of the spectra are publicly available[4].

In Figure 1, we plot the S/G classifier from SExtractor for the targets with spectroscopic redshifts (a) $z < 0.005$, which are predominantly Galactic stars; and (b) $z > 0.005$, which are exclusively distant galaxies. As one expects, the majority of the $z < 0.005$ objects have S/G near unity; the exceptions are primarily objects blended with some other source which was not de-blended by the SExtractor algorithm. In contrast, the extragalactic sources primarily have low S/G classifiers although we note that 8% have S/G > 0.98. We caution that our targeting criteria may have missed a subset of very compact galaxies.

3. The Survey Fields

In this section, we present the imaging data, photometry, and results from the WFCCD spectroscopy for each field. We also comment briefly on any obvious associations between the galaxies we detect and known (published) absorbers along the quasar sightlines. We stress that about half of these fields have been survey for galaxies by other efforts (e.g. SDSS). Our dicussion, however, is primarily limited to the galaxies from our LCO/WFCCD survey. Table 4 summarizes properties of the galaxies discovered in the 20 fields restricted to $0.005 < z < (z_{\rm em} + 0.01)$. Tables 5–23 summarize the photometry and spectroscopy of objects in each field.

In the following, we convert the apparent R-band magnitude of each galaxy with a measured redshift into a luminosity relative to L^*. For the latter, we adopt the Sloan r-band value from Blanton et al. (2003) as measured from the Sloan Digital Sky Survey which corresponds to $z \approx 0.1$: $r^* = -20.44 + 5 \log h_{100}$. With the cosmology we have adopted, this yields $r^* = -21.12$ mag.

For each galaxy, we assess the spectral type from the E_C and L_C coefficients as follows (based in part on a visual inspection of several tens of the galaxies):

- Early-type: $E_C > 0.6$ and $L_C < 0.6$
- Late-type: $E_C < 0.8$ and $L_C > 0.4$, or $E_C < 0$ and $L_C > 0.2$, or $E_C < 0$ and $L_C < 0$.

[4]http://www.ucolick.org/∼xavier/WFCCDOVI/index.html

Galaxies with any other pair of coefficient values are labelled 'unknown'. For every galaxy with an impact parameter $\rho < 300\,\mathrm{kpc}$ we have visually verified each spectral type, placing each into either the late or early-type category.

We then imposed a k-correction to the apparent magnitude using a redshifted template spectrum integrated with an R-band filter. We use an E/S0 template for the early-type galaxies, and an Sc template for the late-type systems. No correction was made for galaxies classified as unknown. This k-correction generally amounts to only a tenth or few tenths correction to the magnitudes, with larger values for more distant galaxies ($z > 0.2$). Finally, we converted the k-corrected, apparent R-band magnitudes into luminosities relative to L^* with the luminosity distance calculated using the assumed WMAP cosmology.

In total, we obtained spectra for 2933 sources and confirmed 2800 redshifts. Of these, there are 1198 galaxies with $0.005 < z < (z_{\mathrm{em}} - 0.01)$ which are suitable for studying the association between galaxies and absorption lines in the low-z IGM. The properties of these galaxies are summarized in Table 4. Lastly, Table 1 lists the spectroscopic completeness of each field as a function of magnitude limit and angular offset from the quasar, e.g. $C^{5'}_{19.5}$ gives the completeness percentile to $R = 19.5\,\mathrm{mag}$ and $\theta_{\mathrm{max}} = 5'$ offset from the quasar.

3.1. Q0026+1259

To date this quasar has no published list of IGM absorption lines, presumably because its UV spectroscopic dataset is relatively sparse. Figure 2 shows the field and marks the galaxies surrounding the quasar with measured redshifts. Figure 3 shows a histogram of the redshifts of the galaxies in the field surrounding the quasar. There is a relatively large 'spike' at the quasar redshift ($z_{\mathrm{em}} = 0.142$) which marks a galaxy group (several $L \approx L*$ galaxies lie within $\rho = 300\,\mathrm{kpc}$). One identifies no other significant large-scale structures foreground to the quasar in our LCO/WFCCD survey. Table 5 summarizes the photometry and spectroscopy for galaxies and stars in the field surrounding Q0026+1259.

3.2. Ton S 180

The Ton S 180 sightline has been surveyed for Lyα absorption by (Penton et al. 2004, STIS/G140M spectra) and for O VI absorption by (Danforth et al. 2006, *FUSE)*. The latter report O VI absorbers at $z = 0.0234, 0.0436$ and $z = 0.0456$, each of which shows a galaxy within an impact parameter of $\rho < 300\,\mathrm{kpc}$ and within a velocity offset of $|\delta v| < 300\mathrm{km\ s^{-1}}$.

None of these were reported in Stocke et al. (2006)[5] presumably because these galaxies were fainter than the magnitude limit of their galaxy compilation. Wakker & Savage (2009) also associated galaxies at $z \approx 0$ with Lyα and O VI absorption along this sightline.

Figure 4 shows the field and marks the galaxies surrounding the quasar with measured redshifts. Given the low emission redshift of the quasar, there are only a handful of galaxies identified in its foreground. One also notes several bright galaxies coincident with the quasar redshift and at relatively small impact parameter ($\rho \approx 300\,$kpc). Figure 5 shows a histogram of the redshifts of the galaxies in the field surrounding the quasar. Table 6 summarizes the photometry and spectroscopy of our survey for galaxies and stars in the field surrounding Ton S 180.

3.3. Ton S 210

Although the quasar Ton S 210 has an impressive UV spectroscopic dataset, there is no published survey for IGM absorption beyond the very local universe (Wakker & Savage 2009). Coincidentally, we have discovered very few galaxies foreground to the quasar to our magnitude limit (Figure 6, Table 4) despite obtaining spectra for 71 extragalactic sources (Figure 7, Table 7). None of the foreground sources lie at close impact parameter.

3.4. PKS0312−770

We previously published the spectrum of a galaxy associated with the $z \approx 0.21$ Lyman limit system toward PKS0312−770 (Lehner et al. 2009). The sightline has also been surveyed by several groups for Lyα and O VI absorption (Danforth & Shull 2008; Thom & Chen 2008; Tripp et al. 2008). Tripp et al. (2008) report two O VI absorbers at $z = 0.1589$ and $z = 0.19827$ where we identify bright galaxies in our survey but only at large impact parameters ($\rho > 500\,$kpc). We also identify a galaxy at $z = 0.0736$ with $\rho = 954\,$kpc that may be associated with the 'void' absorber reported by Stocke et al. (2006). It has a luminosity $L \approx 0.1L*$ which places it below their survey limit.

Tables 8 summarizes the photometry and spectroscopy for galaxies and stars in the field surrounding PKS0312–770. Figure 8 displays our imaging data which covers a rectangular $15' \times 32'$ field of view, and Figure 9 shows a redshift histogram for the field.

---

[5]Indeed, they remarked that the O VI absorber at $z = 0.436$ was the "most isolated" of their sample with no bright galaxy within 1 Mpc.

3.5. PKS0405–123

This field has received significant attention over the past decade, largely because of its relatively high redshift but also because it exhibits several strong O VI absorbers (Chen & Prochaska 2000; Prochaska et al. 2004; Chen et al. 2005; Prochaska et al. 2006; Williger et al. 2006; Tripp et al. 2008; Howk et al. 2009; Wakker & Savage 2009; Savage et al. 2010). We published the results of our galaxy survey in Chen et al. (2005) and Prochaska et al. (2006); here we only summarize properties of the galaxies close to the sightline (Table 4). We also remind the reader that our galaxy survey had non-uniform spectral and imaging coverage beyond the inner $\approx 20' \times 20'$ field-of-view.

3.6. PKS0558–504

This quasar has a very limited UV spectral dataset, and the only IGM analysis has been performed at $z \approx 0$ (Wakker & Savage 2009). By chance, our survey also shows no galaxies at low impact parameters (Tables 9 and Table 4). Figure 10 shows the field and marks the galaxies surrounding the quasar with measured redshifts and Figure 11 presents a redshift histogram.

3.7. PG1004+130

This sightline has been analyzed for Lyα absorption by Bowen et al. (2002) who associated a cluster of low z Lyα absorption lines with a bright nearby galaxy (UGC 5454). A relatively high quality *FUSE* dataset exists but has not yet been surveyed for O VI absorption. As discussed in Prochaska et al. (in prep), we have also analyzed these UV datasets for Lyα and O VI absorption at the redshifts of the galaxies in our LCO/WFCCD survey with small impact parameter to the sightline (Table 4).

The photometry and spectroscopy of our full survey is listed in Table 10 and Figure 12 shows the field and marks the galaxies surrounding the quasars with determined redshifts. Figure 13 provides a redshift histogram.

3.8. HE1029-140

This quasar has a modest UV spectral dataset and has been analyzed for Lyα absorption by Penton et al. (2004). Figure 14 shows the field and marks the few galaxies with $z < z_{\rm em}$

that we have identified in the LCO/WFCCD survey. Table 11 summarizes the photometry and spectroscopy of all objects in the field and Figure 15 gives a redshift histogram of the galaxies from our survey.

3.9. PG1116+215

This sightline has been studied by Tripp et al. (1998) and Sembach et al. (2004) for absorption lines and associated galaxies, along with several other more recent analyses (Tripp et al. 2008; Danforth & Shull 2008; Wakker & Savage 2009). They identify three O VI systems foreground to the quasar at $z = 0.0597, 0.13879$ and 0.1655. Each of these is associated with a galaxy at $\rho \leq 150\,\mathrm{kpc}$ in our survey. For the $z = 0.0597$ system, we identify 6 galaxies within 1 Mpc including several with $L \gtrsim L^*$ which suggests a group environment (Table 4). None of these galaxies were identified in previous surveys.

Table 12 summarizes the photometry and spectroscopy for the objects that we surveyed in the field surrounding PG1116+215. Figure 16 presents an image of the field and marks the galaxies surrounding the quasar with determined $z < z_{\mathrm{em}}$ and Figure 17 shows a redshift histogram of the full galaxy survey.

3.10. PG1211+143

Tumlinson et al. (2005) analyzed this field for IGM absorption lines and corresponding galaxies. They reported a pair of O VI systems at $z = 0.0513$ and 0.0645 and associated these with $L \approx L*$ galaxies at $\rho \approx 150\,\mathrm{kpc}$. Our survey includes these two galaxies (Table 4) and an additional, fainter galaxy at significantly smaller impact parameter for the system at $z = 0.0646$ ($\rho = 70\,\mathrm{kpc}$). We also identify additional galaxies associated with the galaxy group at $z = 0.0513$. Wakker & Savage (2009) also analyzed this field, focusing on $z \approx 0$.

Table 13 summarizes the photometry and spectroscopy for galaxies and stars in the field surrounding PG1211+143. Figure 18 shows the field and marks the galaxies surrounding the quasar while Figure 19 gives a galaxy redshift histogram.

3.11. PG1216+069

This sightline has been studied for absorption by multiple groups (Tripp et al. 2008; Thom & Chen 2008; Danforth & Shull 2008; Chen & Mulchaey 2009; Wakker & Savage 2009)

with O VI systems reported at $z = 0.1236, 0.268$ and 0.282. Our survey reveals galaxies at every redshift, but only the lowest redshift system shows an example with small impact parameter ($\rho = 85\,\mathrm{kpc}$). In addition, we report an overdensity of galaxies at $z = 0.0805$ (5 galaxies within 1 Mpc including an L^* galaxy; Table 4) which is associated with strong Lyα absorption but no apparent O VI gas to a sensitive limit.

The sightline is also notable for intersecting Virgo, and Tripp et al. (2005) report on a strong H I absorber near the NGC 4261 group ($z = 0.0063$). No apparent O VI absorption is detected at the redshift of either structure although the equivalent width limits are poor from the *FUSE* spectra at these wavelengths.

Table 14 summarizes the photometry and spectroscopy, Figure 20 shows the field and marks the galaxies surrounding the quasars with determined redshifts. Figure 21 shows a histogram of the redshifts of the galaxies in the field surrounding the quasar.

3.12. 3C273

Because of its very high UV flux, this quasar and the field around it have been the subject of many previous studies including some of the first galaxy surveys along quasar sightlines (Morris et al. 1993). Tripp et al. (2008) report O VI detections at several redshifts, all at column densities that lie below the sensitivity limit of most other UV spectral datasets, i.e. $N(\mathrm{O}^{+5}) < 10^{13.5}\,\mathrm{cm}^{-2}$. None of these absorbers shows a corresponding galaxy in our survey with $\rho < 300\,\mathrm{kpc}$, but we do identify galaxies at larger impact parameter (Table 4). Wakker & Savage (2009) also analyzed this field, focusing on $z \approx 0$.

Table 15 summarizes the photometry and spectroscopy for galaxies and stars in the field surrounding 3C273. Figure 22 shows the field and marks the galaxies surrounding the quasars with determined redshifts. Figure 23 shows a histogram of the redshifts of the galaxies in the field surrounding the quasar.

3.13. Q1230+095

This quasar has a very sparse UV spectral dataset and there is no published list of IGM absorption. We emphasize that the quasar's redshift ($z_{\mathrm{em}} = 0.415$) make it a very promising sightline for studying the IGM/galaxy connection. Furthermore, there is a set of galaxies at small impact parameters revealed by our survey (Figure 24, Table 4). We encourage observations with the *HST*/COS instrument. Table 16 summarizes the full photometry and spectroscopy for objects in the field surrounding Q1230+095 and Figure 25 histograms the

galaxy redshifts.

3.14. PKS1302-102

This field has been surveyed for Lyα and O VI absorption by several groups (Danforth et al. 2006; Cooksey et al. 2008; Danforth & Shull 2008; Thom & Chen 2008; Tripp et al. 2008; Wakker & Savage 2009). These groups have reported O VI detections at multiple redshifts: $z = 0.0423, 0.0647, 0.0940, 0.0989, 0.1453, 0.1916, 0.2256$, and 0.2274. Our survey has revealed nearly 100 galaxies foreground to the quasar including several at impact parameters $\rho < 100\,$kpc (see also Cooksey et al. 2008). We detect galaxy within 300 kpc and with $|\delta v| < 400$km s^{-1} for each absorber at $z < 0.2$ except at $z = 0.0989$. This includes two sub-$L*$ galaxies that lie at low impact parameter ($\rho < 100\,$kpc; Table 4, Figure 26). Table 17 summarizes the photometry and spectroscopy for galaxies and stars in the field and Figure 27 presents a redshift histogram of all galaxies.

3.15. PG1307+085

This quasar has only a sparse dataset of UV spectroscopy and there is no published list for Lyα or O VI absorption systems. Its relatively high redshift ($z_{\rm em} = 0.155$) marks it as a valuable sightline for future study and our survey provides a modest set of galaxies for cross-correlation analysis (Table 4). The full photometry and spectroscopy for objects from our survey in the field are listed in Table 18. Figure 28 presents an R-band image of the field and marks the surrounding galaxies with $z < z_{\rm em}$. Figure 29 shows a redshift histogram for the galaxies we have discovered.

3.16. MRK1383

Despite its low redshift and correspondingly small pathlength, this sightline has been studied extensively for Lyα and O VI absorption (Danforth et al. 2006; Danforth & Shull 2008; Wakker & Savage 2009). Our survey reveals only a handful of galaxies with $z < z_{\rm em}$ (Table 4, Figure 30), but we also note that this field has one of the lowest completeness levels to $R = 19.5\,$mag (80%). Table 19 summarizes the photometry and spectroscopy for galaxies and stars in the field surrounding MRK1383. Figure 30 provides an image of the field and marks the foreground galaxies, and Figure 31 shows a redshift histogram for the galaxies.

3.17. Q1553+113

This quasar boasts only a short *FUSE* exposure and no additional UV spectroscopy. It has been surveyed for IGM absorption only at $z \approx 0$ by Wakker & Savage (2009). Given the extensive dataset of galaxies that we have discovered in the foreground (Table 4, Figure 32), we encourage future observations with *HST*/COS. The photometry and spectroscopy for objects from our survey in the field are listed in Table 20 and a redshift histogram for the galaxies is provided by Figure 33.

3.18. PKS2005-489

This sightline has been surveyed for Lyα and O VI absorption over the relatively short pathlength provided by this $z = 0.071$ AGN (Penton et al. 2004; Danforth et al. 2006; Danforth & Shull 2008). There are no O VI systems reported. Our survey reveals two sets of foreground galaxies at redshifts $z \approx 0.045$ and 0.057, but none at very close impact parameter to the sightline (Figure 34, Table 4). Table 21 summarizes the photometry and spectroscopy for all objects in the field surrounding PKS2005–489. Figure 35 presents a redshift histogram for all of the galaxies in our survey.

3.19. FJ2155-092

The quasar FJ2155–092, also known as PHL 1811, has a high quality UV spectral dataset. Jenkins et al. (2005) has published an analysis of the Lyman limit system at $z = 0.081$ and its neighboring galaxies. Other groups have examined the spectra for Lyα and O VI absorption (Tripp et al. 2008; Danforth & Shull 2008; Wakker & Savage 2009). Altogether, the sightline boasts four O VI systems at $z = 0.0788, 0.1326, 0.1581$ and 0.1769, all of which have a neighboring galaxy in our survey with $\rho < 350\,\mathrm{kpc}$ and $|\delta v| < 400\mathrm{km\ s^{-1}}$ but none at very low impact parameter. Figure 36 shows the field and marks the galaxies foreground to the quasar with determined redshifts. Table 22 lists the photometry and spectroscopy for galaxies and stars throughout the field and a redshift histogram of the galaxies is given by Figure 37.

3.20. PKS2155-304

This sightline has received significant attention, primarily because of the claimed (and debated) O VII and O VIII absorption at $z \approx 0.055$ (Fang et al. 2002; Cagnoni et al. 2003). The high quality UV spectral datasets have also been surveyed for Lyα and O VI absorption (who report detections at $z = 0.0541$ and 0.0571 Danforth et al. 2006; Danforth & Shull 2008; Wakker & Savage 2009). We associate each of these with a bright ($L > L*$) galaxy in our survey but at relatively large impact parameter ($\rho \sim 500\,$kpc). The photometry and spectroscopy for our survey of the the field is given in Table 23. We show an image of the field and mark the foreground galaxies in Figure 38 and present a redshift histogram for all of the galaxies in Figure 39. We note that our deeper survey reveals no additional galaxies at $z \approx 0.055$ from the ones first reported by (see Table 4; Shull et al. 2003).

4. Summary

This paper serves to define our LCO/WFCCD galaxy survey which was designed to study the IGM/galaxy connection at $z \lesssim 0.2$. We have listed R-band photometry for objects in each field, identified the objects which satisfy our targeting criteria, provide (online) the extracted and coadded 1D spectra, and tabulate the redshifts for all sources with an unambiguous identification. Table 4 summarizes properties of the galaxies discovered in the 20 fields restricted to $0.005 < z < (z_{\rm em} + 0.01)$. Again, we note that approximately half of the fields have been surveyed for galaxies by other groups that our results should not be considered a complete census. This table and the redshift histograms reveal the types of galaxy overdensities that are typical of other low z galaxy surveys.

Figure 40 presents a color-magnitude diagram for the galaxies, and summarizes the redshift, luminosity, and impact parameter distributions of the sample. The set of galaxies with $z < (z_{\rm em} - 0.01)$ is predominantly at redshifts $z = 0.1$ – 0.3, with luminosities $L = 0.1$–$5L^*$, and located at impact parameters of several hundred kpc from the quasar. These distributions are a complex convolution of the magnitude limit and angular extent of the survey fields, and the emission redshift distribution of the targeted quasars. For example, the impact parameter distribution does not scale as $N \propto \rho$ because the fixed angular extent of the survey restricts galaxies to $\rho < 1\,$Mpc at $z < 0.1$. Nevertheless, Figure 40 provides an overview of this survey's utility for probing the low z IGM.

To crudely assess the completeness and global characteristics of the survey, we have also constructed an R-band luminosity function from the dataset. Specifically, we restricted the survey of each field to $R_{\rm max} = 19.5\,$mag, $\theta_{\rm max} = 10'$, and $0.02 < z < min[(z_{\rm em} - 0.01), 0.2]$.

The maximum redshift was imposed to minimize effects from having targeted fields with a known, luminous quasar and also to facilitate comparison with the Sloan Digital Sky Survey (SDSS). We calculated the effective comoving volume $V_{\rm eff}$ for a given absolute magnitude M and evaluated the luminosity function,

$$\Phi(M) = \frac{n_{\rm gal}}{V_{\rm eff}\,\Delta M} \quad , \tag{1}$$

within magnitude bins of $\Delta M = 0.5\,{\rm mag}$. The analysis was further restricted to the 17 fields which have a completeness percentile $C^{10'}_{19.5} > 70\%$ (Table 1). The raw evaluation of $\Phi(M)$ is shown as black points in the lower panel of Figure 41, where the error bars reflect only Poisson uncertainty (1σ equivalent) in $n_{\rm gal}$. Upper limits correspond to 95% c.l. We have also performed a jack-knife analysis of the survey and recover similar scatter in the measurements albeit with a bias toward lower values.

We have also attempted to correct for incompleteness in the survey, using two approaches. The blue stars in the figure include a completeness correction estimated by scaling $n_{\rm gal}$ in each field by its corresponding completeness, i.e. $1/C^{10'}_{19.5}$. This increases $\Phi(M)$ in nearly every bin by $\approx 20\%$, i.e. the correction is essentially independent of apparent magnitude. As Figure 42 demonstrates, however, the survey has higher incompleteness for fainter galaxies. Therefore, we have used the results given in Figure 42 to increment the contribution of each galaxy to $\Phi(M)$ according to each galaxy's apparent magnitude. These results are shown as the cyan diamonds in Figure 41.

Overplotted on our evaluations of $\Phi(M)$ are the luminosity functions derived for the r-band from the Sloan Digital Sky Survey (Blanton et al. 2003; Montero-Dorta & Prada 2009), transformed to our assumed cosmology (e.g. $h = 0.72$). The agreement between our evaluation and the SDSS estimations is remarkably good. The only significant deviation is at the bright-end where we have detected 2–3× more galaxies than predicted by the SDSS luminosity functions. The offset could be the result of an Eddington bias in our estimation of $\Phi(M)$ and/or a modest offset between our R-band photometry and the SDSS r-band (there is one notable for some of these galaxies which are also observed by SDSS). We also emphasize that the number of galaxies in these deviant bins is small (~ 20; upper panel of Figure 41). We conclude, therefore, that our combined survey provides a reasonably representative sample of galaxies for low-z IGM analysis.

In future papers (e.g. Prochaska et al. 2011, in prep), we explore the association of galaxies and their structures to the IGM with particular focus on H I Lyα and O VI absorption. We also encourage the acquisition of new, more sensitive UV spectral datasets (i.e. with *HST*/COS) to further enhance this galaxy survey.

J. X. P. is partially supported by an NSF CAREER grant (AST–0548180). We recognize the terrific staff at Las Campanas Observatory who were instrumental in carrying out this program. We kindly thank R. Weymann who built the WFCCD spectrograph and supported this program.

REFERENCES

Barton, E. J., & Cooke, J. 2009, AJ, 138, 1817

Bergeron, J., & Boisse, P. 1991, Advances in Space Research, 11, 241

Bertin, E., & Arnouts, S. 1996, Astronomy and Astrophysics Supplement, 117, 393

Blanton, M. R., et al. 2003, ApJ, 594, 186

Bowen, D. V., Jimenez, R., Jenkins, E. B., & Pettini, M. 2001, ApJ, 547, 39

Bowen, D. V., Pettini, M., & Blades, J. C. 2002, ApJ, 580, 169

Cagnoni, I., Nicastro, F., Maraschi, L., Treves, A., & Tavecchio, F. 2003, New A Rev., 47, 561

Cen, R., & Ostriker, J. P. 1999, ApJ, 514, 1

Chen, H., Helsby, J. E., Gauthier, J., Shectman, S. A., Thompson, I. B., & Tinker, J. L. 2010, ApJ, 714, 1521

Chen, H., & Mulchaey, J. S. 2009, ApJ, 701, 1219

Chen, H.-W., & Prochaska, J. X. 2000, ApJ, 543, L9

Chen, H.-W., Prochaska, J. X., Weiner, B. J., Mulchaey, J. S., & Williger, G. M. 2005, ApJ, 629, L25

Cooksey, K. L., Prochaska, J. X., Chen, H.-W., Mulchaey, J. S., & Weiner, B. J. 2008, ApJ, 676, 262

Danforth, C. W., & Shull, J. M. 2008, ApJ, 679, 194

Danforth, C. W., Shull, J. M., Rosenberg, J. L., & Stocke, J. T. 2006, ApJ, 640, 716

Davé, R., et al. 2001, ApJ, 552, 473

Dunkley, J., et al. 2009, ApJS, 180, 306

Fang, T., & Bryan, G. L. 2001, ApJ, 561, L31

Fang, T., Marshall, H. L., Lee, J. C., Davis, D. S., & Canizares, C. R. 2002, ApJ, 572, L127

Howk, J. C., Ribaudo, J. S., Lehner, N., Prochaska, J. X., & Chen, H. 2009, MNRAS, 396, 1875

Jenkins, E. B., Bowen, D. V., Tripp, T. M., & Sembach, K. R. 2005, ApJ, 623, 767

Landolt, A. U. 1992, AJ, 104, 372

Lanzetta, K. M., Bowen, D. V., Tytler, D., & Webb, J. K. 1995, ApJ, 442, 538

Lehner, N., Prochaska, J. X., Kobulnicky, H. A., Cooksey, K. L., Howk, J. C., Williger, G. M., & Cales, S. L. 2009, ApJ, 694, 734

Montero-Dorta, A. D., & Prada, F. 2009, MNRAS, 399, 1106

Morris, S. L., Weymann, R. J., Dressler, A., McCarthy, P. J., Smith, B. A., Terrile, R. J., Giovanelli, R., & Irwin, M. 1993, ApJ, 419, 524

Oppenheimer, B. D., & Davé, R. 2009, MNRAS, 395, 1875

Penton, S. V., Stocke, J. T., & Shull, J. M. 2004, ApJS, 152, 29

Prochaska, J. X., Chen, H.-W., Howk, J. C., Weiner, B. J., & Mulchaey, J. 2004, ApJ, 617, 718

Prochaska, J. X., Weiner, B. J., Chen, H.-W., & Mulchaey, J. S. 2006, ApJ, 643, 680

Savage, B. D., et al. 2010, ApJ, 719, 1526

Savage, B. D., Sembach, K. R., Tripp, T. M., & Richter, P. 2002, ApJ, 564, 631

Scannapieco, E., Pichon, C., Aracil, B., Petitjean, P., Thacker, R. J., Pogosyan, D., Bergeron, J., & Couchman, H. M. P. 2006, MNRAS, 365, 615

Sembach, K. R., Tripp, T. M., Savage, B. D., & Richter, P. 2004, ApJS, 155, 351

Shone, A. M., Morris, S. L., Crighton, N., & Wilman, R. J. 2010, MNRAS, 402, 2520

Shull, J. M., Stocke, J. T., & Penton, S. 1996, AJ, 111, 72

Shull, J. M., Tumlinson, J., & Giroux, M. L. 2003, ApJ, 594, L107

Steidel, C. C. 1993, in Astrophysics and Space Science Library, Vol. 188, The Environment and Evolution of Galaxies, ed. J. M. Shull & H. A. Thronson, 263–+

Stocke, J. T., Penton, S. V., Danforth, C. W., Shull, J. M., Tumlinson, J., & McLin, K. M. 2006, ApJ, 641, 217

Stocke, J. T., Shull, J. M., Penton, S., Donahue, M., & Carilli, C. 1995, ApJ, 451, 24

Stoughton, C., et al. 2002, AJ, 123, 485

Thom, C., & Chen, H. 2008, ApJ, 683, 22

Tripp, T. M., Aracil, B., Bowen, D. V., & Jenkins, E. B. 2006, ApJ, 643, L77

Tripp, T. M., Jenkins, E. B., Bowen, D. V., Prochaska, J. X., Aracil, B., & Ganguly, R. 2005, ApJ, 619, 714

Tripp, T. M., Lu, L., & Savage, B. D. 1998, ApJ, 508, 200

Tripp, T. M., & Savage, B. D. 2000, ApJ, 542, 42

Tripp, T. M., Sembach, K. R., Bowen, D. V., Savage, B. D., Jenkins, E. B., Lehner, N., & Richter, P. 2008, ApJS, 177, 39

Tumlinson, J., Shull, J. M., Giroux, M. L., & Stocke, J. T. 2005, ApJ, 620, 95

Wakker, B. P., & Savage, B. D. 2009, ApJS, 182, 378

Wiersma, R. P. C., Schaye, J., Dalla Vecchia, C., Booth, C. M., Theuns, T., & Aguirre, A. 2010, MNRAS, 409, 132

Williger, G. M., Heap, S. R., Weymann, R. J., Davé, R., Ellingson, E., Carswell, R. F., Tripp, T. M., & Jenkins, E. B. 2006, ApJ, 636, 631

Table 1. Summary of Fields Surveyed

Quasar	RA (J2000)	DEC (J2000)	$z_{\rm em}$	*HST* UV Spectroscopic Datasets	*FUSE*[a]	$R_{\rm max}$	$N^{b}_{\rm spec}$	$C^{5'}_{19.5}$	$C^{10'}_{19.5}$
Q0026+1259	00:29:13.8	+13:16:04	0.142	GHRS/(G270M)	20	20.0	60	100	91
Ton S 180	00:57:20.0	–22:22:56	0.062	STIS/(G140M,G230MB)	132	19.7	7	100	93
Ton S 210	01:21:51.5	–28:20:57	0.116	STIS/(E140M,E230M)	57	20.0	7	86	90
PKS0312-77	03:11:55.2	–76:51:51	0.223	STIS/(E140M)		20.0	56	100	97
PKS0405-123	04:07:48.4	–12:11:37	0.573	STIS/(E140M,G230M); GHRS/(G160M,G200M)	71	20.0	565	100	97
PKS0558-504	05:59:47.4	–50:26:52	0.137	STIS/(G230MB)	400	20.0	16	100	99
PG1004+130	10:07:26.1	+12:48:56	0.240	STIS/(G140M)	85	19.5	61	74	71
HE1029-140	10:31:54.3	–14:16:51	0.086	STIS/(G140M)		19.8	8	100	95
PG1116+215	11:19:08.70	+21:19:18.	0.176	STIS/(G140M,E140M,E230M); GHRS/(G140L)	76	20.0	74	76	79
PG1211+143	12:14:17.7	+14:03:13.	0.081	STIS/(G140M,E140M); GHRS/(G140L,G270M)	52	19.5	25	61	56
PG1216+069	12:19:20.9	+06:38:38	0.331	STIS/(E140M); GHRS/(G140L)	13	20.0	101	100	89
3C273	12:29:6.70	+02:03:9.0	0.158	STIS/(E140M); GHRS/(FG130,FG190,FG270,G160M)	42	20.0	32	81	84
Q1230+0947	12:33:25.8	+09:31:23.	0.415	GHRS/(G140L)	13	19.5	99	83	77
PKS1302-102	13:05:33.0	–10:33:19	0.286	STIS/(E140M)	140	19.5	63	89	65
PG1307+085	13:09:47.0	+08:19:49.	0.155	STIS/(G230MB)	11	19.5	41	79	75
MRK1383	14:29:06.4	+01:17:06.0	0.086	STIS/(E140M,G140M)	64	19.5	5	79	68
Q1553+113	15:55:43.0	+11:11:24.	0.360		20	20.0	106	90	85
PKS2005-489	20:09:25.4	–48:49:54.0	0.071	STIS/(G140M)	48	20.0	32	97	97
FJ2155-0922	21:55:01.5	–09:22:25.0	0.192	STIS/(E140M,G230MB)	46	20.0	105	100	95
PKS2155-304	21:58:51.8	–30:13:30.0	0.116	STIS/(E140M); GHRS/(G160M,ECH-B,G140L)	123	20.0	43	96	96

Note. — Columns 9 and 10 list the completeness percent of the spectroscopic survey in each field to $R = 19.5$ mag for a radius of 5 and 10 arcminutes respectively.

[a]Total integration time in ks.

[b]Number of spectroscopically determined galaxy redshifts for objects with $0.005 < z < z_{\rm em}$.

Table 2. Log of Imaging Observations

Field	UT Date	CCD	Filter	Exp.	Conditions
Q0026+1259	26 Oct 2000	SITe1	B	2x450s	Photometric
			R	3x600s	Photometric
Q0046+112	26 Oct 2000	SITe1	B	2x450s	Photometric
			R	3x600s	Photometric
Ton S 180	26 Oct 2000	SITe1	B	2x450s	Photometric
			R	3x600s	Photometric
HE0153−4520	14 Sep 2001	SITe3	B	5x450s	Photometric
			R	6x600s	Photometric
Ton S 210	26 Oct 2000	SITe1	B	2x450s	Photometric
			R	3x600s	Photometric
	02 Oct 2002	SITe3	R	12x600s	Cirrus
	03 Oct 2002	SITe3	R	9x600s	
	04 Oct 2002	SITe3	R	13x600s	
PKS0312−770	02 Oct 2002	SITe3	R	6x450s	Cirrus
	04 Oct 2002	SITe3	R	3x600s	
PKS0405−123	26 Oct 2000	SITe1	B	2x450s	Windy, photometric
			R	5x600s	Windy, photometric
	03 Oct 2002	SITe3	R	18x600s	
	04 Oct 2002	SITe3	R	16x600s	
HE0450−2958	26 Feb 2001	SITe1	B	2x450s	Photometric
			R	3x600s	Photometric
AKN 120	23 Feb 2001	SITe1	B	2x450s	Photometric
			R	4x600s	Photometric
PKS0558−504	26 Oct 2000	SITe1	B	2x450s	Windy, photometric
			R	4x600s	Windy, photometric
B0736+017	21 Feb 2001	SITe1	B	2x450s	Photometric
			R	4x600s	Photometric
PG0832+25	26 Feb 2001	SITe1	B	2x450s	Photometric
			R	3x600s	Photometric
IR0914−6206	21 Feb 2001	SITe1	B	2x450s	Photometric
			R	3x600s	Photometric
PG1001+054	24 Feb 2001	SITe1	B	2x450s	Photometric
			R	4x600s	Photometric
PG1004+130	24 Feb 2001	SITe1	B	2x500s	Photometric
			R	4x600s	Photometric
PG1011−040	24 Feb 2001	SITe1	B	2x450s	Photometric
			R	3x600s	Photometric

Table 2—Continued

Field	UT Date	CCD	Filter	Exp.	Conditions
HE1015−1618	27 Feb 2001	SITe1	B	2x450s	Photometric
			R	3x600s	Photometric
HE1029−140	23 Feb 2001	SITe1	B	2x500s	Photometric
			R	3x600s	Photometric
	08 Apr 2003	SITe3	B	13x600s	Cirrus
HE1050−2711	28 Feb 2001	SITe1	B	2x450s	Photometric
			R	3x600s	Photometric
HE1115−1735	27 Feb 2001	SITe1	B	2x450s	Photometric
			R	3x600s	Photometric
PG1116+215	21 Feb 2001	SITe1	B	3x600s	Photometric
			R	6x600s	Photometric
	23 Feb 2001		B	3x600s	Photometric
			R	3x600s	Photometric
HE1122−1649	23 Feb 2001	SITe1	B	2x500s	Photometric
			R	3x600s	Photometric
MRK 1298	07 Apr 2002	SITe3	B	6x600s	Photometric
			R	12x600s	Photometric
PG1126+215	25 Feb 2001	SITe1	R	7x600s	Photometric
PG1211+143	09 Apr 2002	SITe3	B	6x600s	Photometric
			R	14x600s	Photometric
PG1216+069	25 Feb 2001	SITe1	B	2x600s	Photometric
			R	4x600s	Photometric
	26 Feb 2001		B	4x600s	Photometric
			R	7x600s	Photometric
3C273	27 Feb 2001	SITe1	B	6x600s	Photometric
			R	12x600s	Photometric
LBQS1230+0947	24 Feb 2001	SITe1	B	2x450s	Photometric
			R	4x600s	Photometric
PKS1302−102	21 Feb 2001	SITe1	B	2x450s	Photometric
			R	1x600s	Photometric
	23 Feb 2001	SITe1	B	1x450s	Photometric
			R	3x600s	Photometric
PG1307+085	21 Feb 2001	SITe1	B	2x450s	Photometric
			R	3x600s	Photometric
	08 Apr 2002	SITe3	R	7x600s	Photometric
			B	4x600s	Photometric
HE1326−0516	01 Mar 2001	SITe1	B	2x450s	Cirrus

Table 2—Continued

Field	UT Date	CCD	Filter	Exp.	Conditions
			R	2x600s	Cirrus
PKS1352+183	23 Feb 2001	SITe1	B	2x450s	Photometric
			R	3x600s	Photometric
	07 Apr 2002	SITe3	B	2x600s	Photometric
			R	3x600s	Photometric
MRK 1383	24 Feb 2001	SITe1	B	2x450s	Photometric
			R	2x600s	Photometric
	08 Apr 2002	SITe3	B	2x600s	Photometric
			R	3x600s	Photometric
	09 Apr 2002	SITe3	B	1x600s	Photometric
			R	2x600s	Photometric
RJ1556+11	25 Feb 2001	SITe1	B	2x450s	Photometric
			R	3x600s	Photometric
PKS2005−489	07 Apr 2002	SITe3	B	2x600s	Photometric
			R	5x600s	Photometric
	08 Apr 2002		R	8x600s	Photometric
	09 Apr 2002	SITe3	B	2x600s	Photometric
			R	3x600s	Photometric
	02 Oct 2002	SITe3	R	9x600s	Cirrus
	03 Oct 2002	SITe3	R	9x600s	Cirrus
	04 Oct 2002	SITe3	R	6x600s	
B2145+067	14 Sep 2001	SITe3	B	4x450s	Photometric
			R	6x600s	Photometric
FJ2155−0922	26 Oct 2000	SITe1	B	2x450s	Photometric
			R	3x600s	Photometric
PKS2155−304	26 Oct 2000	SITe1	B	2x450s	Photometric
			R	3x600s	Photometric
Q2251−178	30 Oct 2000	SITe1	B	2x450s	Cirrus
			R	5x600s	Cirrus

Table 3. Log of WFCCD Observations

Field	UT Date	Mask	Exp.	Conditions
Q0026+1259	31 Oct 2002	M1	3600	Clear
	01 Nov 2002	M2	3600	Clear
	02 Nov 2002	M3	3600	Clear
	03 Nov 2002	M4	3600	Clear
	04 Nov 2002	M5	3600	Clear
	05 Nov 2002	M6	1800	Clear
	06 Nov 2002	M6	1800	Clear
Ton S 180	10 Sep 2001	M1	5400	Photometric
	12 Sep 2001	M2	7200	Clear, poor seeing
	14 Sep 2001	M3	3600	Clear
	15 Sep 2001	M4	3600	Clear
	16 Sep 2001	M5	3600	Clear
Ton S 210	12 Sep 2001	M1	5400	Cirrus
	13 Sep 2001	M2	3600	Clear
	13 Sep 2001	M4	3600	Clear
	14 Sep 2001	M3	3600	Clear
PKS0312−770	01 Nov 2002	M1	3600	Clear
	01 Nov 2002	M2	3600	Clear
	02 Nov 2002	M3	3000	Clear
	03 Nov 2002	M4	3300	Clear
	04 Nov 2002	M5	3600	Clear
PKS0405−123	13 Sep 2001	M1	3600	Cirrus
	14 Sep 2001	M3	3600	Clear
	15 Sep 2001	M4	3600	Clear
	16 Sep 2001	M2	3600	Clear
	31 Oct 2002	M5	3600	Clear
	31 Oct 2002	S	1800	Clear
	02 Nov 2002	EE1	3600	Clear
	02 Nov 2002	EE2	3600	Clear
	02 Nov 2002	EE3	3000	Clear
	03 Nov 2002	NN1	3000	Clear
	03 Nov 2002	NN2	3000	Clear
	03 Nov 2002	NN3	3000	Clear
	03 Nov 2002	NN4	3300	Clear
	04 Nov 2002	WW1	3600	Clear
	04 Nov 2002	WW2	3600	Clear
	04 Nov 2002	WW3	3600	Clear

Table 3—Continued

Field	UT Date	Mask	Exp.	Conditions
	04 Nov 2002	WW4	3600	Clear
	05 Nov 2002	SS1	4200	Clear
	05 Nov 2002	SS2	3600	Clear
	05 Nov 2002	SS3	3600	Clear
	05 Nov 2002	SS4	3600	Clear
PKS0558−504	13 Sep 2001	M1	3600	Cirrus
	14 Sep 2001	M3	3600	Clear
	15 Sep 2001	M4	3600	Clear
	16 Sep 2001	M2	3600	Clear
	31 Oct 2002	M5	4200	Clear
	01 Nov 2002	M6	3600	Clear
	01 Nov 2002	M7	1800	Clear
	02 Nov 2002	M7	1800	Clear
	06 Nov 2002	M2	1800	Clear
PG1001+054	22 Apr 2001	S0	3600	Photometric
PG1004+130	31 May 2003	M1	3600	Cirrus
	01 Jun 2003	M2	3600	Cirrus
	02 Jun 2003	M3	3600	Clear
HE1029−140	18 Apr 2001	S0	3600	Photometric
	19 Apr 2001	B0	5400	Photometric
	20 Apr 2001	B1	3600	Light cirrus
	21 Apr 2001	S1	3600	Cirrus
PG1116+215	18 Apr 2001	B0	3600	Photometric
	18 Apr 2001	B1	3600	Photometric
	19 Apr 2001	S0	5400	Photometric
	20 Apr 2001	B2	3600	Light cirrus
	22 Apr 2001	F1	3600	Photometric
	05 Jun 2003	F1	3600	Clouds
	06 Jun 2003	F1	5400	Clear
PG1211+143	31 May 2003	M2	3600	Cirrus
	01 Jun 2003	M3	3600	Cirrus
	02 Jun 2003	M1	3600	Clear
PG1216+069	03 Jun 2003	M1	5400	Clear
	03 Jun 2003	M2	5150	Cirrus
	03 Jun 2003	M3	3600	Clear
	03 Jun 2003	M4	3600	Clear
	06 Jun 2003	M2	3600	Clear

Table 3—Continued

Field	UT Date	Mask	Exp.	Conditions
3C273	17 Apr 2001	B1	1800	Light cirrus
	18 Apr 2001	B1	3600	Photometric
	19 Apr 2001	S0	3600	Photometric
	20 Apr 2001	S1	5400	Light cirrus
	20 Apr 2001	S0	2700	Light cirrus
	21 Apr 2001	B2	5400	Cirrus
	22 Apr 2001	S2	3600	Photometric
	01 Jun 2003	B0	3600	Clear
Q1230+09	21 Apr 2001	S0	3600	Cirrus
	21 Apr 2001	B0	3600	Cirrus
	22 Apr 2001	S1	3600	Photometric
	22 Apr 2001	B1	3600	Photometric
	02 Jun 2003	M8	1800	Clear
	04 Jun 2003	B0	3600	Clear
	05 Jun 2003	M8	3600	Cirrus
PKS1302−102	17 Apr 2001	S0	3600	Light cirrus
	18 Apr 2001	B0	3600	Photometric
	19 Apr 2001	B1	3600	Photometric
	21 Apr 2001	B2	3600	Cirrus
PG1307+085	31 May 2003	B0	3600	Cirrus
	05 Jun 2003	B1	3600	Cirrus
	06 Jun 2003	S0	3600	Clear
Q1307+085	20 Apr 2001	S0	4500	Light cirrus
MRK 1383	17 Apr 2001	B0	5400	Light cirrus
	18 Apr 2001	S0	3600	Photometric
	19 Apr 2001	S1	5400	Photometric
	20 Apr 2001	S0	2700	Light cirrus
	21 Apr 2001	B1	3600	Cirrus
	22 Apr 2001	S2	3600	Photometric
	31 May 2003	B0	3600	Photometric
Q1553+113	18 Apr 2001	t0	3600	Photometric
	19 Apr 2001	t1	2700	Photometric
	20 Apr 2001	t1	3600	Light cirrus
	21 Apr 2001	t2	3600	Cirrus
	22 Apr 2001	t2	2700	Photometric
	04 Jun 2003	M1	3600	Clear
	04 Jun 2003	M2	3600	Clear

Table 3—Continued

Field	UT Date	Mask	Exp.	Conditions
	05 Jun 2003	M3	5400	Clear
	06 Jun 2003	M1	3600	Clear
PKS2005−489	31 May 2003	M1	3600	Light cirrus
	31 May 2003	M5	5400	Light cirrus
	01 Jun 2003	M2	3600	Clear
	01 Jun 2003	M3	5400	Clear
	01 Jun 2003	M4	5400	Clear
	03 Jun 2003	M6	6600	Bad seeing
	04 Jun 2003	M7	5400	Clear
	04 Jun 2003	M2	1800	Clear
	05 Jun 2003	M8	5289	Cirrus
FJ2155−092	10 Sep 2001	M1	3600	Photometric
	13 Sep 2001	M2	3600	Clear
	15 Sep 2001	M3	3600	Clear
	15 Sep 2001	M4	3600	Clear
	16 Sep 2001	M5	3600	Clear
	01 Nov 2002	M6	3600	Clear
	02 Nov 2002	M7	3000	Clear
PKS2155−304	10 Sep 2001	M1	3600	Photometric
	11 Sep 2001	M2	3600	Cloudy
	12 Sep 2001	M2	3600	Clear
	14 Sep 2001	M3	3600	Clear
	14 Sep 2001	M4	3600	Clear
	15 Sep 2001	M2	3600	Clear
	16 Sep 2001	M5	3600	Clear
	31 Oct 2002	M6	3600	Clear

Table 4. Summary of Galaxies at $z < z_{\rm em} + 0.01$

ID	RA (J2000)	DEC (J2000)	$z_{\rm gal}$	L^a ($L*$)	ρ^b (h_{72}^{-1} kpc)	Type^c
Q0026+1259: $0.005 < z < (z_{\rm em} - 0.01)$						
Q0026+1259_1303	00:29:09.2	+13:16:28	0.03295	0.02	44	Late
Q0026+1259_1500	00:29:01.3	+13:13:12	0.03346	0.03	158	Late
Q0026+1259_1143	00:29:15.3	+13:20:57	0.03931	1.38	214	Early
Q0026+1259_1140	00:29:16.4	+13:21:52	0.08043	0.11	497	Unkn
Q0026+1259_1722	00:28:53.5	+13:24:19	0.05645	0.56	595	Late
Q0026+1259_1103	00:29:17.7	+13:23:26	0.08073	0.08	634	Unkn
Q0026+1259_1901	00:28:45.5	+13:20:08	0.08062	0.06	695	Early
Q0026+1259_902	00:29:23.4	+13:09:41	0.11253	1.09	781	Late
Q0026+1259_1125	00:29:16.0	+13:10:03	0.13138	0.18	791	Unkn
Q0026+1259_512	00:29:37.5	+13:10:21	0.09614	1.96	821	Early
Q0026+1259_108	00:29:53.3	+13:10:50	0.07379	0.19	879	Early
Q0026+1259_2045	00:28:39.0	+13:19:02	0.10711	0.14	1007	Early
Q0026+1259_2141	00:28:34.3	+13:07:05	0.10499	0.36	1437	Early
Q0026+1259: $(z_{\rm em} - 0.01) < z < (z_{\rm em} + 0.01)$						
Q0026+1259_1095	00:29:17.9	+13:16:50	0.14736	0.20	186	Early
Q0026+1259_1341	00:29:07.6	+13:16:06	0.14599	0.95	219	Early
Q0026+1259_989	00:29:21.2	+13:16:44	0.14802	0.27	285	Late
Q0026+1259_1013	00:29:20.2	+13:17:15	0.14651	2.79	286	Early
Q0026+1259_963	00:29:22.2	+13:16:06	0.14183	0.21	294	Early
Q0026+1259_1148	00:29:15.4	+13:13:25	0.14487	0.17	381	Late
Q0026+1259_925	00:29:23.4	+13:14:39	0.14480	0.29	398	Late
Q0026+1259_764	00:29:28.7	+13:14:32	0.14553	1.06	575	Late
Q0026+1259_1110	00:29:17.2	+13:20:01	0.14655	0.49	582	Late
Q0026+1259_1421	00:29:04.4	+13:12:17	0.14009	0.95	614	Early
Q0026+1259_756	00:29:28.9	+13:13:15	0.14267	0.56	662	Early
Q0026+1259_978	00:29:21.5	+13:20:32	0.13849	0.50	668	Early
Q0026+1259_636	00:29:33.9	+13:16:31	0.14397	0.45	716	Late
Q0026+1259_686	00:29:32.1	+13:18:10	0.14693	0.60	725	Early
Q0026+1259_1562	00:28:59.1	+13:12:12	0.13920	0.37	730	Late
Q0026+1259_1587	00:28:58.3	+13:12:07	0.14689	0.36	792	Early
Q0026+1259_842	00:29:26.1	+13:11:02	0.14238	0.23	827	Late
Q0026+1259_1280	00:29:09.6	+13:10:13	0.14561	0.75	847	Early
Q0026+1259_1126	00:29:15.6	+13:10:03	0.14550	1.29	859	Late
Q0026+1259_527	00:29:37.7	+13:17:16	0.14507	0.90	870	Early
Q0026+1259_559	00:29:36.8	+13:18:46	0.13875	0.16	872	Unkn
Q0026+1259_1518	00:29:01.5	+13:21:42	0.13732	0.71	872	Late
Q0026+1259_1353	00:29:07.6	+13:22:20	0.14677	0.41	929	Late
Q0026+1259_545	00:29:37.3	+13:19:09	0.14485	0.65	945	Early
Q0026+1259_1558	00:29:00.1	+13:22:16	0.13872	0.34	971	Late
Q0026+1259_1699	00:28:53.9	+13:10:13	0.13949	0.69	1056	Early

Table 4—Continued

ID	RA (J2000)	DEC (J2000)	$z_{\rm gal}$	L^a ($L*$)	ρ^b (h_{72}^{-1} kpc)	Type^c
Q0026+1259_444	00:29:40.0	+13:19:24	0.14612	9.92	1056	Early
Q0026+1259_1498	00:29:01.2	+13:09:13	0.14462	0.59	1069	Early
Q0026+1259_342	00:29:44.4	+13:15:47	0.14398	2.37	1086	Early
Q0026+1259_1716	00:28:52.9	+13:10:26	0.14420	0.82	1086	Late
Q0026+1259_1505	00:29:02.3	+13:08:48	0.14533	5.51	1112	Early
Q0026+1259_1659	00:28:55.6	+13:09:37	0.14550	1.05	1124	Early
Q0026+1259_1091	00:29:18.4	+13:24:13	0.13910	1.06	1132	Early
Q0026+1259_1434	00:29:03.3	+13:08:23	0.14350	0.44	1144	Early
Q0026+1259_1468	00:29:01.5	+13:08:27	0.14653	1.14	1177	Early
Q0026+1259_1507	00:29:01.2	+13:24:13	0.13965	4.76	1206	Early
Q0026+1259_272	00:29:48.0	+13:18:07	0.14646	0.19	1265	Late
Q0026+1259_227	00:29:49.7	+13:13:55	0.14268	0.21	1296	Late
Q0026+1259_2003	00:28:40.1	+13:11:50	0.14091	1.01	1309	Late
Q0026+1259_1169	00:29:15.5	+13:25:23	0.14272	0.57	1311	Late
Q0026+1259_1344	00:29:08.3	+13:25:40	0.13917	0.17	1335	Late
Q0026+1259_345	00:29:45.0	+13:21:11	0.14610	1.18	1339	Early
Q0026+1259_187	00:29:51.2	+13:17:30	0.14655	1.81	1362	Early
Q0026+1259_1496	00:29:01.1	+13:06:17	0.14609	0.34	1471	Early
Q0026+1259_1815	00:28:49.0	+13:07:02	0.14126	0.50	1523	Early
Q0026+1259_2173	00:28:33.3	+13:11:53	0.14363	0.99	1545	Late
Q0026+1259_301	00:29:47.1	+13:23:15	0.14579	0.86	1574	Early
TONS180: $0.005 < z < (z_{\rm em} - 0.01)$						
TONS180_2295	00:57:04.0	–22:26:51	0.02336	0.02	148	Late
TONS180_2149	00:57:08.5	–22:18:29	0.04562	0.38	265	Early
TONS180_433	00:57:57.3	–22:16:40	0.04596	0.67	569	Early
TONS180: $(z_{\rm em} - 0.01) < z < (z_{\rm em} + 0.01)$						
TONS180_1570	00:57:23.9	–22:19:40	0.06348	0.12	233	Unkn
TONS180_2332	00:57:02.9	–22:23:52	0.06244	0.77	295	Early
TONS180_2284	00:57:03.7	–22:25:10	0.06198	2.43	310	Early
TONS180_3307	00:56:36.1	–22:32:24	0.05574	0.12	879	Early
TONS210: $0.005 < z < (z_{\rm em} - 0.01)$						
TONS210_542	01:22:18.4	–28:17:19	0.06730	1.31	552	Early
TONS210_2075	01:21:10.6	–28:14:13	0.06714	0.76	881	Late
TONS210: $(z_{\rm em} - 0.01) < z < (z_{\rm em} + 0.01)$						
TONS210_1700	01:21:26.2	–28:19:13	0.11817	0.22	783	Late
TONS210_1746	01:21:24.4	–28:15:31	0.11774	2.14	1034	Late
TONS210_1228	01:21:48.7	–28:12:07	0.11584	1.39	1040	Late

Table 4—Continued

ID	RA (J2000)	DEC (J2000)	$z_{\rm gal}$	L^a ($L*$)	ρ^b (h_{72}^{-1} kpc)	Type^c
TONS210_1929	01:21:16.5	–28:22:05	0.11816	0.26	1052	Late
TONS210_2100	01:21:10.0	–28:15:44	0.11621	1.00	1367	Early
PKS0312-77: $0.005 < z < (z_{\rm em} - 0.01)$						
PKS0312-77_1339	03:11:57.8	–76:51:55	0.20264	0.63	127	Late
PKS0312-77_2947	03:12:01.7	–76:55:17	0.05935	0.29	245	Late
PKS0312-77_1515	03:11:55.2	–76:50:03	0.20382	0.35	335	Late
PKS0312-77_1616	03:11:58.5	–76:48:55	0.11919	1.85	367	Late
PKS0312-77_1936	03:12:14.1	–76:45:55	0.06119	0.32	502	Late
PKS0312-77_2903	03:11:54.9	–76:55:33	0.19821	0.79	680	Early
PKS0312-77_672	03:12:31.1	–76:43:25	0.05142	4.90	692	Early
PKS0312-77_711	03:12:31.6	–76:42:28	0.04931	0.26	706	Early
PKS0312-77_1920	03:12:45.0	–76:46:03	0.05115	0.29	768	Early
PKS0312-77_2859	03:12:52.4	–76:56:23	0.05205	0.10	854	Early
PKS0312-77_2543	03:11:02.4	–77:00:05	0.05292	1.48	898	Early
PKS0312-77_2457	03:11:26.9	–77:01:37	0.07443	0.08	954	Early
PKS0312-77_2011	03:11:46.4	–76:45:10	0.15307	0.69	1046	Early
PKS0312-77_906	03:11:56.6	–76:59:05	0.15322	0.74	1080	Late
PKS0312-77_1657	03:13:14.2	–76:48:41	0.05064	0.04	1108	Early
PKS0312-77_954	03:12:19.8	–76:57:02	0.16007	0.40	1247	Late
PKS0312-77_2851	03:13:25.7	–76:56:25	0.05294	0.43	1334	Early
PKS0312-77_2215	03:11:27.4	–77:00:44	0.11997	0.29	1366	Late
PKS0312-77_2609	03:10:19.3	–76:59:47	0.05076	0.06	1401	Late
PKS0312-77_2671	03:10:18.7	–76:58:30	0.05232	1.15	1429	Early
PKS0312-77_1460	03:11:22.8	–76:50:41	0.19465	0.29	1476	Late
PKS0312-77_1381	03:12:38.4	–76:51:32	0.15921	1.25	1665	Early
PKS0312-77_1354	03:12:31.8	–76:51:46	0.19874	0.67	1686	Early
PKS0312-77_659	03:14:01.5	–76:42:27	0.05202	1.34	1872	Early
PKS0312-77_2563	03:12:22.4	–77:00:20	0.18823	0.34	1919	Early
PKS0312-77_1906	03:14:23.6	–76:46:15	0.05016	0.07	2060	Unkn
PKS0312-77_2629	03:10:36.0	–76:59:23	0.09856	0.73	2159	Late
PKS0312-77_2041	03:12:38.8	–76:44:53	0.18734	0.65	2272	Early
PKS0312-77_1075	03:11:06.8	–76:54:18	0.20288	1.89	2305	Early
PKS0312-77_1469	03:12:48.4	–76:50:33	0.19822	1.18	2453	Late
PKS0312-77_2205	03:12:38.7	–77:00:43	0.18857	1.21	2477	Early
PKS0312-77_1894	03:11:07.4	–76:46:15	0.20467	0.78	2478	Late
PKS0312-77_1398	03:13:04.1	–76:51:24	0.15893	0.22	2648	Early
PKS0312-77_2667	03:10:31.5	–76:58:46	0.12576	0.28	2778	Early
PKS0312-77_1007	03:10:54.2	–76:55:09	0.19847	0.40	2865	Late
PKS0312-77_779	03:12:49.9	–76:43:09	0.20398	1.53	3041	Early
PKS0312-77_1405	03:13:37.4	–76:51:22	0.11959	0.41	3089	Early
PKS0312-77_1608	03:13:05.0	–76:49:08	0.19697	0.72	3226	Early
PKS0312-77_1231	03:10:44.4	–76:53:00	0.20704	0.53	3366	Unkn
PKS0312-77_2668	03:10:45.6	–76:58:55	0.20300	1.28	3508	Early

Table 4—Continued

ID	RA (J2000)	DEC (J2000)	$z_{\rm gal}$	L^a ($L*$)	ρ^b (h_{72}^{-1} kpc)	Type^c
PKS0312-77_1513	03:10:38.1	–76:50:01	0.20191	0.31	3600	Late
PKS0312-77_1697	03:10:33.5	–76:48:09	0.20448	1.10	3901	Late
PKS0312-77_2727	03:13:35.9	–76:58:13	0.16166	0.19	4047	Late
PKS0312-77_784	03:10:29.8	–76:42:59	0.19566	0.58	4197	Early
PKS0312-77_757	03:10:23.8	–76:42:42	0.19629	0.48	4479	Late
PKS0312-77_937	03:13:55.0	–76:58:09	0.16166	0.61	4767	Late
PKS0312-77_1427	03:10:12.6	–76:50:57	0.20480	0.60	4828	Late
PKS0312-77_683	03:13:44.1	–76:42:02	0.20714	1.16	5499	Early
PKS0312-77_1360	03:14:36.1	–76:51:48	0.15894	0.75	6179	Early
PKS0312-77_765	03:14:02.4	–76:42:56	0.20675	0.45	6263	Late
PKS0312-77: $(z_{\rm em} - 0.01) < z < (z_{\rm em} + 0.01)$						
PKS0312-77_1799	03:13:34.4	–76:47:19	0.22852	1.62	5166	Early
PKS0312-77_1803	03:13:37.4	–76:47:18	0.22876	1.92	5321	Early
PKS0312-77_1209	03:14:10.3	–76:53:20	0.22636	1.22	6875	Early
PKS0312-77_1210	03:14:18.9	–76:53:20	0.23077	0.55	7418	Early
PKS0312-77_2738	03:14:26.8	–76:58:11	0.22669	1.20	7825	Early
PKS0312-77_1207	03:14:34.9	–76:53:21	0.22511	0.75	8089	Late
PKS0405-123: $0.005 < z < (z_{\rm em} - 0.01)$						
PKS0405-123_1753	04:07:51.2	–12:11:38	0.16704	2.14	115	Late
PKS0405-123_2034	04:07:44.0	–12:12:09	0.15321	0.98	181	Early
PKS0405-123_1967	04:07:45.9	–12:11:09	0.36124	6.60	214	Early
PKS0405-123_1786	04:07:50.6	–12:12:25	0.29761	1.88	245	Early
PKS0405-123_1457	04:07:58.1	–12:12:24	0.09645	0.15	256	Late
PKS0405-123_2099	04:07:42.7	–12:11:33	0.20302	1.07	262	Early
PKS0405-123_1602	04:07:54.2	–12:14:45	0.09649	0.15	347	Unkn
PKS0405-123_1601	04:07:54.2	–12:14:50	0.09671	1.36	355	Early
PKS0405-123_948	04:08:09.6	–12:21:01	0.03109	0.01	376	Early
PKS0405-123_1463	04:07:58.3	–12:07:38	0.07673	0.11	381	Late
PKS0405-123_41184	04:07:59.3	–11:51:32	0.01681	0.00	388	Early
PKS0405-123_1081	04:08:06.6	–12:12:50	0.08002	1.40	399	Early
PKS0405-123_1698	04:07:52.6	–12:15:49	0.09056	0.07	410	Unkn
PKS0405-123_32259	04:07:25.8	–12:23:05	0.03026	0.03	434	Late
PKS0405-123_30012	04:07:58.7	–12:18:03	0.05902	0.03	443	Unkn
PKS0405-123_2757	04:07:27.3	–12:10:35	0.08145	0.36	462	Unkn
PKS0405-123_1970	04:07:45.7	–12:15:04	0.13386	0.52	467	Late
PKS0405-123_2288	04:07:38.5	–12:11:56	0.20424	0.43	468	Late
PKS0405-123_1807	04:07:50.2	–12:09:52	0.32516	2.32	476	Early
PKS0405-123_2063	04:07:43.1	–12:15:08	0.13389	0.25	501	Late
PKS0405-123_2262	04:07:38.7	–12:12:49	0.20294	3.53	505	Early
PKS0405-123_2867	04:07:24.5	–12:10:41	0.08126	0.21	516	Early
PKS0405-123_993	04:08:09.6	–12:07:45	0.07697	0.06	536	Early

Table 4—Continued

ID	RA (J2000)	DEC (J2000)	$z_{\rm gal}$	L^a ($L*$)	ρ^b (h_{72}^{-1} kpc)	Type^c
PKS0405-123_2716	04:07:26.7	–12:21:29	0.04321	0.02	537	Unkn
PKS0405-123_40370	04:07:32.9	–11:56:39	0.03189	0.01	551	Early
PKS0405-123_1728	04:07:51.8	–12:13:16	0.42531	6.16	585	Early
PKS0405-123_2421	04:07:35.7	–12:11:54	0.20224	0.34	591	Late
PKS0405-123_2254	04:07:39.7	–12:05:42	0.09705	0.20	632	Late
PKS0405-123_40848	04:07:52.1	–11:53:25	0.03104	0.33	633	Late
PKS0405-123_31252	04:07:56.9	–12:29:53	0.03233	0.06	665	Early
PKS0405-123_20617	04:06:24.9	–12:12:58	0.02869	0.01	673	Unkn
PKS0405-123_2273	04:07:39.0	–12:08:50	0.20283	1.53	679	Early
PKS0405-123_1715	04:07:52.3	–12:14:08	0.30986	1.79	689	Early
PKS0405-123_2999	04:07:20.4	–12:18:28	0.06676	0.06	702	Late
PKS0405-123_1503	04:07:57.4	–12:07:41	0.16166	0.99	706	Late
PKS0405-123_2311	04:07:37.3	–12:16:14	0.13359	0.50	714	Late
PKS0405-123_1316	04:08:01.9	–12:11:40	0.24842	1.29	736	Late
PKS0405-123_41237	04:07:20.6	–11:50:57	0.03050	0.07	745	Early
PKS0405-123_2110	04:07:43.2	–12:02:49	0.08052	0.08	756	Unkn
PKS0405-123_1473	04:07:57.9	–12:09:52	0.32031	1.04	772	Late
PKS0405-123_3138	04:07:17.3	–12:12:45	0.09801	0.11	796	Unkn
PKS0405-123_40321	04:06:32.9	–11:56:35	0.02954	0.54	799	Late
PKS0405-123_1520	04:07:57.0	–12:10:03	0.42672	3.89	834	Early
PKS0405-123_1345	04:08:01.6	–12:07:51	0.17883	0.56	847	Early
PKS0405-123_2784	04:07:26.6	–12:12:52	0.16085	0.43	866	Late
PKS0405-123_1659	04:07:54.4	–12:03:07	0.09698	0.39	868	Late
PKS0405-123_11389	04:09:20.8	–12:02:05	0.03228	0.04	902	Unkn
PKS0405-123_42002	04:08:09.3	–11:46:33	0.03166	0.02	907	Early
PKS0405-123_2458	04:07:34.6	–12:13:22	0.29511	1.20	950	Early
PKS0405-123_2698	04:07:29.0	–12:09:50	0.20106	0.45	957	Late
PKS0405-123_2973	04:07:22.3	–12:03:53	0.09709	0.24	1017	Late
PKS0405-123_2142	04:07:41.2	–12:15:31	0.29640	2.01	1062	Late
PKS0405-123_1710	04:07:52.9	–12:06:46	0.24447	0.90	1070	Late
PKS0405-123_1470	04:07:57.6	–12:14:55	0.32801	2.51	1072	Early
PKS0405-123_3082	04:07:19.9	–12:03:34	0.09733	0.16	1083	Early
PKS0405-123_32313	04:08:10.6	–12:22:56	0.08199	0.39	1090	Early
PKS0405-123_42900	04:06:55.8	–11:40:55	0.02953	0.01	1105	Unkn
PKS0405-123_2285	04:07:40.0	–12:07:20	0.28152	1.58	1136	Late
PKS0405-123_21284	04:05:44.0	–12:05:41	0.03228	0.02	1142	Early
PKS0405-123_2485	04:07:32.9	–12:22:11	0.09860	0.39	1148	Late
PKS0405-123_3432	04:07:10.2	–12:09:04	0.11753	0.64	1176	Late
PKS0405-123_10258	04:08:35.3	–12:16:01	0.08992	0.43	1178	Late
PKS0405-123_3386	04:07:10.8	–12:19:50	0.09171	0.45	1194	Early
PKS0405-123_258	04:08:27.4	–12:22:01	0.08193	0.27	1232	Late
PKS0405-123_3428	04:07:09.9	–12:13:42	0.12574	0.46	1241	Early
PKS0405-123_21663	04:06:19.4	–12:01:29	0.04682	0.05	1257	Late
PKS0405-123_32180	04:07:35.7	–12:23:43	0.09739	0.08	1262	Late
PKS0405-123_2813	04:07:25.9	–12:14:17	0.23610	1.84	1306	Early

Table 4—Continued

ID	RA (J2000)	DEC (J2000)	$z_{\rm gal}$	L^a ($L*$)	ρ^b (h_{72}^{-1} kpc)	Type^c
PKS0405-123_3390	04:07:10.9	–12:17:47	0.11519	0.09	1312	Unkn
PKS0405-123_10727	04:08:50.8	–12:11:00	0.08180	0.07	1347	Late
PKS0405-123_1288	04:08:02.1	–12:16:38	0.25409	0.70	1349	Early
PKS0405-123_2598	04:07:31.2	–12:12:50	0.42526	6.84	1389	Early
PKS0405-123_1039	04:08:08.1	–12:12:04	0.36101	6.62	1397	Early
PKS0405-123_2489	04:07:34.3	–12:07:04	0.29288	1.29	1411	Early
PKS0405-123_3018	04:07:21.3	–12:03:25	0.13373	0.97	1412	Late
PKS0405-123_270	04:08:27.5	–12:16:03	0.13360	0.42	1429	Early
PKS0405-123_11489	04:08:30.5	–12:00:25	0.09034	0.07	1449	Unkn
PKS0405-123_11155	04:09:03.1	–12:05:25	0.06961	0.21	1466	Late
PKS0405-123_10552	04:08:50.4	–12:12:52	0.09158	0.09	1486	Early
PKS0405-123_1236	04:08:04.8	–12:08:12	0.36151	2.79	1507	Early
PKS0405-123_1785	04:07:50.5	–12:15:47	0.54816	3.83	1508	Late
PKS0405-123_875	04:08:12.5	–12:08:37	0.26072	1.59	1523	Early
PKS0405-123_1206	04:08:03.3	–12:22:39	0.13364	0.29	1550	Late
PKS0405-123_10309	04:08:52.8	–12:15:36	0.08987	0.77	1558	Late
PKS0405-123_1419	04:07:58.9	–12:17:25	0.29717	1.55	1580	Early
PKS0405-123_1893	04:07:48.3	–12:04:12	0.24507	0.66	1599	Late
PKS0405-123_32400	04:08:12.9	–12:22:29	0.13103	0.17	1631	Late
PKS0405-123_2622	04:07:30.2	–12:17:19	0.25768	0.64	1632	Late
PKS0405-123_1559	04:07:54.9	–12:19:26	0.22909	0.67	1639	Late
PKS0405-123_2541	04:07:32.2	–12:18:27	0.23607	1.24	1667	Early
PKS0405-123_887	04:08:11.6	–12:14:37	0.30987	1.17	1672	Early
PKS0405-123_2778	04:07:26.6	–12:07:27	0.29296	4.06	1681	Early
PKS0405-123_838	04:08:12.9	–12:14:01	0.31042	1.46	1683	Late
PKS0405-123_31118	04:07:19.4	–12:30:41	0.07910	0.31	1707	Late
PKS0405-123_2970	04:07:21.9	–12:04:58	0.20234	2.22	1748	Early
PKS0405-123_366	04:08:25.0	–12:16:36	0.17706	1.16	1750	Early
PKS0405-123_2272	04:07:38.6	–12:16:35	0.43396	2.09	1750	Late
PKS0405-123_586	04:08:19.5	–12:14:27	0.23950	0.89	1759	Late
PKS0405-123_11470	04:08:57.5	–12:00:50	0.08209	0.80	1763	Late
PKS0405-123_917	04:08:11.4	–12:06:18	0.26140	1.94	1771	Early
PKS0405-123_11433	04:09:00.1	–12:01:16	0.08187	2.33	1788	Late
PKS0405-123_31271	04:07:41.8	–12:29:51	0.09569	0.34	1819	Late
PKS0405-123_10176	04:09:10.7	–12:17:16	0.08174	0.18	1842	Late
PKS0405-123_604	04:08:18.8	–12:16:05	0.23630	2.20	1852	Late
PKS0405-123_3623	04:07:05.8	–12:08:47	0.17963	0.51	1870	Late
PKS0405-123_1309	04:08:01.5	–12:18:30	0.29885	1.27	1900	Late
PKS0405-123_187	04:08:29.4	–12:16:55	0.17736	1.14	1940	Early
PKS0405-123_2214	04:07:39.3	–12:21:51	0.20311	1.29	1960	Late
PKS0405-123_615	04:08:18.4	–12:17:23	0.23653	0.89	1989	Late
PKS0405-123_41101	04:06:56.9	–11:51:48	0.08087	0.05	2016	Late
PKS0405-123_10900	04:09:12.6	–12:08:59	0.09121	0.44	2020	Late
PKS0405-123_2586	04:07:31.2	–12:18:02	0.33581	1.62	2081	Late
PKS0405-123_32226	04:08:05.3	–12:23:31	0.17465	0.66	2095	Early

Table 4—Continued

ID	RA (J2000)	DEC (J2000)	$z_{\rm gal}$	L^a ($L*$)	ρ^b (h_{72}^{-1} kpc)	Type^c
PKS0405-123_2276	04:07:37.7	–12:22:29	0.20314	0.53	2096	Late
PKS0405-123_20890	04:06:09.9	–12:10:07	0.08047	0.06	2097	Early
PKS0405-123_10498	04:09:17.0	–12:13:38	0.09080	0.11	2109	Early
PKS0405-123_10839	04:08:38.7	–12:09:39	0.17708	2.00	2137	Early
PKS0405-123_289	04:08:27.2	–12:14:12	0.24012	0.54	2138	Unkn
PKS0405-123_31862	04:07:03.4	–12:25:29	0.11867	0.60	2142	Late
PKS0405-123_10565	04:08:45.8	–12:12:41	0.15356	1.02	2148	Early
PKS0405-123_40471	04:07:25.5	–11:55:56	0.13110	0.26	2180	Late
PKS0405-123_30806	04:07:57.1	–12:33:20	0.09643	1.41	2184	Early
PKS0405-123_3289	04:07:14.6	–12:03:23	0.20330	1.76	2204	Early
PKS0405-123_983	04:08:08.9	–12:18:50	0.29899	1.20	2208	Early
PKS0405-123_410	04:08:24.2	–12:10:47	0.29310	1.37	2211	Late
PKS0405-123_729	04:08:16.3	–12:05:48	0.28952	1.22	2214	Late
PKS0405-123_31433	04:07:53.8	–12:28:37	0.13107	1.62	2229	Late
PKS0405-123_469	04:08:23.2	–12:08:55	0.29401	1.17	2243	Late
PKS0405-123_972	04:08:09.2	–12:19:15	0.29734	1.54	2294	Early
PKS0405-123_691	04:08:17.4	–12:05:30	0.28860	2.13	2304	Late
PKS0405-123_10246	04:08:54.5	–12:16:15	0.13558	0.63	2311	Late
PKS0405-123_41345	04:06:59.7	–11:50:18	0.09059	0.10	2321	Late
PKS0405-123_1397	04:07:59.1	–12:18:46	0.40610	2.58	2322	Late
PKS0405-123_614	04:08:18.2	–12:20:45	0.21697	0.58	2322	Unkn
PKS0405-123_658	04:08:18.5	–12:03:50	0.24711	0.70	2350	Late
PKS0405-123_3475	04:07:09.2	–12:10:51	0.28360	2.02	2352	Late
PKS0405-123_2871	04:07:24.1	–12:18:04	0.32927	1.10	2354	Late
PKS0405-123_31983	04:08:08.9	–12:25:00	0.17254	0.82	2356	Late
PKS0405-123_41852	04:06:55.7	–11:47:18	0.08102	0.34	2364	Late
PKS0405-123_1181	04:08:05.4	–12:03:00	0.29454	1.74	2366	Late
PKS0405-123_3340	04:07:13.0	–12:04:52	0.24121	0.59	2369	Early
PKS0405-123_11603	04:09:14.5	–11:58:55	0.09079	0.87	2369	Early
PKS0405-123_10458	04:09:08.4	–12:14:09	0.11674	0.51	2385	Late
PKS0405-123_1610	04:07:55.6	–12:01:57	0.28960	2.76	2392	Early
PKS0405-123_30847	04:06:51.1	–12:32:46	0.09021	0.21	2407	Unkn
PKS0405-123_514	04:08:22.2	–12:04:59	0.26142	0.73	2430	Early
PKS0405-123_10470	04:08:34.0	–12:13:50	0.24021	1.65	2471	Early
PKS0405-123_40291	04:07:25.1	–11:57:11	0.16587	1.12	2472	Early
PKS0405-123_2808	04:07:26.9	–12:02:58	0.29051	1.34	2479	Late
PKS0405-123_3300	04:07:13.2	–12:18:58	0.24568	0.52	2480	Late
PKS0405-123_31993	04:07:49.6	–12:24:55	0.20279	0.48	2487	Early
PKS0405-123_41527	04:06:33.7	–11:49:04	0.08098	0.06	2502	Unkn
PKS0405-123_2170	04:07:40.3	–12:20:16	0.36092	3.28	2508	Early
PKS0405-123_10882	04:08:26.7	–12:09:00	0.30841	1.59	2526	Early
PKS0405-123_10556	04:09:08.1	–12:12:50	0.12625	0.53	2528	Early
PKS0405-123_32346	04:08:02.9	–12:22:44	0.24586	1.47	2531	Early
PKS0405-123_3492	04:07:09.1	–12:07:37	0.28370	0.98	2541	Early
PKS0405-123_10253	04:09:00.7	–12:16:10	0.13793	1.07	2544	Late

Table 4—Continued

ID	RA (J2000)	DEC (J2000)	$z_{\rm gal}$	L^a ($L*$)	ρ^b (h_{72}^{-1} kpc)	Type^c
PKS0405-123_3123	04:07:18.5	–12:02:40	0.25342	0.73	2576	Late
PKS0405-123_3360	04:07:12.4	–12:08:37	0.34253	3.01	2586	Early
PKS0405-123_907	04:08:11.8	–12:04:32	0.36168	1.91	2596	Late
PKS0405-123_21111	04:06:08.4	–12:07:39	0.09941	0.38	2600	Early
PKS0405-123_40537	04:06:52.7	–11:55:18	0.12070	0.50	2609	Late
PKS0405-123_30260	04:07:40.0	–12:39:24	0.08990	1.60	2618	Early
PKS0405-123_1150	04:08:06.6	–12:02:05	0.29782	1.54	2621	Late
PKS0405-123_10112	04:09:02.1	–12:18:03	0.13535	0.36	2624	Late
PKS0405-123_3466	04:07:09.7	–12:06:41	0.29122	2.29	2649	Early
PKS0405-123_1570	04:07:54.8	–12:22:13	0.29882	2.56	2669	Early
PKS0405-123_30799	04:06:36.4	–12:33:01	0.09172	2.44	2674	Early
PKS0405-123_32584	04:06:55.5	–12:20:53	0.17812	2.66	2721	Early
PKS0405-123_3415	04:07:10.8	–12:08:02	0.34165	2.63	2733	Early
PKS0405-123_10692	04:08:44.0	–12:11:15	0.21664	2.52	2737	Early
PKS0405-123_98	04:08:32.0	–12:17:07	0.26016	1.86	2754	Early
PKS0405-123_3519	04:07:10.4	–12:07:52	0.33747	1.93	2755	Late
PKS0405-123_42607	04:07:30.9	–11:42:48	0.09105	0.14	2768	Unkn
PKS0405-123_32555	04:06:54.6	–12:21:04	0.17799	0.82	2770	Late
PKS0405-123_11108	04:08:34.6	–12:05:59	0.24540	1.10	2775	Late
PKS0405-123_32098	04:07:03.9	–12:24:05	0.17798	0.70	2813	Late
PKS0405-123_31417	04:07:48.6	–12:28:42	0.17488	0.70	2839	Late
PKS0405-123_221	04:08:29.0	–12:13:28	0.34660	2.76	2843	Early
PKS0405-123_909	04:08:10.5	–12:20:47	0.32837	2.88	2844	Early
PKS0405-123_427	04:08:23.3	–12:17:53	0.32943	2.83	2857	Early
PKS0405-123_3056	04:07:19.5	–12:18:21	0.38190	2.51	2885	Early
PKS0405-123_31321	04:06:48.7	–12:29:08	0.12506	0.69	2887	Late
PKS0405-123_1957	04:07:45.5	–12:22:20	0.33512	3.33	2892	Early
PKS0405-123_1919	04:07:46.3	–12:22:26	0.33531	3.63	2916	Early
PKS0405-123_2974	04:07:22.5	–12:02:57	0.34363	1.84	2954	Early
PKS0405-123_30002	04:06:41.7	–12:17:54	0.17449	1.74	2954	Early
PKS0405-123_43005	04:07:41.0	–11:40:19	0.09098	0.32	2976	Late
PKS0405-123_3557	04:07:06.8	–12:08:14	0.34182	5.38	2977	Early
PKS0405-123_32340	04:07:48.3	–12:22:42	0.33451	2.87	2980	Early
PKS0405-123_32926	04:06:41.7	–12:18:30	0.17433	0.58	2988	Late
PKS0405-123_42613	04:06:57.8	–11:42:36	0.09084	0.15	3000	Early
PKS0405-123_324	04:08:32.0	–12:07:09	0.30934	0.88	3005	Late
PKS0405-123_32344	04:07:15.6	–12:22:33	0.25417	1.02	3028	Late
PKS0405-123_3788	04:07:06.3	–12:07:56	0.34086	1.92	3031	Late
PKS0405-123_30574	04:07:14.1	–12:35:00	0.12063	0.91	3031	Early
PKS0405-123_40500	04:07:42.7	–11:55:49	0.21101	1.62	3053	Late
PKS0405-123_1050	04:08:08.8	–12:01:37	0.34217	3.98	3058	Early
PKS0405-123_41377	04:07:04.2	–11:50:02	0.12616	0.21	3064	Late
PKS0405-123_30544	04:07:12.8	–12:35:13	0.12104	0.19	3078	Late
PKS0405-123_21326	04:06:12.5	–12:05:17	0.12435	0.31	3097	Late
PKS0405-123_32644	04:07:05.2	–12:20:33	0.25386	1.53	3103	Early

Table 4—Continued

ID	RA (J2000)	DEC (J2000)	$z_{\rm gal}$	L^a ($L*$)	ρ^b (h_{72}^{-1} kpc)	Type^c
PKS0405-123_32334	04:07:44.0	–12:22:43	0.35981	2.98	3145	Early
PKS0405-123_41036	04:07:26.5	–11:52:20	0.16517	0.82	3177	Early
PKS0405-123_31215	04:07:29.3	–12:30:05	0.17610	0.50	3187	Late
PKS0405-123_31150	04:07:32.4	–12:30:31	0.17594	1.75	3224	Early
PKS0405-123_553	04:08:21.1	–12:04:45	0.40444	4.11	3235	Early
PKS0405-123_31145	04:07:33.8	–12:30:37	0.17633	0.47	3236	Late
PKS0405-123_42430	04:07:21.0	–11:43:47	0.11081	0.34	3239	Early
PKS0405-123_31423	04:07:07.7	–12:28:30	0.17389	2.93	3258	Early
PKS0405-123_2390	04:07:37.0	–12:01:42	0.43489	2.16	3260	Late
PKS0405-123_42509	04:06:32.9	–11:43:09	0.09236	0.08	3285	Unkn
PKS0405-123_3630	04:07:05.5	–12:09:57	0.40812	2.04	3299	Unkn
PKS0405-123_529	04:08:20.5	–12:19:15	0.39232	5.16	3300	Early
PKS0405-123_996	04:08:08.3	–12:21:19	0.40773	4.11	3321	Early
PKS0405-123_32041	04:07:26.4	–12:24:32	0.27848	1.22	3325	Early
PKS0405-123_847	04:08:14.0	–12:01:14	0.34310	2.70	3333	Early
PKS0405-123_40674	04:07:35.3	–11:54:35	0.21125	0.43	3342	Late
PKS0405-123_312	04:08:26.9	–12:12:10	0.51655	4.99	3360	Late
PKS0405-123_452	04:08:24.0	–12:02:41	0.33525	3.77	3391	Early
PKS0405-123_2496	04:07:33.2	–12:20:56	0.49917	6.25	3438	Early
PKS0405-123_10053	04:08:45.3	–12:18:48	0.24482	0.72	3441	Late
PKS0405-123_31316	04:07:04.7	–12:29:18	0.17429	0.84	3444	Early
PKS0405-123_20178	04:06:10.3	–12:17:25	0.13840	0.34	3446	Unkn
PKS0405-123_20498	04:06:25.1	–12:14:21	0.17389	0.54	3469	Early
PKS0405-123_21834	04:05:43.3	–11:59:11	0.10005	0.74	3477	Early
PKS0405-123_40354	04:07:14.4	–11:56:39	0.22806	1.56	3515	Late
PKS0405-123_21840	04:06:03.3	–11:59:18	0.12005	0.25	3516	Late
PKS0405-123_30394	04:08:13.3	–12:36:42	0.13847	0.17	3540	Late
PKS0405-123_3406	04:07:10.2	–12:19:13	0.38100	2.89	3562	Late
PKS0405-123_10616	04:08:33.6	–12:12:02	0.43548	4.29	3581	Early
PKS0405-123_10615	04:08:33.8	–12:12:03	0.43530	11.40	3600	Early
PKS0405-123_10136	04:08:52.7	–12:17:39	0.23689	0.73	3618	Late
PKS0405-123_10159	04:08:53.3	–12:17:26	0.23592	1.58	3619	Early
PKS0405-123_30779	04:07:34.3	–12:33:32	0.17105	1.45	3622	Early
PKS0405-123_3253	04:07:15.3	–12:02:55	0.40649	13.03	3640	Early
PKS0405-123_411	04:08:23.5	–12:19:07	0.43391	4.50	3647	Late
PKS0405-123_31286	04:06:54.8	–12:29:23	0.17499	0.65	3695	Late
PKS0405-123_30714	04:07:34.2	–12:34:01	0.17098	1.01	3698	Early
PKS0405-123_11455	04:08:32.1	–12:00:58	0.28960	1.74	3713	Late
PKS0405-123_30693	04:07:34.2	–12:34:13	0.17084	0.99	3728	Late
PKS0405-123_32006	04:07:28.7	–12:24:46	0.33054	2.01	3741	Early
PKS0405-123_31606	04:06:44.8	–12:27:08	0.17816	0.78	3745	Early
PKS0405-123_32058	04:08:11.4	–12:24:35	0.32725	1.90	3757	Early
PKS0405-123_40838	04:07:50.0	–11:53:39	0.23512	1.38	3758	Late
PKS0405-123_31919	04:07:31.8	–12:25:10	0.32876	5.63	3762	Early
PKS0405-123_11333	04:08:23.2	–12:02:45	0.40479	4.21	3770	Early

Table 4—Continued

ID	RA (J2000)	DEC (J2000)	$z_{\rm gal}$	L^a ($L*$)	ρ^b (h_{72}^{-1} kpc)	Type^c
PKS0405-123_31963	04:06:35.7	–12:24:45	0.17763	0.38	3770	Early
PKS0405-123_21409	04:06:17.6	–12:04:21	0.16497	0.46	3772	Late
PKS0405-123_30811	04:07:08.8	–12:33:10	0.16729	0.46	3800	Late
PKS0405-123_31969	04:07:27.8	–12:24:55	0.33317	6.47	3819	Early
PKS0405-123_41580	04:07:49.1	–11:49:07	0.18187	0.37	3854	Late
PKS0405-123_30210	04:07:43.3	–12:37:47	0.15099	4.73	3857	Unkn
PKS0405-123_10833	04:09:20.5	–12:09:56	0.17641	0.48	3864	Late
PKS0405-123_31822	04:06:54.0	–12:25:43	0.21774	2.16	3865	Late
PKS0405-123_118	04:08:31.2	–12:21:21	0.33226	1.74	3874	Early
PKS0405-123_21319	04:05:47.3	–12:05:17	0.12585	0.19	3902	Late
PKS0405-123_3499	04:07:09.3	–12:03:16	0.40877	3.26	3914	Late
PKS0405-123_21459	04:06:30.5	–12:03:48	0.20275	1.35	3916	Early
PKS0405-123_30561	04:08:02.7	–12:35:18	0.17214	0.41	3927	Unkn
PKS0405-123_41676	04:07:14.4	–11:48:16	0.16490	1.77	3931	Late
PKS0405-123_10098	04:09:04.3	–12:18:15	0.21748	0.78	3964	Early
PKS0405-123_10078	04:08:56.8	–12:18:34	0.24533	1.81	3990	Early
PKS0405-123_10074	04:09:04.5	–12:18:38	0.21743	1.69	4002	Early
PKS0405-123_21390	04:05:43.9	–12:04:21	0.12480	1.99	4004	Early
PKS0405-123_11294	04:09:05.2	–12:03:25	0.21041	0.52	4014	Early
PKS0405-123_31265	04:08:05.5	–12:29:52	0.24258	1.23	4016	Early
PKS0405-123_41714	04:07:56.4	–11:48:18	0.18229	0.33	4017	Unkn
PKS0405-123_31721	04:07:54.0	–12:26:40	0.33134	2.78	4034	Early
PKS0405-123_11396	04:08:48.0	–12:01:55	0.26254	1.69	4037	Late
PKS0405-123_11487	04:08:38.2	–12:00:29	0.28979	1.69	4069	Early
PKS0405-123_21391	04:05:42.8	–12:04:21	0.12598	0.58	4069	Early
PKS0405-123_21074	04:06:06.5	–12:08:03	0.16520	0.36	4075	Late
PKS0405-123_30445	04:08:03.8	–12:36:15	0.17140	0.34	4076	Late
PKS0405-123_21296	04:06:05.1	–12:05:38	0.15934	0.43	4078	Late
PKS0405-123_40517	04:07:06.5	–11:55:32	0.24059	0.90	4084	Early
PKS0405-123_33037	04:06:52.2	–12:17:55	0.33444	2.39	4132	Early
PKS0405-123_32168	04:06:37.1	–12:23:28	0.21174	4.71	4135	Early
PKS0405-123_40547	04:07:05.8	–11:55:21	0.24066	1.80	4135	Early
PKS0405-123_41448	04:08:08.6	–11:49:54	0.20198	0.72	4151	Early
PKS0405-123_31723	04:07:44.9	–12:26:36	0.35073	2.03	4161	Early
PKS0405-123_41391	04:08:05.4	–11:50:15	0.21020	0.42	4183	Unkn
PKS0405-123_30965	04:06:47.2	–12:31:47	0.17435	1.24	4191	Late
PKS0405-123_21376	04:05:38.2	–12:04:32	0.12551	0.25	4193	Early
PKS0405-123_21377	04:05:37.8	–12:04:22	0.12510	1.97	4198	Early
PKS0405-123_40652	04:07:31.1	–11:54:39	0.28404	1.92	4200	Late
PKS0405-123_10251	04:08:49.3	–12:16:13	0.32714	2.05	4212	Late
PKS0405-123_40177	04:07:28.0	–11:58:01	0.37967	1.71	4228	Late
PKS0405-123_41422	04:08:04.8	–11:50:04	0.21120	0.76	4228	Early
PKS0405-123_31667	04:07:50.2	–12:27:04	0.34705	1.92	4255	Early
PKS0405-123_31607	04:07:36.4	–12:27:22	0.32901	3.19	4260	Early
PKS0405-123_32194	04:06:47.4	–12:23:19	0.25439	1.43	4261	Early

Table 4—Continued

ID	RA (J2000)	DEC (J2000)	$z_{\rm gal}$	L^a ($L*$)	ρ^b (h_{72}^{-1} kpc)	Type^c
PKS0405-123_21381	04:06:21.0	–12:04:38	0.20164	1.38	4263	Early
PKS0405-123_31005	04:07:11.0	–12:31:39	0.21163	1.00	4271	Early
PKS0405-123_30315	04:08:14.3	–12:37:09	0.17137	0.34	4305	Unkn
PKS0405-123_31300	04:07:52.5	–12:29:34	0.28359	0.92	4314	Late
PKS0405-123_31916	04:07:56.6	–12:25:21	0.42641	3.65	4347	Early
PKS0405-123_31003	04:06:42.2	–12:31:31	0.17814	1.03	4361	Late
PKS0405-123_11089	04:09:02.8	–12:06:18	0.26426	5.69	4412	Early
PKS0405-123_41188	04:06:32.7	–11:51:08	0.16524	0.62	4420	Early
PKS0405-123_42077	04:07:03.6	–11:45:58	0.16456	1.27	4421	Early
PKS0405-123_40308	04:06:55.1	–11:56:57	0.25813	1.78	4439	Late
PKS0405-123_21375	04:06:16.8	–12:04:42	0.20121	0.52	4441	Late
PKS0405-123_20589	04:06:20.8	–12:13:23	0.22543	0.53	4448	Late
PKS0405-123_30944	04:06:35.4	–12:31:52	0.17410	1.54	4510	Early
PKS0405-123_21008	04:06:12.1	–12:08:50	0.20265	0.69	4521	Late
PKS0405-123_40682	04:06:58.3	–11:54:22	0.24049	1.41	4533	Early
PKS0405-123_32976	04:06:36.9	–12:18:11	0.28236	1.73	4551	Late
PKS0405-123_31991	04:07:15.8	–12:24:47	0.38500	2.75	4552	Early
PKS0405-123_40504	04:07:15.0	–11:55:41	0.30794	2.43	4566	Late
PKS0405-123_30761	04:06:35.9	–12:33:22	0.16977	0.89	4588	Late
PKS0405-123_42162	04:06:58.6	–11:45:23	0.16468	1.62	4590	Early
PKS0405-123_21590	04:06:17.6	–12:02:10	0.20302	1.29	4595	Early
PKS0405-123_42163	04:06:58.1	–11:45:17	0.16465	2.83	4612	Early
PKS0405-123_31901	04:06:49.1	–12:25:10	0.26811	1.31	4629	Early
PKS0405-123_10223	04:09:12.0	–12:16:40	0.24476	1.46	4641	Early
PKS0405-123_30908	04:08:13.4	–12:32:37	0.24004	1.71	4658	Early
PKS0405-123_41780	04:08:09.4	–11:48:01	0.21109	1.27	4659	Early
PKS0405-123_40133	04:06:54.9	–11:58:16	0.29540	1.39	4662	Early
PKS0405-123_41685	04:06:37.6	–11:48:05	0.16522	0.35	4669	Late
PKS0405-123_21397	04:06:12.1	–12:04:26	0.20194	0.45	4672	Late
PKS0405-123_20478	04:05:54.4	–12:14:19	0.17325	0.82	4717	Late
PKS0405-123_10298	04:09:14.3	–12:15:50	0.24463	1.62	4719	Late
PKS0405-123_10299	04:09:14.0	–12:15:50	0.24566	1.26	4719	Early
PKS0405-123_30726	04:07:59.1	–12:34:01	0.23976	3.64	4790	Early
PKS0405-123_41111	04:07:06.2	–11:51:45	0.24090	4.09	4791	Early
PKS0405-123_31434	04:07:23.1	–12:28:30	0.32985	1.17	4798	Late
PKS0405-123_20725	04:06:10.9	–12:11:42	0.21813	1.33	4817	Early
PKS0405-123_20722	04:06:29.5	–12:11:49	0.29162	1.41	4823	Early
PKS0405-123_10935	04:08:46.4	–12:08:12	0.45708	4.66	4849	Early
PKS0405-123_30739	04:08:10.5	–12:34:02	0.23631	1.58	4849	Early
PKS0405-123_21122	04:05:36.9	–12:07:22	0.15001	0.45	4850	Late
PKS0405-123_11634	04:08:42.7	–11:58:11	0.30797	2.28	4854	Early
PKS0405-123_41694	04:07:42.1	–11:48:20	0.23431	0.72	4869	Early
PKS0405-123_21382	04:06:21.3	–12:04:38	0.24133	0.79	4874	Late
PKS0405-123_30575	04:07:33.1	–12:35:07	0.22883	0.51	4880	Late
PKS0405-123_21790	04:06:29.5	–11:59:55	0.24109	0.59	4884	Late

Table 4—Continued

ID	RA (J2000)	DEC (J2000)	$z_{\rm gal}$	L^a ($L*$)	ρ^b (h_{72}^{-1} kpc)	Type^c
PKS0405-123_20844	04:06:02.2	–12:10:32	0.20054	1.06	4919	Early
PKS0405-123_11606	04:08:58.4	–11:58:49	0.26378	3.77	4938	Early
PKS0405-123_42990	04:07:56.7	–11:40:32	0.16528	0.84	4941	Late
PKS0405-123_20274	04:05:43.7	–12:16:12	0.16597	0.31	5012	Late
PKS0405-123_10751	04:09:24.1	–12:10:51	0.23735	1.65	5048	Early
PKS0405-123_40606	04:06:46.8	–11:54:57	0.25767	0.90	5076	Late
PKS0405-123_43154	04:07:56.6	–11:39:35	0.16501	0.77	5083	Late
PKS0405-123_42816	04:07:03.2	–11:41:32	0.16497	0.72	5088	Late
PKS0405-123_10532	04:08:52.5	–12:13:11	0.43514	3.99	5101	Early
PKS0405-123_20194	04:06:27.7	–12:17:18	0.28988	1.97	5103	Early
PKS0405-123_31133	04:07:43.4	–12:30:43	0.33092	4.43	5107	Early
PKS0405-123_20259	04:06:12.8	–12:16:32	0.23795	1.02	5150	Late
PKS0405-123_21672	04:06:04.6	–12:01:20	0.20021	0.62	5157	Late
PKS0405-123_11655	04:08:58.6	–12:19:33	0.33286	1.88	5158	Early
PKS0405-123_31795	04:07:05.0	–12:25:58	0.37177	3.70	5172	Early
PKS0405-123_20417	04:06:24.8	–12:15:04	0.29160	1.72	5179	Early
PKS0405-123_40587	04:06:43.7	–11:54:56	0.25794	3.14	5201	Late
PKS0405-123_20664	04:06:22.9	–12:12:30	0.29040	5.01	5216	Early
PKS0405-123_11114	04:09:05.9	–12:06:00	0.31849	3.69	5244	Early
PKS0405-123_20652	04:06:22.4	–12:12:40	0.29028	3.69	5245	Early
PKS0405-123_20776	04:06:21.7	–12:11:19	0.28886	1.42	5261	Late
PKS0405-123_20622	04:06:22.0	–12:12:54	0.29084	4.32	5282	Early
PKS0405-123_20651	04:06:22.2	–12:12:42	0.29348	1.27	5297	Early
PKS0405-123_41874	04:07:03.6	–11:47:11	0.21781	0.53	5305	Late
PKS0405-123_32497	04:06:30.4	–12:21:22	0.28989	3.15	5307	Early
PKS0405-123_11404	04:08:50.5	–12:01:49	0.37820	2.82	5337	Late
PKS0405-123_40871	04:06:58.1	–11:53:13	0.28418	3.29	5347	Early
PKS0405-123_42851	04:08:25.6	–11:41:35	0.18221	4.07	5395	Early
PKS0405-123_43269	04:06:58.1	–11:59:01	0.40516	8.64	5396	Early
PKS0405-123_20610	04:06:22.2	–12:13:06	0.30133	1.29	5399	Late
PKS0405-123_41797	04:07:42.5	–11:47:47	0.26204	2.64	5410	Early
PKS0405-123_41119	04:07:26.1	–11:51:47	0.32452	2.53	5417	Early
PKS0405-123_32318	04:06:40.9	–12:22:32	0.33689	3.55	5418	Early
PKS0405-123_41809	04:07:40.1	–11:47:41	0.26054	1.91	5418	Late
PKS0405-123_41870	04:07:42.8	–11:47:20	0.26029	3.60	5484	Early
PKS0405-123_40685	04:07:31.5	–11:54:31	0.42597	2.28	5498	Late
PKS0405-123_41266	04:06:56.8	–11:50:47	0.25934	1.12	5509	Early
PKS0405-123_30763	04:07:49.8	–12:33:44	0.29978	1.58	5516	Late
PKS0405-123_41265	04:06:56.5	–11:50:47	0.25953	0.98	5518	Early
PKS0405-123_21096	04:06:18.7	–12:07:57	0.28922	2.13	5522	Early
PKS0405-123_21172	04:05:57.7	–12:07:04	0.21785	0.94	5534	Early
PKS0405-123_32012	04:06:30.8	–12:24:26	0.28193	2.96	5551	Early
PKS0405-123_30999	04:06:43.9	–12:31:33	0.24704	1.30	5564	Unkn
PKS0405-123_41998	04:06:58.0	–11:46:20	0.21750	0.62	5568	Early
PKS0405-123_41295	04:07:33.0	–11:50:44	0.32542	2.32	5596	Late

Table 4—Continued

ID	RA (J2000)	DEC (J2000)	$z_{\rm gal}$	L^a ($L*$)	ρ^b (h_{72}^{-1} kpc)	Type^c
PKS0405-123_20504	04:06:02.9	–12:14:09	0.24083	1.12	5640	Late
PKS0405-123_10856	04:09:19.8	–12:09:35	0.29519	1.92	5660	Early
PKS0405-123_20974	04:06:14.0	–12:09:09	0.28270	1.02	5676	Late
PKS0405-123_20849	04:06:05.7	–12:10:29	0.25360	2.36	5685	Early
PKS0405-123_10005	04:08:52.3	–11:58:04	0.34455	3.06	5735	Early
PKS0405-123_42041	04:07:45.3	–11:46:18	0.26195	1.11	5736	Early
PKS0405-123_11141	04:09:20.4	–12:05:45	0.28926	1.19	5774	Late
PKS0405-123_42099	04:07:46.3	–11:46:00	0.26104	2.03	5788	Late
PKS0405-123_32257	04:06:35.3	–12:22:57	0.33656	2.58	5796	Early
PKS0405-123_31170	04:07:58.7	–12:30:35	0.40701	3.25	5824	Early
PKS0405-123_20816	04:06:27.0	–12:10:56	0.37136	2.74	5845	Early
PKS0405-123_32211	04:06:34.7	–12:23:07	0.33649	4.47	5852	Early
PKS0405-123_21112	04:06:13.2	–12:07:43	0.28974	1.34	5870	Late
PKS0405-123_20425	04:06:20.4	–12:14:58	0.32691	2.04	5880	Early
PKS0405-123_20535	04:05:57.2	–12:13:51	0.23839	0.96	5892	Early
PKS0405-123_11592	04:09:11.2	–11:59:00	0.28967	2.64	5904	Early
PKS0405-123_21528	04:05:53.9	–12:02:49	0.21765	3.70	5907	Early
PKS0405-123_42922	04:08:26.2	–11:41:10	0.20231	0.78	5944	Early
PKS0405-123_20949	04:05:48.9	–12:09:20	0.21937	1.45	5944	Early
PKS0405-123_20086	04:05:42.0	–12:18:12	0.20042	1.01	5971	Early
PKS0405-123_20976	04:06:09.1	–12:09:04	0.28334	3.59	5977	Early
PKS0405-123_40696	04:06:49.8	–11:54:14	0.32550	1.69	5992	Late
PKS0405-123_10369	04:09:16.8	–12:15:07	0.33574	2.26	6024	Early
PKS0405-123_20497	04:05:47.0	–12:14:09	0.21864	0.76	6030	Late
PKS0405-123_20577	04:06:12.1	–12:13:27	0.30094	2.79	6030	Early
PKS0405-123_42858	04:06:44.1	–11:41:09	0.18733	0.57	6041	Late
PKS0405-123_42801	04:06:37.0	–11:41:26	0.18419	1.52	6067	Late
PKS0405-123_21485	04:06:14.4	–12:03:19	0.29112	1.19	6084	Early
PKS0405-123_42983	04:06:42.9	–11:40:15	0.18338	0.38	6101	Early
PKS0405-123_40353	04:06:42.7	–11:56:32	0.34481	2.46	6105	Early
PKS0405-123_42425	04:06:40.1	–11:43:38	0.20302	0.61	6126	Late
PKS0405-123_20343	04:06:09.1	–12:15:41	0.29099	1.37	6142	Early
PKS0405-123_20952	04:06:05.7	–12:09:22	0.28328	3.58	6173	Early
PKS0405-123_21564	04:06:14.1	–12:02:28	0.29171	0.89	6183	Late
PKS0405-123_42305	04:07:24.7	–11:44:37	0.26091	1.79	6244	Late
PKS0405-123_42550	04:06:37.9	–11:42:58	0.20313	0.58	6289	Late
PKS0405-123_31340	04:06:46.3	–12:29:04	0.33702	1.30	6303	Late
PKS0405-123_42447	04:07:08.7	–11:43:40	0.24094	0.81	6319	Early
PKS0405-123_30770	04:07:40.9	–12:33:38	0.36965	6.53	6332	Early
PKS0405-123_42060	04:06:39.7	–11:45:56	0.23146	1.00	6385	Late
PKS0405-123_30568	04:07:30.9	–12:35:06	0.33301	2.20	6398	Late
PKS0405-123_10122	04:09:20.3	–12:18:00	0.33506	3.59	6414	Early
PKS0405-123_20999	04:05:42.5	–12:08:46	0.22593	0.94	6414	Late
PKS0405-123_30406	04:07:35.3	–12:36:28	0.31137	1.07	6415	Late
PKS0405-123_41650	04:07:30.5	–11:48:33	0.34593	2.99	6445	Early

Table 4—Continued

ID	RA (J2000)	DEC (J2000)	$z_{\rm gal}$	L^a ($L*$)	ρ^b (h_{72}^{-1} kpc)	Type^c
PKS0405-123_40441	04:06:32.6	–11:55:53	0.32578	4.52	6495	Early
PKS0405-123_41659	04:06:31.7	–11:48:12	0.24364	0.98	6498	Early
PKS0405-123_21399	04:06:16.3	–12:04:26	0.34412	3.29	6593	Early
PKS0405-123_20044	04:05:41.0	–12:18:41	0.22544	0.65	6608	Early
PKS0405-123_42902	04:07:38.3	–11:41:07	0.24615	0.76	6621	Late
PKS0405-123_21109	04:06:12.5	–12:07:44	0.34263	2.32	6623	Early
PKS0405-123_40928	04:06:43.4	–11:52:48	0.33115	2.42	6628	Early
PKS0405-123_10430	04:09:15.9	–12:14:30	0.40271	3.82	6667	Early
PKS0405-123_41821	04:07:52.0	–11:47:41	0.35873	2.47	6729	Early
PKS0405-123_20943	04:06:07.3	–12:09:30	0.32909	1.74	6731	Early
PKS0405-123_20342	04:05:36.1	–12:15:32	0.22601	1.57	6759	Early
PKS0405-123_42350	04:08:19.2	–11:44:30	0.28403	1.98	6768	Early
PKS0405-123_20793	04:06:06.0	–12:11:04	0.33221	2.51	6841	Early
PKS0405-123_20887	04:06:06.1	–12:10:09	0.33198	1.65	6843	Late
PKS0405-123_41908	04:06:50.6	–11:46:54	0.28341	0.93	6857	Late
PKS0405-123_41974	04:06:52.0	–11:46:31	0.28508	1.35	6926	Early
PKS0405-123_20500	04:06:01.6	–12:14:12	0.31674	1.50	6939	Late
PKS0405-123_20095	04:05:55.2	–12:18:13	0.28286	1.36	6952	Early
PKS0405-123_41971	04:07:44.0	–11:46:46	0.35981	2.65	7002	Early
PKS0405-123_21262	04:06:05.5	–12:06:07	0.33125	2.10	7015	Early
PKS0405-123_20165	04:05:55.4	–12:17:27	0.29068	1.68	7036	Early
PKS0405-123_20383	04:05:56.9	–12:15:17	0.30170	1.82	7036	Early
PKS0405-123_42210	04:06:42.3	–11:45:01	0.25946	3.22	7040	Early
PKS0405-123_20307	04:05:56.2	–12:15:59	0.30028	1.08	7085	Late
PKS0405-123_10898	04:09:22.0	–12:09:03	0.40103	5.10	7096	Early
PKS0405-123_21982	04:05:55.2	–12:18:56	0.29087	3.87	7131	Early
PKS0405-123_41858	04:08:06.4	–11:47:32	0.37942	3.01	7135	Early
PKS0405-123_20580	04:06:00.4	–12:13:22	0.32706	1.86	7157	Unkn
PKS0405-123_20188	04:05:52.6	–12:17:10	0.28899	2.09	7159	Early
PKS0405-123_20509	04:05:35.9	–12:13:54	0.24534	2.43	7168	Early
PKS0405-123_21424	04:05:59.6	–12:04:06	0.31011	1.76	7199	Early
PKS0405-123_21633	04:06:18.2	–12:01:47	0.38290	4.40	7204	Early
PKS0405-123_42843	04:07:07.0	–11:41:22	0.26082	0.96	7220	Late
PKS0405-123_20441	04:05:59.7	–12:14:42	0.32655	3.22	7226	Early
PKS0405-123_30375	04:08:00.8	–12:36:44	0.36814	3.02	7233	Early
PKS0405-123_42257	04:06:52.7	–11:44:48	0.28376	2.85	7247	Early
PKS0405-123_41372	04:07:07.2	–11:50:05	0.40679	4.32	7252	Early
PKS0405-123_30180	04:07:19.8	–12:38:02	0.33011	1.25	7287	Late
PKS0405-123_42183	04:06:47.4	–11:45:18	0.28339	2.38	7287	Early
PKS0405-123_42969	04:06:53.9	–11:40:25	0.24267	1.45	7289	Early
PKS0405-123_20466	04:05:58.5	–12:14:26	0.32714	3.89	7303	Early
PKS0405-123_42330	04:06:54.4	–11:44:11	0.28398	10.32	7337	Early
PKS0405-123_41834	04:06:39.9	–11:47:19	0.29606	2.26	7344	Early
PKS0405-123_20050	04:05:56.5	–12:18:43	0.31287	1.65	7408	Early
PKS0405-123_20431	04:05:45.0	–12:14:43	0.28345	1.77	7429	Early

Table 4—Continued

ID	RA (J2000)	DEC (J2000)	$z_{\rm gal}$	L^a ($L*$)	ρ^b (h_{72}^{-1} kpc)	Type^c
PKS0405-123_42733	04:06:46.1	–11:41:53	0.25401	1.10	7434	Late
PKS0405-123_41479	04:07:45.2	–11:49:43	0.49610	6.32	7459	Early
PKS0405-123_20158	04:05:46.5	–12:17:27	0.28597	1.58	7481	Early
PKS0405-123_30617	04:06:44.1	–12:34:34	0.33169	1.75	7483	Late
PKS0405-123_42773	04:07:08.4	–11:41:45	0.28153	4.55	7511	Early
PKS0405-123_41902	04:06:35.5	–11:46:52	0.29573	3.20	7589	Early
PKS0405-123_20424	04:05:41.1	–12:14:48	0.28262	2.18	7646	Early
PKS0405-123_30186	04:08:02.8	–12:38:07	0.36889	4.48	7652	Early
PKS0405-123_42841	04:07:05.9	–11:41:19	0.28197	4.63	7667	Early
PKS0405-123_30397	04:06:51.9	–12:36:19	0.33753	2.78	7688	Early
PKS0405-123_42486	04:07:35.1	–11:43:33	0.34206	3.74	7698	Early
PKS0405-123_42530	04:06:48.1	–11:43:08	0.28419	1.66	7737	Late
PKS0405-123_42645	04:07:34.0	–11:42:39	0.33180	2.43	7794	Early
PKS0405-123_20207	04:05:38.4	–12:16:55	0.27922	4.74	7808	Early
PKS0405-123_20970	04:05:50.5	–12:09:05	0.32874	1.24	7848	Late
PKS0405-123_21102	04:05:51.0	–12:07:47	0.32911	2.34	7856	Early
PKS0405-123_20406	04:05:59.3	–12:15:05	0.37360	1.60	7925	Late
PKS0405-123_21143	04:05:49.1	–12:07:17	0.32769	1.62	7976	Early
PKS0405-123_21666	04:05:58.2	–12:01:21	0.34092	2.00	7994	Late
PKS0405-123_20082	04:05:46.5	–12:18:15	0.31265	2.73	8000	Early
PKS0405-123_21667	04:05:57.7	–12:01:17	0.34160	4.81	8040	Early
PKS0405-123_33059	04:08:10.4	–12:39:28	0.36844	2.93	8118	Late
PKS0405-123_30791	04:07:19.3	–12:39:04	0.37120	2.86	8160	Early
PKS0405-123_42809	04:07:01.8	–11:41:34	0.30759	1.37	8176	Early
PKS0405-123_20482	04:05:46.9	–12:14:18	0.34399	1.61	8335	Late
PKS0405-123_21696	04:05:47.5	–12:00:48	0.31927	3.40	8352	Early
PKS0405-123_43118	04:06:56.0	–11:39:31	0.28591	5.98	8360	Early
PKS0405-123_43083	04:07:12.1	–11:39:44	0.30762	3.89	8411	Early
PKS0405-123_43069	04:08:12.3	–11:40:07	0.32434	1.67	8432	Early
PKS0405-123_43130	04:07:10.6	–11:39:31	0.30748	1.81	8487	Early
PKS0405-123_20693	04:05:35.1	–12:11:56	0.31309	3.22	8555	Early
PKS0405-123_21833	04:05:51.3	–11:59:18	0.33782	1.93	8582	Early
PKS0405-123_43052	04:06:36.8	–11:39:51	0.28380	1.46	8747	Early
PKS0405-123_21915	04:05:43.7	–11:58:16	0.32856	2.93	8994	Early
PKS0405-123_42876	04:08:12.4	–11:41:24	0.38158	1.88	9001	Late
PKS0405-123_42758	04:06:43.3	–11:41:42	0.33100	2.61	9078	Early
PKS0405-123_42737	04:07:08.6	–11:41:58	0.38011	2.95	9116	Early
PKS0405-123_43048	04:07:59.6	–11:40:12	0.38158	2.98	9218	Early
PKS0405-123_43008	04:06:32.5	–11:40:01	0.33145	2.52	9834	Early
PKS0405-123_42982	04:07:33.9	–11:40:30	0.43173	4.15	9859	Early
PKS0405-123_21877	04:05:53.8	–11:58:46	0.43309	2.64	9903	Late
PKS0405-123_21480	04:05:37.9	–12:03:13	0.42616	4.62	10524	Late
PKS0405-123_21907	04:05:52.1	–11:58:23	0.49528	6.72	10860	Early

PKS0405-123: $(z_{\rm em} - 0.01) < z < (z_{\rm em} + 0.01)$

Table 4—Continued

ID	RA (J2000)	DEC (J2000)	$z_{\rm gal}$	L^a ($L*$)	ρ^b (h_{72}^{-1} kpc)	Type^c
PKS0405-123_1163	04:08:05.2	–12:13:25	0.57350	14.88	1683	Early
PKS0558-504: $0.005 < z < (z_{\rm em} - 0.01)$						
PKS0558-504_2349	05:59:35.1	–50:28:45	0.09482	0.17	354	Late
PKS0558-504_2159	05:59:40.0	–50:31:18	0.11618	0.62	566	Early
PKS0558-504_1049	06:00:19.8	–50:16:35	0.05592	0.81	796	Early
PKS0558-504_407	06:00:42.3	–50:31:18	0.05704	0.05	894	Late
PKS0558-504_2990	05:59:13.0	–50:26:46	0.11586	0.25	1010	Late
PKS0558-504_2948	05:59:13.5	–50:29:23	0.11611	1.42	1039	Early
PKS0558-504_1689	05:59:55.9	–50:35:52	0.11530	0.20	1084	Late
PKS0558-504_717	06:00:31.2	–50:30:35	0.11941	0.24	1397	Early
PKS0558-504_3276	05:59:04.1	–50:18:03	0.10833	0.13	1544	Late
PKS0558-504: $(z_{\rm em} - 0.01) < z < (z_{\rm em} + 0.01)$						
PKS0558-504_2156	05:59:41.7	–50:25:48	0.13809	0.33	242	Late
PKS0558-504_2075	05:59:44.9	–50:21:37	0.14643	0.25	756	Late
PKS0558-504_1173	06:00:15.0	–50:22:29	0.13818	2.79	1119	Early
PKS0558-504_2689	05:59:22.9	–50:31:57	0.14662	0.23	1141	Late
PKS0558-504_1664	05:59:56.9	–50:34:31	0.14525	0.52	1143	Early
PKS0558-504_902	06:00:25.0	–50:25:27	0.13882	0.17	1306	Late
PKS0558-504_3144	05:59:06.9	–50:31:02	0.14091	0.48	1520	Late
PG1004+130: $0.005 < z < (z_{\rm em} - 0.01)$						
PG1004+130_1870	10:07:06.5	+12:53:51	0.00922	0.01	74	Late
PG1004+130_1984	10:07:02.7	+12:56:19	0.00898	0.00	97	Early
PG1004+130_1683	10:07:10.9	+12:39:05	0.00968	0.05	117	Early
PG1004+130_1203	10:07:30.7	+12:53:50	0.02967	0.05	168	Late
PG1004+130_2015	10:06:59.9	+12:46:16	0.03041	0.05	241	Unkn
PG1004+130_1061	10:07:34.5	+12:52:09	0.07041	2.40	290	Early
PG1004+130_1408	10:07:22.6	+12:47:10	0.16481	0.71	310	Early
PG1004+130_1459	10:07:21.4	+12:52:11	0.08929	0.12	323	Early
PG1004+130_1351	10:07:25.5	+12:59:11	0.03107	0.05	357	Early
PG1004+130_1504	10:07:20.1	+12:53:24	0.07342	0.11	369	Early
PG1004+130_260	10:08:05.1	+12:56:50	0.03190	0.15	448	Late
PG1004+130_1588	10:07:17.3	+12:53:42	0.11245	0.48	602	Late
PG1004+130_1332	10:07:25.3	+12:53:04	0.16742	3.58	665	Early
PG1004+130_1745	10:07:10.6	+12:50:04	0.19314	1.34	723	Late
PG1004+130_2301	10:06:49.8	+12:49:50	0.07929	0.40	763	Late
PG1004+130_1485	10:07:21.2	+12:56:00	0.12337	0.29	891	Late
PG1004+130_1017	10:07:38.0	+12:55:45	0.12325	0.20	924	Unkn
PG1004+130_695	10:07:49.4	+12:47:23	0.16428	0.45	952	Late

Table 4—Continued

ID	RA (J2000)	DEC (J2000)	$z_{\rm gal}$	L^a ($L*$)	ρ^b (h_{72}^{-1} kpc)	Type^c
PG1004+130_1120	10:07:34.0	+12:54:57	0.16598	0.87	1009	Early
PG1004+130_1567	10:07:16.7	+12:42:33	0.16343	0.84	1068	Early
PG1004+130_1006	10:07:38.4	+12:55:09	0.16469	0.58	1098	Early
PG1004+130_1417	10:07:21.7	+12:42:33	0.19662	0.92	1179	Late
PG1004+130_2118	10:06:56.8	+12:54:29	0.13550	0.57	1236	Late
PG1004+130_827	10:07:44.0	+12:42:34	0.16695	0.78	1245	Late
PG1004+130_595	10:07:53.3	+12:54:18	0.15060	1.28	1275	Late
PG1004+130_722	10:07:49.1	+12:54:48	0.16547	0.84	1307	Late
PG1004+130_1401	10:07:22.1	+12:41:31	0.19874	1.40	1374	Late
PG1004+130_634	10:07:51.1	+12:45:26	0.21372	2.11	1395	Late
PG1004+130_932	10:07:39.7	+12:42:14	0.21410	1.57	1465	Late
PG1004+130_279	10:08:04.2	+12:52:24	0.15028	0.50	1490	Unkn
PG1004+130_576	10:07:53.0	+12:43:17	0.18278	0.76	1512	Early
PG1004+130_403	10:07:58.7	+12:44:23	0.18553	1.10	1627	Late
PG1004+130_914	10:07:40.5	+12:40:42	0.19630	1.58	1637	Early
PG1004+130_982	10:07:39.5	+12:57:31	0.19421	2.02	1667	Early
PG1004+130_756	10:07:48.0	+12:56:47	0.19427	1.27	1732	Early
PG1004+130_831	10:07:45.5	+12:58:42	0.19274	2.93	1959	Early
PG1004+130_2220	10:06:53.7	+12:54:52	0.22018	0.81	1998	Unkn
PG1004+130_411	10:07:57.5	+12:38:34	0.20753	2.69	2471	Early
PG1004+130: $(z_{\rm em}-0.01)<z<(z_{\rm em}+0.01)$						
PG1004+130_1366	10:07:24.2	+12:48:36	0.24264	1.09	120	Early
PG1004+130_1400	10:07:23.0	+12:48:59	0.23979	1.57	165	Early
PG1004+130_1387	10:07:23.2	+12:48:01	0.24796	4.30	250	Early
PG1004+130_1676	10:07:13.6	+12:48:10	0.24774	1.15	695	Early
PG1004+130_1673	10:07:13.2	+12:47:14	0.24829	9.44	791	Early
PG1004+130_1128	10:07:32.7	+12:45:31	0.24671	1.24	823	Early
PG1004+130_876	10:07:42.6	+12:47:56	0.24734	1.71	923	Early
PG1004+130_1780	10:07:09.1	+12:47:42	0.24982	1.30	964	Late
PG1004+130_1797	10:07:08.6	+12:46:43	0.24829	3.01	1067	Early
PG1004+130_1052	10:07:34.9	+12:44:28	0.24752	3.18	1081	Early
PG1004+130_1066	10:07:34.5	+12:44:09	0.24526	1.91	1128	Early
PG1004+130_1917	10:07:04.9	+12:51:10	0.23692	1.99	1210	Early
PG1004+130_1897	10:07:04.8	+12:46:44	0.24923	2.43	1256	Early
PG1004+130_1204	10:07:31.2	+12:55:14	0.24768	1.02	1402	Early
PG1004+130_2046	10:06:59.2	+12:49:33	0.24810	2.88	1467	Late
PG1004+130_636	10:07:52.2	+12:52:31	0.24097	1.89	1588	Early
PG1004+130_2169	10:06:54.9	+12:50:07	0.24808	2.06	1717	Early
PG1004+130_2181	10:06:54.3	+12:49:29	0.24785	2.18	1732	Late
PG1004+130_694	10:07:50.4	+12:57:00	0.24721	3.01	2196	Early
PG1004+130_415	10:08:00.0	+12:56:35	0.24723	1.19	2483	Late
PG1004+130_2444	10:06:45.1	+12:55:09	0.23650	0.84	2518	Late
PG1004+130_365	10:08:00.0	+12:40:22	0.24016	1.73	2561	Late

Table 4—Continued

ID	RA (J2000)	DEC (J2000)	$z_{\rm gal}$	L^a ($L*$)	ρ^b (h_{72}^{-1} kpc)	Type^c
PG1004+130_239	10:08:06.1	+12:57:40	0.24689	3.84	2883	Early
HE1029-140: $0.005 < z < (z_{\rm em} - 0.01)$						
HE1029-140_2238	10:31:41.4	–14:12:49	0.05083	0.03	287	Early
HE1029-140_2254	10:31:40.2	–14:14:01	0.07459	0.79	357	Early
HE1029-140_771	10:32:21.7	–14:11:53	0.07462	0.15	672	Late
HE1029-140_217	10:32:36.9	–14:06:57	0.05430	0.03	860	Unkn
HE1029-140: $(z_{\rm em} - 0.01) < z < (z_{\rm em} + 0.01)$						
HE1029-140_1628	10:31:57.5	–14:15:11	0.08584	0.44	166	Unkn
HE1029-140_1336	10:32:04.4	–14:11:53	0.08646	0.38	506	Late
HE1029-140_541	10:32:28.1	–14:11:51	0.08622	0.14	890	Late
HE1029-140_140	10:32:37.7	–14:15:30	0.08602	0.62	988	Early
PG1116+215: $0.005 < z < (z_{\rm em} - 0.01)$						
PG1116+215_2071	11:19:05.5	+21:17:33	0.06002	0.10	124	Early
PG1116+215_2028	11:19:06.7	+21:18:29	0.13829	2.04	130	Early
PG1116+215_1849	11:19:12.2	+21:18:52	0.16595	0.34	156	Early
PG1116+215_2154	11:19:03.1	+21:16:23	0.05939	0.02	207	Early
PG1116+215_2048	11:19:05.4	+21:15:38	0.05873	0.39	238	Early
PG1116+215_1571	11:19:19.8	+21:22:28	0.06128	0.12	280	Early
PG1116+215_2663	11:18:48.7	+21:14:41	0.04134	0.41	310	Early
PG1116+215_1691	11:19:16.5	+21:18:54	0.16480	0.25	317	Late
PG1116+215_1905	11:19:09.6	+21:11:22	0.04086	0.03	358	Unkn
PG1116+215_1987	11:19:08.9	+21:22:55	0.13440	0.27	485	Late
PG1116+215_808	11:19:38.4	+21:21:42	0.06063	0.24	512	Early
PG1116+215_2081	11:19:05.0	+21:15:03	0.13842	0.80	594	Late
PG1116+215_1152	11:19:29.5	+21:14:56	0.08346	0.17	597	Late
PG1116+215_1312	11:19:24.3	+21:10:30	0.05899	1.42	615	Early
PG1116+215_674	11:19:42.0	+21:26:10	0.06138	0.06	717	Unkn
PG1116+215_2	11:18:29.2	+21:14:00	0.06038	1.32	730	Early
PG1116+215_643	11:19:42.2	+21:17:48	0.08339	0.16	747	Late
PG1116+215_1524	11:19:19.7	+21:11:13	0.08370	0.32	752	Late
PG1116+215_1613	11:19:16.8	+21:14:57	0.16525	1.15	762	Late
PG1116+215_1610	11:19:18.0	+21:15:04	0.16588	2.73	768	Early
PG1116+215_2635	11:18:50.0	+21:16:11	0.13873	0.21	769	Late
PG1116+215_2140	11:19:02.7	+21:09:48	0.09202	0.24	921	Late
PG1116+215_1677	11:19:16.4	+21:13:24	0.16619	0.45	988	Early
PG1116+215_2536	11:18:52.3	+21:12:12	0.13158	0.18	1072	Late
PG1116+215_2498	11:18:53.0	+21:08:32	0.09120	0.51	1089	Early
PG1116+215_1672	11:19:16.3	+21:12:32	0.16628	0.99	1118	Late
PG1116+215_1534	11:19:19.3	+21:12:42	0.16614	1.70	1131	Early

Table 4—Continued

ID	RA (J2000)	DEC (J2000)	$z_{\rm gal}$	L^a ($L*$)	ρ^b (h_{72}^{-1} kpc)	Type^c
PG1116+215_116	11:19:57.4	+21:15:27	0.08967	0.87	1197	Early
PG1116+215_1253	11:19:26.0	+21:12:31	0.16376	5.46	1266	Early
PG1116+215_3236	11:18:32.7	+21:18:14	0.14607	1.19	1298	Late
PG1116+215_2416	11:18:55.4	+21:10:05	0.13412	0.27	1304	Late
PG1116+215_2137	11:19:03.1	+21:11:02	0.16527	3.88	1329	Late
PG1116+215_609	11:19:42.8	+21:14:19	0.13968	0.63	1362	Early
PG1116+215_2851	11:18:43.1	+21:13:05	0.16645	0.77	1421	Late
PG1116+215_429	11:19:47.8	+21:15:44	0.13855	2.59	1426	Early
PG1116+215_3433	11:18:27.4	+21:20:13	0.14536	0.99	1476	Early
PG1116+215_2861	11:18:42.4	+21:10:47	0.14933	2.22	1568	Early
PG1116+215_2251	11:18:59.5	+21:09:38	0.16540	0.39	1575	Late
PG1116+215_15	11:18:26.0	+21:22:53	0.14719	0.21	1622	Late
PG1116+215_656	11:19:41.2	+21:11:52	0.15350	0.19	1645	Late
PG1116+215_1407	11:19:22.8	+21:08:47	0.15313	0.38	1652	Late
PG1116+215_3132	11:18:35.4	+21:12:00	0.16607	0.35	1760	Late
PG1116+215_340	11:19:52.4	+21:25:05	0.16592	0.73	1969	Late
PG1116+215_3508	11:19:59.6	+21:12:10	0.14621	1.08	2091	Late
PG1116+215_118	11:19:57.1	+21:13:01	0.16587	0.63	2172	Early
PG1116+215: $(z_{\rm em}-0.01)<z<(z_{\rm em}+0.01)$						
PG1116+215_1958	11:19:07.8	+21:19:15	0.17744	0.95	35	Early
PG1116+215_2049	11:19:06.4	+21:19:07	0.17503	0.52	97	Early
PG1116+215_2003	11:19:07.8	+21:18:41	0.17707	1.40	109	Early
PG1116+215_1818	11:19:13.2	+21:20:11	0.17584	2.09	239	Early
PG1116+215_1770	11:19:14.1	+21:15:46	0.16695	0.71	605	Early
PG1116+215_2467	11:18:55.0	+21:17:57	0.17405	1.89	608	Early
PG1116+215_1652	11:19:16.7	+21:14:28	0.16696	2.51	836	Early
PG1116+215_1236	11:19:27.7	+21:17:41	0.17601	0.57	837	Early
PG1116+215_1081	11:19:30.6	+21:18:07	0.17692	1.10	939	Early
PG1116+215_1083	11:19:31.4	+21:18:06	0.17571	1.40	970	Late
PG1116+215_1201	11:19:28.3	+21:15:16	0.17188	1.00	1040	Late
PG1116+215_1767	11:19:14.1	+21:12:54	0.16674	0.65	1043	Early
PG1116+215_2528	11:18:52.4	+21:14:31	0.17677	3.03	1052	Early
PG1116+215_2843	11:18:43.3	+21:14:27	0.17651	1.23	1336	Unkn
PG1116+215_2928	11:18:41.3	+21:14:35	0.17577	0.98	1385	Late
PG1116+215_517	11:19:47.1	+21:22:29	0.17428	0.79	1675	Late
PG1116+215_390	11:19:49.5	+21:16:27	0.17410	0.89	1752	Early
PG1116+215_377	11:19:49.6	+21:13:30	0.17372	2.09	1942	Early
PG1116+215_170	11:19:56.4	+21:19:19	0.17355	0.93	1968	Late
PG1116+215_242	11:19:53.6	+21:15:01	0.17362	1.57	1985	Early
PG1116+215_140	11:19:57.2	+21:18:07	0.17408	0.42	2019	Early
PG1116+215_147	11:19:56.5	+21:15:30	0.17445	0.92	2081	Early
PG1116+215_1060	11:19:31.2	+21:08:00	0.17366	0.68	2084	Early
PG1116+215_84	11:19:58.5	+21:16:38	0.17345	1.24	2101	Late

Table 4—Continued

ID	RA (J2000)	DEC (J2000)	$z_{\rm gal}$	L^a ($L*$)	ρ^b (h_{72}^{-1} kpc)	Type^c
PG1116+215_19	11:18:24.5	+21:12:43	0.17686	1.83	2155	Early
PG1116+215_3452	11:18:26.2	+21:11:36	0.17366	0.54	2163	Early
PG1116+215_451	11:19:46.7	+21:09:21	0.17278	0.47	2262	Early
PG1116+215_313	11:19:51.1	+21:09:12	0.17266	1.26	2408	Early
PG1116+215_98	11:19:57.3	+21:08:38	0.17377	0.72	2671	Early
PG1211+143: $0.005 < z < (z_{\rm em} - 0.01)$						
PG1211+143_2215	12:14:13.9	+14:03:31	0.06461	0.08	69	Late
PG1211+143_2360	12:14:09.5	+14:04:21	0.05113	0.83	131	Late
PG1211+143_2503	12:14:19.8	+14:05:10	0.06438	0.74	141	Early
PG1211+143_2409	12:14:06.9	+14:04:38	0.05199	0.09	173	Late
PG1211+143_3249	12:14:06.3	+14:08:54	0.05102	0.08	355	Late
PG1211+143_3512	12:14:13.6	+14:10:22	0.05123	0.22	405	Late
PG1211+143_3234	12:13:57.0	+14:08:54	0.05149	0.40	433	Late
PG1211+143_3602	12:14:01.1	+14:11:07	0.05221	1.21	509	Early
PG1211+143_3700	12:14:00.6	+14:11:39	0.05094	1.62	526	Early
PG1211+143_103	12:14:21.4	+14:13:04	0.04990	0.43	541	Early
PG1211+143_61	12:14:06.2	+14:12:54	0.05081	1.29	562	Early
PG1211+143_3769	12:13:55.5	+14:12:00	0.05032	0.62	573	Early
PG1211+143_3337	12:14:54.8	+14:09:11	0.05100	0.13	616	Early
PG1211+143: $(z_{\rm em} - 0.01) < z < (z_{\rm em} + 0.01)$						
PG1211+143_2014	12:14:25.4	+14:02:25	0.08110	0.08	180	Early
PG1211+143_2681	12:14:24.0	+14:06:00	0.08104	0.07	275	Unkn
PG1211+143_2389	12:14:39.5	+14:04:16	0.08020	0.11	472	Early
PG1211+143_3051	12:14:31.9	+14:07:54	0.08154	0.30	507	Late
PG1211+143_2573	12:14:46.2	+14:05:32	0.08061	1.87	640	Early
PG1211+143_2574	12:14:47.6	+14:05:45	0.08094	4.41	676	Early
PG1211+143_3693	12:14:20.2	+14:11:20	0.08026	0.09	691	Late
PG1211+143_1361	12:14:45.3	+13:58:30	0.08038	1.30	710	Early
PG1211+143_2534	12:14:49.9	+14:05:08	0.08145	1.14	712	Early
PG1211+143_1243	12:14:45.7	+13:58:30	0.08068	1.32	720	Early
PG1211+143_2492	12:14:54.0	+14:04:50	0.08110	0.89	791	Early
PG1211+143_2717	12:14:54.7	+14:06:07	0.08009	0.52	822	Early
PG1216+069: $0.005 < z < (z_{\rm em} - 0.01)$						
PG1216+069_2614	12:19:20.6	+06:42:18	0.00810	0.01	34	Early
PG1216+069_2	12:18:38.6	+06:42:29	0.00667	0.03	86	Early
PG1216+069_2476	12:19:23.4	+06:38:20	0.12410	0.65	88	Late
PG1216+069_3477	12:19:03.7	+06:33:43	0.01318	0.01	98	Early
PG1216+069_2980	12:19:14.5	+06:35:33	0.08048	0.06	295	Early
PG1216+069_2671	12:19:20.3	+06:36:57	0.24641	1.76	363	Early

Table 4—Continued

ID	RA (J2000)	DEC (J2000)	$z_{\rm gal}$	L^a ($L*$)	ρ^b (h_{72}^{-1} kpc)	Type^c
PG1216+069_2002	12:19:32.7	+06:41:57	0.08053	0.06	379	Early
PG1216+069_2990	12:19:14.4	+06:37:02	0.17980	0.49	384	Late
PG1216+069_3311	12:19:08.6	+06:39:09	0.12458	0.30	389	Late
PG1216+069_2079	12:19:30.8	+06:43:34	0.08047	2.25	471	Late
PG1216+069_2283	12:19:27.3	+06:44:03	0.08056	0.10	481	Early
PG1216+069_3351	12:19:08.0	+06:38:31	0.18038	0.61	549	Late
PG1216+069_3398	12:19:06.4	+06:39:28	0.18099	2.39	632	Late
PG1216+069_1916	12:19:33.8	+06:42:44	0.12497	1.79	657	Early
PG1216+069_1551	12:19:40.2	+06:40:41	0.13536	2.21	706	Early
PG1216+069_3846	12:18:59.0	+06:40:53	0.12508	0.69	742	Late
PG1216+069_3829	12:18:58.7	+06:35:23	0.11843	0.70	770	Late
PG1216+069_4320	12:18:48.1	+06:33:40	0.08076	0.12	817	Late
PG1216+069_3057	12:19:13.1	+06:44:58	0.12482	3.79	832	Early
PG1216+069_1972	12:19:33.1	+06:40:25	0.28000	0.81	846	Late
PG1216+069_3582	12:19:04.0	+06:41:35	0.19168	1.14	920	Unkn
PG1216+069_1506	12:19:41.2	+06:41:19	0.17983	1.12	978	Late
PG1216+069_1499	12:19:40.1	+06:32:01	0.11914	2.33	984	Late
PG1216+069_1882	12:19:34.8	+06:40:55	0.27950	1.83	991	Late
PG1216+069_2623	12:19:21.8	+06:46:44	0.12312	0.27	1004	Early
PG1216+069_4236	12:18:50.5	+06:40:08	0.13728	1.59	1051	Late
PG1216+069_538	12:19:57.7	+06:29:26	0.07657	0.07	1057	Late
PG1216+069_3730	12:19:00.5	+06:34:30	0.17881	0.36	1107	Late
PG1216+069_1063	12:19:48.5	+06:31:38	0.11905	0.62	1183	Late
PG1216+069_3918	12:18:57.2	+06:34:49	0.17841	0.64	1186	Late
PG1216+069_2452	12:19:23.6	+06:33:46	0.29445	1.59	1207	Early
PG1216+069_2155	12:19:28.3	+06:28:59	0.12284	0.68	1213	Early
PG1216+069_3140	12:19:11.2	+06:34:03	0.29339	1.87	1270	Early
PG1216+069_3411	12:19:06.5	+06:34:51	0.29705	1.49	1288	Early
PG1216+069_4155	12:18:51.9	+06:32:34	0.13848	0.81	1293	Late
PG1216+069_4529	12:18:43.6	+06:36:58	0.13839	0.34	1294	Early
PG1216+069_766	12:19:54.5	+06:38:28	0.16128	1.90	1307	Late
PG1216+069_1310	12:19:44.1	+06:30:30	0.13441	0.44	1334	Late
PG1216+069_1022	12:19:50.9	+06:45:41	0.13545	0.58	1386	Late
PG1216+069_533	12:19:58.7	+06:34:16	0.13756	0.30	1418	Late
PG1216+069_999	12:19:50.3	+06:36:55	0.20613	1.20	1429	Late
PG1216+069_3235	12:19:09.2	+06:31:45	0.21534	0.82	1462	Late
PG1216+069_4176	12:18:51.3	+06:30:31	0.13475	0.42	1468	Late
PG1216+069_3602	12:19:03.0	+06:34:38	0.29511	1.66	1477	Early
PG1216+069_4274	12:18:49.5	+06:36:29	0.20417	1.56	1524	Early
PG1216+069_1192	12:19:46.7	+06:38:17	0.27821	1.21	1533	Late
PG1216+069_3474	12:19:03.8	+06:34:00	0.29585	0.79	1554	Late
PG1216+069_3125	12:19:11.3	+06:31:03	0.21557	1.30	1555	Late
PG1216+069_3476	12:19:04.9	+06:33:39	0.29447	3.92	1569	Early
PG1216+069_663	12:19:55.5	+06:28:07	0.11952	0.50	1644	Late
PG1216+069_2220	12:19:27.6	+06:31:49	0.27661	2.21	1651	Early

Table 4—Continued

ID	RA (J2000)	DEC (J2000)	$z_{\rm gal}$	L^a ($L*$)	ρ^b (h_{72}^{-1} kpc)	Type^c
PG1216+069_1178	12:19:46.6	+06:36:01	0.28083	2.62	1653	Early
PG1216+069_366	12:20:01.9	+06:34:49	0.15706	0.38	1665	Late
PG1216+069_1005	12:19:50.6	+06:42:27	0.22449	2.86	1689	Early
PG1216+069_4626	12:18:41.4	+06:36:49	0.17825	2.92	1691	Late
PG1216+069_894	12:19:53.4	+06:48:18	0.13505	1.06	1694	Late
PG1216+069_975	12:19:51.0	+06:38:22	0.27857	1.56	1787	Early
PG1216+069_700	12:19:56.8	+06:43:14	0.19223	0.83	1807	Early
PG1216+069_2189	12:19:27.8	+06:27:50	0.17480	0.45	1813	Late
PG1216+069_4749	12:18:38.7	+06:36:00	0.17751	0.39	1826	Unkn
PG1216+069_2066	12:19:30.4	+06:31:14	0.27562	0.98	1828	Late
PG1216+069_1166	12:19:46.7	+06:33:48	0.26803	0.77	1856	Late
PG1216+069_2521	12:19:23.6	+06:47:00	0.28006	0.90	1996	Early
PG1216+069_917	12:19:51.3	+06:32:38	0.23669	2.09	2036	Early
PG1216+069_2349	12:19:24.7	+06:30:00	0.27940	1.56	2061	Early
PG1216+069_4257	12:18:49.9	+06:35:23	0.29549	2.36	2071	Early
PG1216+069_264	12:20:03.8	+06:34:23	0.20634	1.14	2186	Early
PG1216+069_550	12:19:58.1	+06:33:45	0.23420	1.31	2195	Late
PG1216+069_2301	12:19:25.4	+06:30:08	0.31406	4.84	2205	Early
PG1216+069_1277	12:19:44.2	+06:31:55	0.29762	1.44	2209	Early
PG1216+069_4432	12:18:45.2	+06:29:52	0.19086	0.46	2227	Late
PG1216+069_4513	12:18:43.3	+06:30:22	0.19194	0.28	2235	Late
PG1216+069_1275	12:19:44.6	+06:31:48	0.29750	1.89	2245	Early
PG1216+069_1371	12:19:42.8	+06:31:15	0.29687	1.72	2276	Early
PG1216+069_2040	12:19:30.6	+06:29:38	0.29815	4.01	2313	Early
PG1216+069_3936	12:18:56.4	+06:31:18	0.29791	1.21	2367	Late
PG1216+069_2755	12:19:17.8	+06:28:32	0.27950	1.40	2401	Late
PG1216+069_480	12:20:00.4	+06:41:45	0.27469	1.95	2430	Late
PG1216+069_3999	12:18:55.0	+06:30:53	0.29325	4.46	2474	Early
PG1216+069_2704	12:19:21.0	+06:48:54	0.31385	2.88	2645	Early
PG1216+069_1076	12:19:48.1	+06:29:24	0.28373	0.98	2750	Early
PG1216+069_4315	12:18:48.1	+06:30:39	0.29345	2.26	2808	Late
PG1216+069_884	12:19:52.0	+06:30:07	0.29788	1.76	2864	Early
PG1216+069_379	12:20:01.4	+06:31:39	0.29665	1.31	3045	Early
PG1216+069_243	12:20:03.9	+06:30:27	0.28295	1.85	3238	Early
PG1216+069: $(z_{\rm em}-0.01) < z < (z_{\rm em}+0.01)$						
PG1216+069_2916	12:19:15.5	+06:36:02	0.33306	8.00	781	Early
PG1216+069_2911	12:19:15.9	+06:35:51	0.33228	1.48	813	Early
PG1216+069_3161	12:19:10.8	+06:35:11	0.33484	3.64	1144	Early
PG1216+069_2859	12:19:16.6	+06:33:50	0.32583	5.27	1297	Early
PG1216+069_2110	12:19:29.8	+06:34:11	0.33666	1.59	1339	Late
PG1216+069_3978	12:18:56.5	+06:39:34	0.32433	1.75	1617	Early
PG1216+069_2296	12:19:27.5	+06:44:31	0.33240	1.98	1636	Early
PG1216+069_2087	12:19:29.9	+06:32:43	0.33212	1.67	1691	Early

Table 4—Continued

ID	RA (J2000)	DEC (J2000)	$z_{\rm gal}$	L^a ($L*$)	ρ^b (h_{72}^{-1} kpc)	Type^c
PG1216+069_3783	12:19:00.3	+06:42:59	0.32284	1.86	1766	Early
PG1216+069_1996	12:19:31.7	+06:32:21	0.33161	1.00	1828	Late
PG1216+069_3698	12:19:01.1	+06:33:12	0.33327	2.47	1965	Early
PG1216+069_679	12:19:56.7	+06:38:34	0.32236	2.07	2350	Early
PG1216+069_3083	12:19:10.6	+06:29:41	0.32227	1.10	2437	Late
PG1216+069_1851	12:19:33.9	+06:29:52	0.32253	2.20	2447	Early
PG1216+069_4377	12:18:48.0	+06:43:23	0.32365	2.85	2491	Late
PG1216+069_307	12:20:03.0	+06:34:55	0.32353	6.07	2934	Early
3C273: $0.005 < z < (z_{\rm em} - 0.01)$						
3C273_5268	12:29:50.5	+02:01:54	0.00621	0.01	79	Early
3C273_288	12:28:30.4	+02:06:30	0.03285	0.15	355	Early
3C273_3806	12:28:51.8	+02:06:03	0.09023	1.11	443	Early
3C273_4002	12:28:48.5	+02:08:26	0.07777	0.17	574	Late
3C273_3400	12:28:58.5	+01:55:05	0.07478	0.05	661	Late
3C273_1930	12:29:23.0	+01:53:03	0.07776	0.04	897	Late
3C273_1958	12:29:24.1	+02:08:12	0.14637	2.02	957	Late
3C273_1991	12:29:23.2	+02:08:22	0.14681	0.34	960	Late
3C273_2500	12:29:12.9	+01:51:10	0.07816	0.07	999	Early
3C273_1429	12:29:31.8	+01:57:50	0.14026	0.17	1140	Early
3C273_787	12:29:41.3	+01:50:56	0.07759	0.17	1231	Late
3C273_259	12:28:25.6	+01:58:40	0.11979	0.24	1354	Early
3C273_404	12:29:48.0	+01:53:29	0.10272	0.30	1496	Early
3C273: $(z_{\rm em} - 0.01) < z < (z_{\rm em} + 0.01)$						
3C273_2747	12:29:11.6	+02:03:13	0.15846	0.90	191	Early
3C273_3356	12:28:59.9	+02:01:54	0.15969	0.88	322	Early
3C273_3774	12:28:52.2	+01:59:11	0.15836	0.30	821	Late
3C273_4085	12:28:45.9	+01:59:42	0.15823	0.88	953	Late
3C273_4287	12:28:42.4	+02:07:50	0.15881	1.33	1177	Early
3C273_1231	12:29:35.4	+02:06:07	0.15876	0.31	1193	Early
3C273_2557	12:29:11.8	+01:55:25	0.15813	4.29	1198	Early
3C273_1104	12:29:37.5	+02:02:37	0.16496	0.34	1222	Late
3C273_4806	12:28:32.5	+02:03:45	0.15921	0.44	1316	Late
3C273_5055	12:28:30.8	+01:59:29	0.15910	0.40	1489	Late
3C273_289	12:28:27.2	+02:02:49	0.15903	4.92	1516	Early
3C273_4931	12:28:30.4	+02:08:37	0.15785	1.23	1616	Early
3C273_4998	12:28:29.2	+02:08:12	0.15847	0.78	1629	Early
3C273_360	12:29:49.1	+02:00:53	0.15761	3.41	1656	Early
3C273_4153	12:28:44.3	+01:53:44	0.15756	0.38	1668	Early
3C273_70	12:28:23.7	+02:07:09	0.15764	1.06	1750	Late
3C273_97	12:28:24.7	+02:08:48	0.16041	0.91	1846	Early
3C273_122	12:28:23.9	+02:10:00	0.16006	1.32	1961	Late

Table 4—Continued

ID	RA (J2000)	DEC (J2000)	$z_{\rm gal}$	L^a ($L*$)	ρ^b (h_{72}^{-1} kpc)	Type^c
3C273_454	12:29:47.3	+01:54:03	0.15776	1.49	2081	Early
Q1230+0947: $0.005 < z < (z_{\rm em} - 0.01)$						
Q1230+0947_1752	12:33:14.6	+09:30:45	0.01181	0.00	39	Late
Q1230+0947_1485	12:33:23.8	+09:32:27	0.09052	0.09	112	Early
Q1230+0947_1396	12:33:26.9	+09:33:35	0.09071	0.14	211	Early
Q1230+0947_1266	12:33:30.2	+09:31:49	0.20680	1.88	227	Early
Q1230+0947_1533	12:33:22.0	+09:33:03	0.12543	0.65	241	Late
Q1230+0947_1459	12:33:24.7	+09:33:28	0.12552	0.32	267	Late
Q1230+0947_1398	12:33:26.7	+09:33:47	0.12447	0.67	303	Early
Q1230+0947_1347	12:33:28.1	+09:32:47	0.25025	1.15	334	Late
Q1230+0947_1345	12:33:27.4	+09:26:01	0.06088	0.12	353	Early
Q1230+0947_1407	12:33:26.3	+09:34:19	0.12469	0.74	369	Early
Q1230+0947_856	12:33:42.3	+09:25:27	0.04664	0.02	370	Early
Q1230+0947_1406	12:33:26.3	+09:34:27	0.12488	2.68	386	Early
Q1230+0947_1893	12:33:09.8	+09:29:41	0.10451	0.87	465	Early
Q1230+0947_1158	12:33:33.5	+09:30:08	0.25164	3.63	507	Early
Q1230+0947_637	12:33:49.2	+09:26:13	0.06128	0.04	517	Late
Q1230+0947_1648	12:33:19.8	+09:39:38	0.05849	0.04	533	Early
Q1230+0947_1707	12:33:16.0	+09:31:09	0.29048	1.85	596	Early
Q1230+0947_1597	12:33:19.2	+09:27:32	0.14578	0.29	597	Early
Q1230+0947_1676	12:33:17.5	+09:35:22	0.14708	0.28	647	Late
Q1230+0947_958	12:33:39.5	+09:30:13	0.20027	0.87	671	Early
Q1230+0947_1980	12:33:06.6	+09:24:43	0.07924	0.27	687	Early
Q1230+0947_922	12:33:40.5	+09:29:11	0.20462	0.82	809	Late
Q1230+0947_1917	12:33:09.1	+09:29:15	0.19947	0.61	861	Late
Q1230+0947_1152	12:33:33.0	+09:21:31	0.08454	0.08	890	Late
Q1230+0947_1755	12:33:14.8	+09:34:18	0.26395	1.66	913	Early
Q1230+0947_1972	12:33:07.7	+09:31:31	0.22460	3.65	913	Early
Q1230+0947_356	12:33:59.7	+09:37:05	0.09061	0.21	968	Early
Q1230+0947_1923	12:33:09.9	+09:38:19	0.12791	0.23	1023	Late
Q1230+0947_1984	12:33:06.4	+09:24:10	0.11737	1.56	1032	Early
Q1230+0947_876	12:33:41.6	+09:28:32	0.25183	2.34	1074	Early
Q1230+0947_787	12:33:45.2	+09:30:01	0.25132	1.30	1112	Early
Q1230+0947_1798	12:33:11.6	+09:21:40	0.10538	0.95	1118	Early
Q1230+0947_889	12:33:42.4	+09:37:54	0.14803	0.91	1121	Late
Q1230+0947_1248	12:33:31.3	+09:36:34	0.23683	2.97	1128	Early
Q1230+0947_2054	12:33:05.2	+09:29:03	0.22375	1.94	1136	Early
Q1230+0947_1566	12:33:21.6	+09:39:42	0.14419	0.36	1187	Late
Q1230+0947_2052	12:33:05.1	+09:28:23	0.22249	2.30	1196	Early
Q1230+0947_713	12:33:47.3	+09:29:28	0.25049	1.47	1252	Early
Q1230+0947_1982	12:33:07.8	+09:34:40	0.26499	1.69	1271	Early
Q1230+0947_743	12:33:47.3	+09:38:24	0.14843	0.36	1284	Late
Q1230+0947_2653	12:32:47.7	+09:35:13	0.12742	0.27	1308	Late

Table 4—Continued

ID	RA (J2000)	DEC (J2000)	$z_{\rm gal}$	L^a ($L*$)	ρ^b (h_{72}^{-1} kpc)	Type^c
Q1230+0947_2632	12:32:48.6	+09:35:28	0.12901	0.28	1310	Late
Q1230+0947_1174	12:33:32.2	+09:24:56	0.23106	1.18	1371	Early
Q1230+0947_2100	12:33:03.6	+09:27:07	0.22435	0.92	1412	Early
Q1230+0947_2133	12:33:02.5	+09:27:21	0.22245	1.00	1418	Early
Q1230+0947_2179	12:33:01.1	+09:27:39	0.22283	1.09	1446	Late
Q1230+0947_2759	12:32:43.3	+09:24:59	0.11551	0.21	1453	Early
Q1230+0947_947	12:33:39.4	+09:25:37	0.25237	1.34	1476	Early
Q1230+0947_1741	12:33:15.5	+09:38:14	0.22909	0.83	1502	Late
Q1230+0947_1236	12:33:31.9	+09:38:39	0.22489	2.08	1506	Early
Q1230+0947_823	12:33:43.0	+09:22:57	0.16640	0.57	1511	Late
Q1230+0947_1782	12:33:14.4	+09:38:14	0.22899	1.14	1521	Early
Q1230+0947_504	12:33:53.8	+09:27:28	0.20662	0.58	1523	Late
Q1230+0947_925	12:33:40.3	+09:25:27	0.25122	1.58	1528	Late
Q1230+0947_757	12:33:45.1	+09:21:50	0.14643	1.19	1536	Late
Q1230+0947_325	12:34:00.8	+09:35:32	0.16748	1.06	1553	Early
Q1230+0947_1693	12:33:15.9	+09:24:04	0.22512	1.07	1559	Early
Q1230+0947_2230	12:32:59.3	+09:27:08	0.22572	1.19	1593	Late
Q1230+0947_2463	12:32:53.1	+09:33:42	0.20655	0.78	1609	Late
Q1230+0947_2231	12:32:58.9	+09:27:01	0.22373	4.81	1613	Early
Q1230+0947_3	12:32:44.6	+09:22:05	0.11526	3.19	1621	Late
Q1230+0947_1049	12:33:36.9	+09:37:13	0.30342	6.95	1626	Early
Q1230+0947_2519	12:32:51.5	+09:32:50	0.20750	0.83	1653	Unkn
Q1230+0947_2416	12:32:54.3	+09:32:33	0.23291	0.90	1654	Late
Q1230+0947_1042	12:33:36.4	+09:25:23	0.30593	1.49	1657	Late
Q1230+0947_2275	12:32:59.5	+09:41:00	0.14560	0.26	1663	Late
Q1230+0947_1498	12:33:22.3	+09:22:38	0.20678	1.92	1666	Early
Q1230+0947_555	12:33:52.0	+09:25:11	0.20131	1.17	1674	Late
Q1230+0947_2754	12:32:43.6	+09:26:14	0.14787	0.30	1697	Early
Q1230+0947_463	12:33:54.8	+09:27:25	0.23310	4.10	1718	Early
Q1230+0947_605	12:33:50.9	+09:30:04	0.33493	2.92	1727	Early
Q1230+0947_2351	12:32:56.1	+09:26:55	0.22430	1.11	1747	Early
Q1230+0947_2618	12:32:48.3	+09:30:10	0.20711	2.15	1795	Late
Q1230+0947_443	12:33:55.4	+09:26:55	0.23353	1.89	1798	Early
Q1230+0947_2222	12:32:59.4	+09:25:12	0.22646	0.90	1839	Early
Q1230+0947_2458	12:32:52.5	+09:27:40	0.22590	1.06	1846	Early
Q1230+0947_2190	12:33:00.2	+09:23:51	0.20558	2.35	1862	Early
Q1230+0947_2660	12:32:47.6	+09:34:07	0.20621	0.65	1877	Early
Q1230+0947_2168	12:33:01.6	+09:26:40	0.29502	2.16	1887	Late
Q1230+0947_410	12:33:56.6	+09:26:24	0.23302	0.86	1908	Late
Q1230+0947_152	12:34:06.9	+09:32:16	0.20227	1.91	1927	Late
Q1230+0947_2130	12:33:03.7	+09:39:57	0.20752	2.48	1939	Early
Q1230+0947_490	12:33:53.9	+09:25:31	0.25107	1.39	2013	Early
Q1230+0947_2238	12:32:58.4	+09:22:57	0.20697	2.04	2059	Early
Q1230+0947_246	12:34:02.3	+09:22:08	0.16568	0.91	2066	Late
Q1230+0947_256	12:34:03.7	+09:37:12	0.20144	1.48	2070	Early

Table 4—Continued

ID	RA (J2000)	DEC (J2000)	$z_{\rm gal}$	L^a ($L*$)	ρ^b (h_{72}^{-1} kpc)	Type^c
Q1230+0947_93	12:34:09.4	+09:34:42	0.20227	0.94	2125	Late
Q1230+0947_202	12:34:05.4	+09:37:05	0.20475	0.82	2152	Early
Q1230+0947_2419	12:32:53.4	+09:24:28	0.22514	1.69	2155	Early
Q1230+0947_2702	12:32:45.1	+09:25:01	0.20560	0.72	2263	Early
Q1230+0947_2552	12:32:51.1	+09:38:17	0.23568	2.90	2325	Early
Q1230+0947_718	12:33:48.1	+09:39:00	0.30711	2.21	2396	Late
Q1230+0947_2606	12:32:49.5	+09:38:25	0.23637	3.17	2410	Late
Q1230+0947_2799	12:34:11.9	+09:37:40	0.20202	3.39	2447	Early
Q1230+0947_38	12:34:12.6	+09:38:18	0.20332	1.02	2546	Late
Q1230+0947_1650	12:34:08.2	+09:27:56	0.29503	2.07	2751	Early
Q1230+0947_111	12:34:08.1	+09:32:00	0.32098	3.87	2773	Early
Q1230+0947_2398	12:32:54.2	+09:24:41	0.35030	3.63	2863	Early
Q1230+0947_36	12:34:11.8	+09:31:48	0.33288	1.99	3085	Late
PKS1302-102: $0.005 < z < (z_{\rm em} - 0.01)$						
PKS1302-102_2033	13:05:32.1	–10:33:56	0.09358	0.19	65	Early
PKS1302-102_1909	13:05:35.3	–10:33:24	0.14530	0.40	83	Late
PKS1302-102_1926	13:05:34.9	–10:34:22	0.19171	0.89	209	Early
PKS1302-102_2447	13:05:20.2	–10:36:30	0.04256	2.58	212	Late
PKS1302-102_2415	13:05:22.6	–10:34:48	0.09328	0.13	291	Early
PKS1302-102_2226	13:05:25.6	–10:39:23	0.04196	0.33	294	Late
PKS1302-102_1027	13:05:58.0	–10:24:50	0.02521	0.01	300	Late
PKS1302-102_2886	13:05:09.1	–10:34:22	0.04674	0.03	311	Early
PKS1302-102_2435	13:05:20.9	–10:34:51	0.09393	5.38	330	Early
PKS1302-102_1576	13:05:43.7	–10:37:22	0.06468	0.05	338	Early
PKS1302-102_2391	13:05:23.7	–10:30:25	0.09331	0.32	360	Late
PKS1302-102_1821	13:05:38.1	–10:31:42	0.22557	0.89	417	Early
PKS1302-102_2051	13:05:31.2	–10:35:42	0.19239	1.53	434	Early
PKS1302-102_2376	13:05:24.2	–10:22:19	0.03655	0.09	456	Early
PKS1302-102_2232	13:05:26.4	–10:35:19	0.19296	0.69	464	Late
PKS1302-102_1712	13:05:41.0	–10:26:42	0.06523	1.95	484	Early
PKS1302-102_2649	13:05:14.8	–10:40:00	0.05687	1.12	499	Early
PKS1302-102_2055	13:05:30.6	–10:36:55	0.13927	0.94	503	Early
PKS1302-102_1664	13:05:42.1	–10:31:33	0.19361	2.22	521	Early
PKS1302-102_2189	13:05:28.5	–10:26:29	0.07120	0.60	526	Early
PKS1302-102_2790	13:05:12.1	–10:34:21	0.09531	0.12	527	Early
PKS1302-102_2063	13:05:30.3	–10:26:17	0.07179	2.40	541	Early
PKS1302-102_1708	13:05:40.1	–10:36:54	0.14292	2.05	564	Early
PKS1302-102_2685	13:05:14.5	–10:37:04	0.09258	0.75	574	Early
PKS1302-102_5	13:04:54.6	–10:39:58	0.04576	0.09	588	Early
PKS1302-102_1375	13:05:49.0	–10:35:04	0.15882	0.61	673	Early
PKS1302-102_2867	13:05:09.2	–10:36:51	0.09523	1.14	684	Early
PKS1302-102_2682	13:05:15.6	–10:27:50	0.09442	1.14	685	Early
PKS1302-102_2143	13:05:28.6	–10:38:14	0.13843	1.20	691	Early

Table 4—Continued

ID	RA (J2000)	DEC (J2000)	$z_{\rm gal}$	L^a ($L*$)	ρ^b (h_{72}^{-1} kpc)	Type^c
PKS1302-102_1711	13:05:41.5	–10:26:24	0.09332	0.22	702	Late
PKS1302-102_2193	13:05:28.4	–10:25:15	0.09402	2.03	795	Early
PKS1302-102_1685	13:05:43.7	–10:25:53	0.10624	0.42	861	Early
PKS1302-102_1920	13:05:34.0	–10:39:59	0.14536	1.07	953	Late
PKS1302-102_1921	13:05:33.3	–10:40:06	0.14500	2.15	966	Late
PKS1302-102_1398	13:05:47.5	–10:41:36	0.11599	0.28	1066	Late
PKS1302-102_1253	13:05:52.3	–10:30:33	0.22690	4.36	1134	Early
PKS1302-102_1238	13:05:53.3	–10:24:07	0.10674	0.87	1149	Late
PKS1302-102_1970	13:05:35.5	–10:28:04	0.27511	1.73	1241	Late
PKS1302-102_107	13:06:21.4	–10:30:37	0.10819	1.05	1374	Early
PKS1302-102_768	13:06:03.8	–10:27:12	0.14202	1.51	1375	Early
PKS1302-102_2000	13:05:34.5	–10:23:15	0.13857	0.27	1379	Late
PKS1302-102_3298	13:04:59.0	–10:39:06	0.13850	0.26	1408	Early
PKS1302-102_1564	13:05:45.5	–10:23:21	0.14685	2.26	1501	Early
PKS1302-102_3074	13:05:05.3	–10:30:20	0.22772	1.39	1538	Early
PKS1302-102_152	13:06:20.7	–10:27:53	0.11608	0.65	1543	Early
PKS1302-102_171	13:06:19.5	–10:34:42	0.13839	1.77	1605	Early
PKS1302-102_3152	13:05:03.0	–10:30:10	0.22584	3.01	1648	Early
PKS1302-102_3208	13:05:01.9	–10:30:19	0.22687	3.70	1695	Early
PKS1302-102_1413	13:05:47.3	–10:40:09	0.25398	1.26	1711	Late
PKS1302-102_1006	13:05:55.8	–10:44:34	0.13790	1.71	1721	Early
PKS1302-102_2573	13:05:18.8	–10:24:06	0.25012	1.61	2161	Early
PKS1302-102_3314	13:04:58.5	–10:38:38	0.24942	4.92	2212	Early
PKS1302-102_2510	13:05:20.7	–10:23:27	0.24852	3.97	2250	Early
PKS1302-102_4	13:04:56.0	–10:29:18	0.27252	4.61	2347	Early
PKS1302-102_2378	13:05:24.9	–10:22:38	0.24786	1.59	2364	Late
PKS1302-102_2726	13:05:14.5	–10:23:07	0.24873	2.93	2441	Early
PKS1302-102_2832	13:05:12.1	–10:23:01	0.24892	3.64	2518	Early
PKS1302-102_2973	13:05:08.4	–10:23:08	0.24882	1.46	2595	Early
PKS1302-102_179	13:06:20.0	–10:26:11	0.24866	4.15	2998	Early
PKS1302-102: $(z_{\rm em} - 0.01) < z < (z_{\rm em} + 0.01)$						
PKS1302-102_1346	13:05:49.2	–10:37:48	0.27732	1.47	1432	Early
PKS1302-102_1587	13:05:44.7	–10:26:50	0.27849	3.21	1684	Early
PKS1302-102_1227	13:05:52.1	–10:38:53	0.27933	1.59	1743	Late
PKS1302-102_3089	13:05:03.9	–10:40:32	0.27789	1.66	2420	Early
PG1307+085: $0.005 < z < (z_{\rm em} - 0.01)$						
PG1307+085_1831	13:09:44.2	+08:20:04	0.12762	2.85	93	Early
PG1307+085_769	13:10:14.0	+08:18:59	0.03373	0.02	257	Late
PG1307+085_1993	13:09:39.9	+08:21:09	0.12794	0.99	283	Early
PG1307+085_1188	13:10:02.0	+08:18:46	0.08716	0.09	357	Early
PG1307+085_2494	13:09:25.0	+08:22:15	0.06835	0.06	440	Early

Table 4—Continued

ID	RA (J2000)	DEC (J2000)	$z_{\rm gal}$	L^a ($L*$)	ρ^b (h_{72}^{-1} kpc)	Type^c
PG1307+085_2318	13:09:29.9	+08:18:11	0.09287	0.18	442	Early
PG1307+085_2281	13:09:31.8	+08:23:26	0.08652	0.19	475	Late
PG1307+085_813	13:10:13.1	+08:24:02	0.08772	1.56	716	Early
PG1307+085_852	13:10:11.2	+08:13:45	0.08711	0.29	782	Early
PG1307+085_1409	13:09:54.8	+08:11:50	0.09227	0.22	790	Early
PG1307+085_2237	13:09:33.8	+08:28:20	0.08552	0.14	821	Late
PG1307+085_1129	13:10:02.8	+08:12:02	0.09275	0.16	843	Early
PG1307+085_2406	13:09:28.6	+08:28:10	0.08650	1.94	866	Early
PG1307+085_2126	13:09:34.8	+08:13:31	0.12666	0.34	886	Early
PG1307+085_385	13:10:25.1	+08:22:45	0.09149	0.35	951	Early
PG1307+085_693	13:10:14.5	+08:12:41	0.09277	0.94	957	Late
PG1307+085_1749	13:09:45.3	+08:12:03	0.12700	1.67	989	Early
PG1307+085_258	13:10:28.3	+08:20:07	0.09253	0.21	997	Early
PG1307+085_213	13:10:29.0	+08:20:36	0.09187	1.60	1010	Early
PG1307+085_152	13:10:31.0	+08:21:13	0.09149	1.50	1060	Early
PG1307+085_137	13:10:31.7	+08:22:12	0.09150	0.86	1092	Early
PG1307+085_109	13:10:31.9	+08:20:28	0.09569	2.60	1118	Early
PG1307+085_95	13:10:32.4	+08:22:34	0.09531	2.59	1157	Early
PG1307+085_32	13:10:35.3	+08:22:21	0.09701	0.28	1243	Late
PG1307+085_2792	13:09:15.1	+08:24:31	0.14375	0.24	1306	Late
PG1307+085_2766	13:09:15.0	+08:14:38	0.14034	0.89	1318	Early
PG1307+085_2839	13:09:12.6	+08:14:16	0.13967	0.47	1408	Early
PG1307+085: $(z_{\rm em}-0.01)<z<(z_{\rm em}+0.01)$						
PG1307+085_1675	13:09:48.4	+08:19:41	0.15304	3.77	57	Early
PG1307+085_1816	13:09:45.0	+08:19:27	0.15242	1.02	89	Early
PG1307+085_1601	13:09:51.1	+08:19:29	0.15336	1.42	163	Early
PG1307+085_1726	13:09:47.3	+08:18:37	0.15365	0.79	178	Early
PG1307+085_1930	13:09:41.9	+08:20:15	0.15234	1.35	200	Early
PG1307+085_1665	13:09:49.6	+08:21:30	0.15407	0.44	272	Late
PG1307+085_1491	13:09:54.0	+08:20:18	0.15563	0.61	276	Early
PG1307+085_1873	13:09:56.0	+08:20:05	0.15089	0.61	335	Late
PG1307+085_1343	13:09:57.5	+08:20:19	0.15272	1.37	399	Early
PG1307+085_1773	13:09:46.2	+08:23:35	0.15250	2.51	561	Early
PG1307+085_2408	13:09:27.4	+08:18:17	0.15320	0.97	761	Early
PG1307+085_874	13:10:10.9	+08:18:09	0.15000	0.33	908	Late
PG1307+085_561	13:10:20.1	+08:22:25	0.15275	1.50	1290	Early
PG1307+085_952	13:10:07.6	+08:10:38	0.15477	2.76	1581	Early
MRK1383: $0.005<z<(z_{\rm em}-0.01)$						
MRK1383_2416	14:28:58.4	+01:13:05	0.02994	0.02	150	Late
MRK1383_438	14:29:42.4	+01:17:50	0.02811	0.01	286	Early
MRK1383_899	14:29:33.8	+01:15:10	0.06748	0.09	515	Unkn

Table 4—Continued

ID	RA (J2000)	DEC (J2000)	$z_{\rm gal}$	L^a ($L*$)	ρ^b (h_{72}^{-1} kpc)	Type^c
MRK1383: $(z_{\rm em}-0.01) < z < (z_{\rm em}+0.01)$						
MRK1383_1589	14:29:17.7	+01:21:00	0.08414	0.37	427	Early
MRK1383_1549	14:29:17.1	+01:08:12	0.08585	0.17	837	Early
Q1553+113: $0.005 < z < (z_{\rm em}-0.01)$						
Q1553+113_2068	15:55:39.0	+11:01:57	0.01507	0.00	163	Late
Q1553+113_1294	15:55:58.0	+11:11:45	0.04168	0.28	174	Early
Q1553+113_2842	15:55:21.0	+11:13:57	0.03953	0.01	265	Early
Q1553+113_2546	15:55:28.5	+11:16:02	0.04208	0.07	274	Late
Q1553+113_2794	15:55:21.1	+11:08:39	0.04493	0.28	302	Late
Q1553+113_2711	15:55:24.6	+11:13:44	0.06286	0.06	349	Early
Q1553+113_2228	15:55:37.0	+11:20:39	0.03552	0.04	371	Early
Q1553+113_138	15:56:27.1	+11:02:51	0.02370	0.01	373	Early
Q1553+113_2548	15:55:29.0	+11:20:04	0.03609	0.02	376	Early
Q1553+113_1683	15:55:49.4	+11:09:11	0.14667	0.25	392	Late
Q1553+113_2790	15:55:22.7	+11:18:10	0.04234	0.03	396	Late
Q1553+113_2595	15:55:27.0	+11:11:40	0.10571	0.57	435	Early
Q1553+113_2608	15:55:26.5	+11:11:55	0.10567	1.00	449	Late
Q1553+113_2215	15:55:36.8	+11:12:43	0.26180	1.50	461	Early
Q1553+113_2336	15:55:33.3	+11:09:48	0.16606	0.35	461	Unkn
Q1553+113_3321	15:55:08.9	+11:06:52	0.04466	0.02	475	Unkn
Q1553+113_2884	15:55:19.3	+11:07:26	0.07075	0.33	537	Early
Q1553+113_1941	15:55:42.8	+11:07:40	0.15197	1.85	551	Early
Q1553+113_4	15:55:00.7	+11:04:26	0.04052	1.14	568	Early
Q1553+113_762	15:56:12.1	+11:13:36	0.07095	0.08	576	Early
Q1553+113_2424	15:55:31.7	+11:12:29	0.21654	1.32	594	Early
Q1553+113_2458	15:55:30.8	+11:11:51	0.21626	0.40	602	Late
Q1553+113_738	15:56:12.7	+11:14:12	0.07124	0.30	604	Late
Q1553+113_2351	15:55:32.3	+11:03:37	0.07085	0.04	622	Early
Q1553+113_1872	15:55:44.6	+11:08:53	0.31491	1.48	654	Late
Q1553+113_2033	15:55:41.9	+11:15:54	0.15220	0.71	669	Late
Q1553+113_1221	15:56:00.5	+11:13:57	0.13503	2.42	681	Late
Q1553+113_1251	15:55:59.2	+11:08:49	0.15152	2.47	710	Early
Q1553+113_1489	15:55:52.5	+11:02:18	0.07124	0.56	714	Early
Q1553+113_2453	15:55:30.3	+11:10:15	0.25550	1.29	745	Early
Q1553+113_2923	15:55:18.3	+11:08:48	0.11502	0.72	782	Early
Q1553+113_3523	15:55:04.5	+11:16:43	0.07224	0.08	846	Early
Q1553+113_3513	15:55:03.5	+11:05:03	0.06738	0.12	847	Unkn
Q1553+113_1590	15:55:51.9	+11:15:36	0.19000	2.09	847	Late
Q1553+113_1175	15:56:01.3	+11:15:53	0.13441	3.26	857	Early
Q1553+113_3657	15:55:00.2	+11:07:13	0.07137	0.22	873	Early
Q1553+113_2501	15:55:29.5	+11:10:22	0.30435	1.54	888	Early

Table 4—Continued

ID	RA (J2000)	DEC (J2000)	$z_{\rm gal}$	L^a ($L*$)	ρ^b (h_{72}^{-1} kpc)	Type^c
Q1553+113_3696	15:54:59.1	+11:07:22	0.07176	1.33	893	Early
Q1553+113_907	15:56:08.4	+11:11:09	0.15256	0.48	945	Late
Q1553+113_3493	15:55:04.5	+11:09:14	0.09487	0.65	972	Early
Q1553+113_1421	15:55:55.9	+11:15:59	0.18762	1.54	987	Late
Q1553+113_2576	15:55:27.5	+11:11:26	0.31467	2.67	996	Early
Q1553+113_2125	15:55:37.9	+11:03:50	0.13309	0.81	1015	Late
Q1553+113_3682	15:54:59.0	+11:03:56	0.07187	0.87	1019	Early
Q1553+113_2910	15:55:19.0	+11:10:05	0.17622	0.26	1025	Late
Q1553+113_2932	15:55:18.3	+11:14:50	0.15182	3.64	1043	Early
Q1553+113_3049	15:55:15.7	+11:13:20	0.15187	0.41	1048	Early
Q1553+113_1645	15:55:51.0	+11:17:29	0.17599	0.93	1072	Early
Q1553+113_2607	15:55:26.4	+11:08:52	0.25496	0.67	1076	Late
Q1553+113_2139	15:55:37.5	+11:02:10	0.11591	0.10	1096	Late
Q1553+113_350	15:56:22.4	+11:12:44	0.10911	3.35	1111	Late
Q1553+113_2992	15:55:17.1	+11:13:08	0.18572	0.28	1164	Late
Q1553+113_1989	15:55:43.2	+11:16:37	0.26175	0.75	1181	Early
Q1553+113_202	15:56:26.4	+11:12:40	0.10931	0.12	1222	Unkn
Q1553+113_1074	15:56:02.0	+11:01:22	0.10787	1.03	1226	Late
Q1553+113_3032	15:55:16.3	+11:18:49	0.12284	1.53	1232	Early
Q1553+113_1441	15:55:54.1	+11:04:13	0.17716	1.36	1290	Early
Q1553+113_142	15:56:28.3	+11:14:59	0.10571	0.28	1291	Early
Q1553+113_1375	15:55:55.7	+11:04:14	0.17619	0.24	1310	Late
Q1553+113_3336	15:55:09.6	+11:18:11	0.12362	1.09	1337	Early
Q1553+113_1008	15:56:05.7	+11:12:47	0.26605	0.64	1339	Late
Q1553+113_2782	15:55:21.7	+11:05:58	0.18837	1.28	1339	Early
Q1553+113_42	15:56:31.3	+11:12:40	0.10820	0.52	1345	Early
Q1553+113_3379	15:55:08.6	+11:18:14	0.12338	0.11	1361	Late
Q1553+113_3314	15:55:10.2	+11:18:56	0.12304	0.44	1378	Late
Q1553+113_3413	15:55:07.6	+11:18:19	0.12383	1.03	1398	Late
Q1553+113_2517	15:55:30.1	+11:22:11	0.13402	1.04	1499	Early
Q1553+113_1224	15:56:00.7	+11:15:11	0.31395	1.13	1505	Late
Q1553+113_911	15:56:08.7	+11:12:49	0.26650	0.59	1512	Late
Q1553+113_3713	15:54:59.9	+11:16:32	0.12823	0.24	1528	Late
Q1553+113_2148	15:55:39.0	+11:19:45	0.19629	0.35	1533	Late
Q1553+113_2374	15:55:32.2	+11:06:25	0.34666	3.66	1553	Early
Q1553+113_3375	15:55:07.9	+11:12:08	0.19138	1.46	1569	Early
Q1553+113_3588	15:55:02.6	+11:10:21	0.16552	0.74	1609	Early
Q1553+113_2695	15:55:25.6	+11:19:55	0.18475	0.57	1661	Late
Q1553+113_887	15:56:08.0	+11:03:47	0.20414	1.03	1851	Early
Q1553+113_3003	15:55:15.6	+11:04:04	0.20892	0.36	1913	Late
Q1553+113_777	15:56:11.8	+11:15:30	0.27901	2.71	1965	Early
Q1553+113_297	15:56:24.3	+11:13:57	0.21568	0.62	2087	Late
Q1553+113_2792	15:55:20.8	+11:01:19	0.20074	1.26	2130	Early
Q1553+113_1118	15:56:01.2	+11:00:31	0.20442	1.84	2217	Early
Q1553+113_1880	15:55:43.7	+11:02:22	0.29952	1.40	2250	Late

Table 4—Continued

ID	RA (J2000)	DEC (J2000)	$z_{\rm gal}$	L^a ($L*$)	ρ^b (h_{72}^{-1} kpc)	Type^c
Q1553+113_3338	15:55:09.1	+11:11:54	0.32875	1.65	2251	Early
Q1553+113_390	15:56:21.6	+11:10:36	0.27872	2.70	2299	Early
Q1553+113_771	15:56:10.4	+11:01:13	0.20413	1.13	2304	Early
Q1553+113_1825	15:55:45.0	+11:02:01	0.29881	1.19	2337	Early
Q1553+113_638	15:56:15.7	+11:18:19	0.25317	2.32	2370	Early
Q1553+113_3220	15:55:11.0	+11:05:59	0.30099	1.30	2412	Late
Q1553+113_2431	15:55:32.2	+11:21:25	0.28032	4.46	2469	Early
Q1553+113_3229	15:55:10.1	+11:00:54	0.20098	0.74	2473	Late
Q1553+113_900	15:56:07.9	+11:04:24	0.33651	1.48	2524	Late
Q1553+113_3255	15:55:10.2	+11:05:25	0.29963	0.99	2525	Late
Q1553+113_233	15:56:25.4	+11:09:59	0.27886	2.19	2538	Early
Q1553+113_1322	15:55:56.8	+11:01:37	0.30008	2.17	2587	Early
Q1553+113_1232	15:55:58.8	+11:01:40	0.29950	5.77	2614	Early
Q1553+113_1139	15:56:01.0	+11:01:30	0.30196	2.17	2721	Early
Q1553+113_1288	15:55:57.4	+11:01:45	0.33635	7.51	2778	Early
Q1553+113_976	15:56:05.6	+11:01:37	0.29919	1.05	2812	Early
Q1553+113_452	15:56:20.6	+11:18:50	0.28001	2.51	2852	Late
Q1553+113_217	15:56:25.8	+11:05:13	0.26839	2.97	2853	Early
Q1553+113_482	15:56:20.1	+11:17:31	0.31428	2.44	2866	Early
Q1553+113_453	15:56:19.5	+11:04:57	0.33639	1.73	3012	Early
Q1553+113_396	15:56:20.7	+11:05:05	0.33600	1.64	3059	Early
Q1553+113_3056	15:55:16.3	+11:21:05	0.32308	2.84	3084	Early
Q1553+113_3825	15:56:29.5	+11:04:00	0.26876	1.90	3182	Early
Q1553+113: $(z_{\rm em}-0.01) < z < (z_{\rm em}+0.01)$						
Q1553+113_2006	15:55:41.1	+11:03:52	0.35777	4.00	2117	Early
PKS2005-489: $0.005 < z < (z_{\rm em}-0.01)$						
PKS2005-489_1929	20:09:40.0	–48:44:44	0.05725	0.24	393	Early
PKS2005-489_7288	20:09:17.5	–48:55:55	0.05773	0.02	397	Early
PKS2005-489_3830	20:08:51.2	–48:51:04	0.05767	0.03	540	Early
PKS2005-489_4260	20:10:04.7	–48:49:57	0.05811	0.74	619	Late
PKS2005-489_3950	20:08:31.8	–48:50:37	0.04445	0.07	657	Early
PKS2005-489_5645	20:09:05.4	–49:00:16	0.05726	0.05	715	Unkn
PKS2005-489_6563	20:10:12.8	–48:57:52	0.04801	0.04	753	Unkn
PKS2005-489_5764	20:10:20.4	–48:58:52	0.04754	0.76	857	Early
PKS2005-489_3636	20:08:28.3	–48:51:34	0.05777	0.03	901	Unkn
PKS2005-489: $(z_{\rm em}-0.01) < z < (z_{\rm em}+0.01)$						
PKS2005-489_4566	20:09:25.3	–48:49:06	0.07042	0.42	60	Early
PKS2005-489_4514	20:09:31.5	–48:49:12	0.07191	0.12	130	Early
PKS2005-489_4342	20:09:32.4	–48:49:39	0.07019	0.18	133	Early

Table 4—Continued

ID	RA (J2000)	DEC (J2000)	$z_{\rm gal}$	L^a ($L*$)	ρ^b (h_{72}^{-1} kpc)	Type^c
PKS2005-489_4903	20:09:41.8	–48:48:12	0.07146	0.04	339	Early
PKS2005-489_2650	20:09:42.9	–48:47:18	0.07233	0.07	393	Early
PKS2005-489_4399	20:09:46.6	–48:49:38	0.07175	0.05	407	Early
PKS2005-489_2678	20:09:47.3	–48:47:02	0.07114	0.37	469	Late
PKS2005-489_7207	20:09:16.9	–48:55:45	0.07702	0.13	509	Late
PKS2005-489_4270	20:08:55.7	–48:49:51	0.07159	0.10	566	Early
PKS2005-489_2025	20:08:55.0	–48:45:00	0.06411	0.12	623	Early
PKS2005-489_6431	20:09:34.4	–48:57:46	0.07126	2.92	624	Early
PKS2005-489_2089	20:10:01.5	–48:45:16	0.06495	0.40	709	Late
PKS2005-489_2442	20:08:44.4	–48:46:22	0.07062	0.57	817	Early
PKS2005-489_3065	20:10:06.6	–48:53:25	0.07031	0.39	819	Early
PKS2005-489_3225	20:08:42.5	–48:52:39	0.07702	1.26	904	Early
PKS2005-489_2281	20:10:18.4	–48:46:11	0.07009	0.26	1032	Early
PKS2005-489_4473	20:08:27.9	–48:49:07	0.07123	0.29	1094	Early
PKS2005-489_1224	20:10:18.1	–48:43:19	0.06969	0.10	1098	Late
PKS2005-489_6310	20:10:13.1	–48:58:42	0.07156	0.07	1133	Late
PKS2005-489_2944	20:08:30.7	–48:53:29	0.07722	0.26	1157	Late
PKS2005-489_4761	20:08:24.9	–48:48:20	0.07160	0.97	1161	Early
PKS2005-489_2463	20:08:24.2	–48:46:33	0.07083	0.04	1185	Unkn
PKS2005-489_4475	20:08:27.1	–48:49:00	0.07734	0.04	1197	Unkn
FJ2155-0922: $0.005 < z < (z_{\rm em} - 0.01)$						
FJ2155-0922_1734	21:54:59.9	–09:22:24	0.08098	0.87	33	Early
FJ2155-0922_1474	21:55:06.5	–09:23:25	0.13262	1.63	212	Late
FJ2155-0922_2091	21:54:50.8	–09:22:33	0.07880	0.16	222	Late
FJ2155-0922_1682	21:55:01.6	–09:20:47	0.15553	0.44	246	Early
FJ2155-0922_1847	21:54:56.6	–09:18:07	0.05165	1.43	251	Early
FJ2155-0922_2033	21:54:52.2	–09:24:37	0.08080	0.07	272	Early
FJ2155-0922_1845	21:54:56.8	–09:27:24	0.05037	0.04	282	Early
FJ2155-0922_2226	21:54:47.5	–09:22:54	0.07765	0.52	289	Late
FJ2155-0922_2225	21:54:47.3	–09:23:05	0.07791	0.05	297	Late
FJ2155-0922_2103	21:54:50.9	–09:20:03	0.07942	0.07	298	Early
FJ2155-0922_1109	21:55:16.4	–09:24:07	0.07376	0.45	323	Early
FJ2155-0922_1202	21:55:14.1	–09:24:34	0.08157	0.20	329	Early
FJ2155-0922_1935	21:54:54.9	–09:23:30	0.17636	2.40	331	Early
FJ2155-0922_1527	21:55:05.0	–09:24:25	0.15815	0.50	336	Late
FJ2155-0922_2019	21:54:53.0	–09:22:03	0.16723	0.55	343	Late
FJ2155-0922_841	21:55:22.7	–09:23:51	0.06004	1.75	357	Early
FJ2155-0922_825	21:55:24.1	–09:23:16	0.05896	1.37	365	Early
FJ2155-0922_840	21:55:23.0	–09:24:13	0.05937	3.30	365	Early
FJ2155-0922_1987	21:54:52.6	–09:26:28	0.07963	0.32	389	Early
FJ2155-0922_846	21:55:23.8	–09:25:25	0.05809	0.02	400	Early
FJ2155-0922_1217	21:55:13.7	–09:18:05	0.07458	0.87	420	Early
FJ2155-0922_2411	21:54:43.1	–09:19:48	0.07838	0.05	438	Early

Table 4—Continued

ID	RA (J2000)	DEC (J2000)	$z_{\rm gal}$	L^a ($L*$)	ρ^b (h_{72}^{-1} kpc)	Type[c]
FJ2155-0922_1497	21:55:06.0	–09:25:09	0.15554	0.70	446	Late
FJ2155-0922_1070	21:55:17.3	–09:17:51	0.07339	3.74	471	Early
FJ2155-0922_1802	21:54:58.4	–09:18:56	0.13541	0.48	478	Early
FJ2155-0922_1795	21:54:58.0	–09:28:30	0.07691	0.09	501	Early
FJ2155-0922_1134	21:55:15.8	–09:27:21	0.07769	0.26	503	Early
FJ2155-0922_864	21:55:23.6	–09:19:06	0.07369	0.04	507	Early
FJ2155-0922_2238	21:54:47.0	–09:28:01	0.07359	0.34	523	Early
FJ2155-0922_2234	21:54:47.9	–09:17:18	0.08199	0.38	530	Late
FJ2155-0922_2957	21:54:26.2	–09:21:49	0.05813	0.05	556	Early
FJ2155-0922_493	21:55:31.7	–09:26:37	0.05939	0.10	557	Early
FJ2155-0922_2031	21:54:53.1	–09:15:58	0.07811	0.79	560	Late
FJ2155-0922_465	21:55:32.4	–09:29:06	0.05013	0.20	561	Unkn
FJ2155-0922_1453	21:55:07.9	–09:13:23	0.05871	1.10	583	Early
FJ2155-0922_218	21:55:38.3	–09:23:37	0.05898	0.17	594	Early
FJ2155-0922_1851	21:54:56.3	–09:29:17	0.08070	0.15	596	Early
FJ2155-0922_2727	21:54:33.2	–09:23:31	0.08006	0.11	605	Early
FJ2155-0922_1119	21:55:16.1	–09:29:09	0.07749	0.12	630	Early
FJ2155-0922_2425	21:54:42.3	–09:21:54	0.13248	0.30	636	Early
FJ2155-0922_2426	21:54:42.5	–09:21:12	0.13220	0.29	645	Late
FJ2155-0922_3021	21:54:23.2	–09:30:04	0.04927	0.04	661	Early
FJ2155-0922_1106	21:55:16.3	–09:29:22	0.07971	0.12	665	Unkn
FJ2155-0922_2480	21:54:41.6	–09:15:46	0.07545	0.21	665	Early
FJ2155-0922_394	21:55:33.6	–09:29:26	0.05819	0.03	673	Late
FJ2155-0922_299	21:55:35.6	–09:29:08	0.05749	0.45	678	Early
FJ2155-0922_879	21:55:22.3	–09:29:07	0.07636	0.36	689	Early
FJ2155-0922_1691	21:55:01.8	–09:14:03	0.07896	0.10	698	Early
FJ2155-0922_2801	21:54:31.1	–09:18:23	0.07732	0.07	703	Early
FJ2155-0922_1832	21:54:57.2	–09:26:55	0.15791	0.33	708	Late
FJ2155-0922_1659	21:55:02.5	–09:13:54	0.07955	0.37	716	Late
FJ2155-0922_2284	21:54:46.9	–09:14:31	0.07862	0.12	723	Early
FJ2155-0922_2670	21:54:35.8	–09:18:37	0.09376	0.30	726	Late
FJ2155-0922_2239	21:54:46.4	–09:30:11	0.07963	0.62	727	Late
FJ2155-0922_2136	21:54:49.0	–09:30:47	0.07779	0.14	736	Late
FJ2155-0922_400	21:55:34.0	–09:19:35	0.08104	0.12	737	Early
FJ2155-0922_297	21:55:36.2	–09:20:17	0.07805	0.50	740	Early
FJ2155-0922_1017	21:55:18.6	–09:23:02	0.18130	0.97	741	Late
FJ2155-0922_2689	21:54:34.6	–09:16:32	0.07854	1.57	742	Early
FJ2155-0922_2896	21:54:28.4	–09:18:49	0.07764	0.09	742	Early
FJ2155-0922_2576	21:54:39.1	–09:15:32	0.07950	0.11	745	Early
FJ2155-0922_2612	21:54:37.2	–09:15:34	0.07813	4.85	757	Early
FJ2155-0922_1871	21:54:56.9	–09:13:13	0.07834	0.36	768	Early
FJ2155-0922_870	21:55:22.7	–09:30:00	0.07864	0.13	772	Early
FJ2155-0922_1668	21:55:00.6	–09:31:28	0.08306	2.98	793	Early
FJ2155-0922_3043	21:54:23.2	–09:14:22	0.05897	1.27	798	Early
FJ2155-0922_2921	21:54:27.0	–09:26:15	0.08080	0.05	804	Early

Table 4—Continued

ID	RA (J2000)	DEC (J2000)	$z_{\rm gal}$	L^a ($L*$)	ρ^b (h_{72}^{-1} kpc)	Type^c
FJ2155-0922_769	21:55:25.0	–09:30:19	0.07835	0.14	817	Early
FJ2155-0922_1848	21:54:56.4	–09:28:28	0.13463	0.33	827	Late
FJ2155-0922_1401	21:55:08.1	–09:31:54	0.08156	0.15	829	Early
FJ2155-0922_1295	21:55:10.8	–09:32:07	0.07850	0.24	830	Early
FJ2155-0922_544	21:55:29.9	–09:29:38	0.07758	1.46	833	Early
FJ2155-0922_2620	21:54:37.7	–09:14:03	0.07867	0.06	854	Early
FJ2155-0922_2800	21:54:30.9	–09:22:11	0.11735	0.39	908	Early
FJ2155-0922_2222	21:54:47.1	–09:28:28	0.13557	0.69	947	Late
FJ2155-0922_2081	21:54:50.9	–09:29:17	0.13635	0.19	995	Late
FJ2155-0922_533	21:55:30.7	–09:23:58	0.13590	1.71	1006	Late
FJ2155-0922_3117	21:54:20.9	–09:29:20	0.07860	0.20	1022	Unkn
FJ2155-0922_1950	21:54:53.7	–09:30:04	0.13503	3.50	1058	Early
FJ2155-0922_2459	21:54:40.8	–09:29:07	0.13573	0.47	1140	Early
FJ2155-0922_2881	21:54:28.8	–09:17:40	0.12045	0.40	1148	Late
FJ2155-0922_547	21:55:31.4	–09:16:09	0.12759	0.20	1246	Early
FJ2155-0922_596	21:55:29.9	–09:18:48	0.16637	0.22	1272	Late
FJ2155-0922_213	21:55:38.9	–09:18:32	0.13540	0.16	1363	Late
FJ2155-0922_2770	21:54:31.4	–09:26:27	0.17112	0.94	1392	Late
FJ2155-0922_3127	21:54:20.8	–09:26:00	0.15062	0.28	1583	Early
FJ2155-0922_192	21:55:39.8	–09:14:52	0.13431	0.47	1626	Late
FJ2155-0922_229	21:55:37.4	–09:31:37	0.13502	1.10	1724	Early
FJ2155-0922_782	21:55:26.2	–09:12:53	0.16758	0.29	1822	Late
FJ2155-0922: $(z_{\rm em}-0.01)<z<(z_{\rm em}+0.01)$						
FJ2155-0922_1719	21:55:00.5	–09:22:49	0.19223	0.59	85	Late
FJ2155-0922_2316	21:54:45.2	–09:22:42	0.19229	1.20	732	Early
FJ2155-0922_2317	21:54:44.7	–09:22:39	0.19202	1.18	752	Early
FJ2155-0922_912	21:55:21.9	–09:23:23	0.19489	0.62	945	Late
FJ2155-0922_2589	21:54:38.3	–09:19:47	0.19677	0.57	1160	Late
FJ2155-0922_480	21:55:32.5	–09:22:05	0.19577	2.44	1412	Early
FJ2155-0922_2684	21:54:35.0	–09:18:18	0.19590	2.33	1414	Early
FJ2155-0922_2743	21:54:33.1	–09:18:36	0.19717	0.58	1471	Late
FJ2155-0922_504	21:55:31.8	–09:18:42	0.19546	2.46	1532	Early
FJ2155-0922_2269	21:54:47.5	–09:14:43	0.19656	0.40	1540	Late
FJ2155-0922_2610	21:54:38.1	–09:15:06	0.19790	0.62	1715	Late
FJ2155-0922_133	21:55:40.9	–09:20:48	0.19273	1.64	1792	Early
FJ2155-0922_1291	21:55:11.8	–09:12:34	0.19681	8.41	1859	Early
FJ2155-0922_2605	21:54:38.2	–09:13:59	0.19755	1.66	1871	Late
FJ2155-0922_2599	21:54:38.6	–09:13:48	0.19699	0.31	1887	Late
FJ2155-0922_404	21:55:33.3	–09:31:41	0.19311	0.39	2198	Early
PKS2155-304: $0.005<z<(z_{\rm em}-0.01)$						
PKS2155-304_2668	21:58:30.5	–30:11:02	0.01694	0.00	113	Early

Table 4—Continued

ID	RA (J2000)	DEC (J2000)	$z_{\rm gal}$	L^a ($L*$)	ρ^b (h_{72}^{-1} kpc)	Type^c
PKS2155-304_2204	21:58:40.8	–30:19:27	0.05705	1.59	406	Early
PKS2155-304_2878	21:58:23.6	–30:17:57	0.04587	0.11	420	Early
PKS2155-304_1153	21:59:08.2	–30:20:54	0.04540	1.14	424	Unkn
PKS2155-304_1862	21:58:49.5	–30:20:32	0.06771	0.15	513	Early
PKS2155-304_2860	21:58:23.8	–30:19:31	0.05407	2.05	544	Early
PKS2155-304_3	21:58:11.4	–30:19:08	0.04528	1.48	576	Late
PKS2155-304_1266	21:59:06.0	–30:18:07	0.09522	0.84	577	Early
PKS2155-304_1135	21:59:09.5	–30:19:21	0.07553	0.11	590	Early
PKS2155-304_2959	21:58:20.9	–30:17:29	0.06758	0.20	630	Late
PKS2155-304_3101	21:58:17.4	–30:20:29	0.06794	0.05	807	Late
PKS2155-304_2476	21:58:34.6	–30:23:02	0.07473	0.04	832	Early
PKS2155-304_838	21:59:16.4	–30:19:29	0.10475	0.41	924	Early
PKS2155-304_1875	21:58:52.2	–30:04:44	0.10586	0.10	952	Early
PKS2155-304_2255	21:58:40.3	–30:22:31	0.10560	0.40	1025	Early
PKS2155-304_3032	21:58:18.7	–30:19:16	0.10585	0.19	1094	Late
PKS2155-304: $(z_{\rm em}-0.01)<z<(z_{\rm em}+0.01)$						
PKS2155-304_1790	21:58:53.3	–30:13:44	0.11706	0.50	55	Early
PKS2155-304_1792	21:58:53.3	–30:14:29	0.11504	0.21	125	Early
PKS2155-304_2009	21:58:48.1	–30:14:20	0.11712	0.19	148	Early
PKS2155-304_1785	21:58:52.3	–30:15:24	0.11611	2.54	225	Early
PKS2155-304_1638	21:58:57.5	–30:12:04	0.12109	0.19	247	Early
PKS2155-304_1517	21:59:00.2	–30:13:44	0.11481	0.11	249	Early
PKS2155-304_1824	21:58:52.3	–30:15:47	0.11559	0.14	270	Early
PKS2155-304_1839	21:58:51.7	–30:15:54	0.11817	1.86	288	Early
PKS2155-304_1381	21:59:03.1	–30:13:23	0.11640	1.50	336	Early
PKS2155-304_2210	21:58:41.5	–30:15:05	0.11536	0.27	352	Early
PKS2155-304_1496	21:59:00.2	–30:15:55	0.11615	0.52	378	Early
PKS2155-304_1389	21:59:03.1	–30:12:05	0.12045	0.88	387	Early
PKS2155-304_2233	21:58:41.5	–30:16:14	0.11620	0.14	442	Early
PKS2155-304_1055	21:59:12.0	–30:14:56	0.11665	0.39	621	Late
PKS2155-304_1214	21:59:07.5	–30:18:39	0.11649	0.76	766	Early
PKS2155-304_1128	21:59:09.8	–30:18:31	0.11624	0.25	796	Late
PKS2155-304_1044	21:59:11.8	–30:18:37	0.11519	0.61	838	Early
PKS2155-304_1331	21:59:04.5	–30:20:07	0.11528	0.50	860	Late
PKS2155-304_2955	21:58:21.1	–30:18:28	0.11614	0.11	1075	Late
PKS2155-304_2923	21:58:21.8	–30:18:50	0.11594	1.33	1082	Late
PKS2155-304_3298	21:58:12.3	–30:14:19	0.11737	0.23	1177	Late
PKS2155-304_351	21:59:31.1	–30:16:14	0.11616	2.45	1202	Early
PKS2155-304_3358	21:58:10.4	–30:12:15	0.11587	1.84	1224	Early
PKS2155-304_3487	21:58:07.4	–30:18:10	0.11591	0.14	1414	Late
PKS2155-304_210	21:59:36.5	–30:09:22	0.11747	0.17	1417	Early
PKS2155-304_2906	21:58:24.0	–30:04:17	0.12371	0.36	1432	Late
PKS2155-304_3357	21:58:11.5	–30:05:27	0.11731	0.17	1531	Late

Table 4—Continued

ID	RA (J2000)	DEC (J2000)	$z_{\rm gal}$	L^a ($L*$)	ρ^b (h_{72}^{-1} kpc)	Type[c]

[a]Luminosity relative to L* as measured from the apparent R-band magnitude. See text for a detailed description.

[b]Impact parameter in physical distance.

[c]The galaxy type is a crude assessment of the spectrum based on a fit of eigenfunctions. See text for a detailed description.

Table 5. Q0026+1259: Object Summary

ID	RA	DEC	B (mag)	R (mag)	S/G[a]	Area ($\square''$)	flg[b]	z
1	00:28:40.3	+13:08:22	11.51 ± 0.11	10.20 ± 0.08	0.69	76.8	0	···
2	00:28:27.4	+13:16:27	18.79 ± 0.12	17.43 ± 0.08	0.96	4.8	0	···
3	00:28:27.6	+13:26:27	19.12 ± 0.12	17.33 ± 0.08	1.00	2.6	0	···
4	00:28:26.8	+13:15:39	19.54 ± 0.12	18.21 ± 0.08	1.00	2.4	0	···
5	00:28:27.2	+13:24:49	20.46 ± 0.14	18.22 ± 0.08	1.00	2.4	0	···
6	00:28:26.4	+13:14:06	21.46 ± 0.23	19.60 ± 0.09	0.14	3.6	0	···
7	00:28:26.1	+13:13:18	21.76 ± 0.27	19.50 ± 0.09	1.00	2.9	0	···
8	00:28:25.8	+13:10:15	23.74 ± 1.00	21.42 ± 0.15	0.19	2.4	0	···
9	00:28:25.8	+13:10:33	21.64 ± 0.24	19.64 ± 0.09	0.87	2.6	0	···
10	00:28:25.9	+13:11:33	20.69 ± 0.16	18.26 ± 0.08	1.00	2.4	0	···

[a]Star/galaxy classifier calculated by SExtractor. Values near unity indicate a stellar-like point-spread function.

[b]This binary flag has the following code: 1: Survey target; 2: Spectrum taken; 4: Redshift measured.

Note. — [The complete version of this table is in the electronic edition of the Journal. The printed edition contains only a sample.]

Table 6. Ton S 180: Object Summary

ID	RA	DEC	B (mag)	R (mag)	S/G[a]	Area ($\square''$)	flg[b]	z
1	00:57:27.9	–22:25:12	9.86 ± 0.08	9.37 ± 0.06	0.69	253.5	0	···
2	00:56:52.8	–22:11:23	12.07 ± 0.08	11.42 ± 0.06	0.95	40.1	0	···
3	00:56:34.2	–22:29:02	15.35 ± 0.09	14.34 ± 0.06	1.00	3.5	0	···
4	00:56:33.8	–22:15:29	19.34 ± 0.10	17.53 ± 0.06	0.02	5.8	0	···
5	00:56:32.1	–22:31:34	21.96 ± 0.20	20.94 ± 0.10	0.82	3.3	0	···
6	00:56:32.0	–22:28:30	19.97 ± 0.11	18.10 ± 0.06	0.48	4.5	0	···
7	00:56:33.0	–22:11:44	19.09 ± 0.10	17.16 ± 0.06	0.88	5.0	0	···
8	00:56:32.4	–22:11:41	23.32 ± 0.54	21.59 ± 0.13	0.20	4.3	0	···
9	00:56:32.0	–22:24:37	21.65 ± 0.18	20.28 ± 0.08	0.12	3.9	0	···
10	00:56:32.6	–22:15:52	21.40 ± 0.15	20.02 ± 0.07	0.31	2.9	0	···

[a]Star/galaxy classifier calculated by SExtractor. Values near unity indicate a stellar-like point-spread function.

[b]This binary flag has the following code: 1: Survey target; 2: Spectrum taken; 4: Redshift measured.

Note. — [The complete version of this table is in the electronic edition of the Journal. The printed edition contains only a sample.]

Table 7. Ton S 210: Object Summary

ID	RA	DEC	B (mag)	R (mag)	S/G[a]	Area ($\square''$)	flg[b]	z
1	01:21:01.7	–28:14:24	16.10 ± 0.10	13.78 ± 0.06	1.00	4.7	0	···
2	01:21:00.1	–28:13:04	18.81 ± 0.09	17.36 ± 0.07	0.47	10.4	0	···
3	01:20:58.4	–28:13:53	19.05 ± 0.09	17.87 ± 0.07	0.13	4.9	0	···
4	01:20:56.6	–28:30:40	21.65 ± 0.23	18.85 ± 0.07	0.19	4.9	0	···
5	01:20:57.4	–28:22:13	19.54 ± 0.10	18.31 ± 0.07	0.02	6.9	0	···
6	01:20:57.7	–28:16:38	19.50 ± 0.09	18.63 ± 0.07	0.09	5.1	0	···
7	01:20:57.2	–28:21:14	20.68 ± 0.12	18.19 ± 0.07	0.99	2.1	0	···
8	01:20:57.1	–28:19:15	24.85 ± 1.70	21.36 ± 0.12	0.98	3.1	0	···
9	01:20:56.6	–28:23:16	22.62 ± 0.29	19.87 ± 0.07	0.99	1.9	0	···
10	01:20:55.9	–28:30:45	22.82 ± 0.43	20.35 ± 0.09	1.00	4.3	0	···

[a]Star/galaxy classifier calculated by SExtractor. Values near unity indicate a stellar-like point-spread function.

[b]This binary flag has the following code: 1: Survey target; 2: Spectrum taken; 4: Redshift measured.

Note. — [The complete version of this table is in the electronic edition of the Journal. The printed edition contains only a sample.]

Table 8. PKS0312-770: Object Summary

ID	RA	DEC	R (mag)	S/G[a]	Area ($\square''$)	flg[b]	z
1	03:11:42.7	–76:33:44	12.65 ± 0.01	1.00	7.2	0	···
2	03:12:28.6	–76:33:42	18.71 ± 0.02	0.12	10.2	0	···
3	03:12:10.2	–76:33:40	17.71 ± 0.01	1.00	4.6	0	···
4	03:14:33.7	–76:33:39	16.63 ± 0.01	1.00	4.6	0	···
5	03:12:34.0	–76:33:31	19.25 ± 0.03	0.85	3.8	0	···
6	03:11:25.3	–76:33:23	20.89 ± 0.08	0.12	7.8	0	···
7	03:12:52.6	–76:33:25	19.44 ± 0.03	0.56	5.2	0	···
8	03:10:19.9	–76:33:15	20.60 ± 0.10	0.98	2.7	0	···
9	03:13:01.0	–76:33:22	21.29 ± 0.12	1.00	5.5	0	···
10	03:14:36.7	–76:33:23	20.19 ± 0.05	0.97	8.1	0	···

[a]Star/galaxy classifier calculated by SExtractor. Values near unity indicate a stellar-like point-spread function.

[b]This binary flag has the following code: 1: Survey target; 2: Spectrum taken; 4: Redshift measured.

Note. — [The complete version of this table is in the electronic edition of the Journal. The printed edition contains only a sample.]

Table 9. PKS0558-504: Object Summary

ID	RA	DEC	B (mag)	R (mag)	S/G[a]	Area ($\square''$)	flg[b]	z
1	05:59:38.2	–50:18:33	10.41 ± 0.09	9.57 ± 0.06	0.69	149.9	0	···
2	05:59:20.5	–50:17:37	11.53 ± 0.09	10.80 ± 0.06	0.73	48.9	0	···
3	05:58:56.4	–50:27:28	12.41 ± 0.09	11.06 ± 0.06	0.75	38.3	0	···
4	05:58:48.3	–50:17:10	9.97 ± 0.09	9.98 ± 0.06	0.69	97.9	0	···
5	05:58:44.9	–50:24:12	10.51 ± 0.09	10.05 ± 0.06	0.69	94.4	0	···
6	05:58:45.6	–50:25:13	14.00 ± 0.09	13.27 ± 0.06	1.00	5.8	0	···
7	05:58:45.7	–50:16:04	12.78 ± 0.09	12.20 ± 0.06	1.00	14.2	0	···
8	05:58:39.9	–50:26:41	18.09 ± 0.09	17.13 ± 0.06	1.00	2.5	0	···
9	05:58:42.0	–50:26:33	12.30 ± 0.09	11.76 ± 0.06	0.98	20.0	0	···
10	05:58:43.5	–50:22:24	13.99 ± 0.09	13.12 ± 0.06	1.00	6.4	0	···

[a]Star/galaxy classifier calculated by SExtractor. Values near unity indicate a stellar-like point-spread function.

[b]This binary flag has the following code: 1: Survey target; 2: Spectrum taken; 4: Redshift measured.

Note. — [The complete version of this table is in the electronic edition of the Journal. The printed edition contains only a sample.]

Table 10. PG1004+130: Object Summary

ID	RA	DEC	B (mag)	R (mag)	S/G[a]	Area ($\square''$)	flg[b]	z
1	10:06:47.3	+12:46:52	8.19 ± 0.00	8.74 ± 0.00	0.69	217.7	0	···
2	10:06:57.9	+12:40:53	10.58 ± 0.00	11.13 ± 0.00	0.75	30.0	0	···
3	10:06:40.6	+12:47:50	21.44 ± 0.24	21.99 ± 0.24	1.00	2.4	0	···
4	10:06:39.5	+12:40:58	19.82 ± 0.06	20.37 ± 0.06	0.22	3.7	0	···
5	10:06:38.8	+12:37:14	17.74 ± 0.01	18.29 ± 0.01	1.00	2.6	0	···
6	10:06:40.1	+12:48:43	21.92 ± 0.30	22.46 ± 0.30	0.97	7.6	0	···
7	10:06:40.3	+12:51:47	17.97 ± 0.01	18.51 ± 0.01	1.00	2.5	0	···
8	10:06:39.4	+12:44:47	19.73 ± 0.07	20.28 ± 0.07	0.12	5.7	0	···
9	10:06:39.5	+12:45:04	21.60 ± 0.29	22.15 ± 0.29	0.35	9.2	0	···
10	10:06:38.5	+12:37:47	19.38 ± 0.05	19.93 ± 0.05	0.15	3.6	0	···

[a]Star/galaxy classifier calculated by SExtractor. Values near unity indicate a stellar-like point-spread function.

[b]This binary flag has the following code: 1: Survey target; 2: Spectrum taken; 4: Redshift measured.

Note. — [The complete version of this table is in the electronic edition of the Journal. The printed edition contains only a sample.]

Table 11. HE1029-140: Object Summary

ID	RA	DEC	B (mag)	R (mag)	S/G[a]	Area ($\square''$)	flg[b]	z
1	10:31:16.6	–14:21:26	14.12 ± 0.00	13.23 ± 0.00	1.00	6.2	0	···
2	10:31:15.3	–14:14:52	15.22 ± 0.00	13.97 ± 0.01	1.00	3.9	0	···
3	10:31:13.1	–14:15:55	16.15 ± 0.01	14.62 ± 0.01	1.00	2.6	0	···
4	10:31:13.4	–14:11:51	16.64 ± 0.01	15.80 ± 0.01	1.00	2.2	0	···
5	10:31:13.9	–14:06:06	18.95 ± 0.03	17.90 ± 0.01	0.87	6.1	7	0.13066
6	10:31:11.8	–14:21:00	16.48 ± 0.01	15.64 ± 0.00	1.00	2.8	0	···
7	10:31:12.5	–14:16:26	17.81 ± 0.01	16.50 ± 0.01	1.00	2.1	0	···
8	10:31:12.2	–14:13:53	19.50 ± 0.05	18.30 ± 0.02	0.28	4.9	7	0.19151
9	10:31:12.5	–14:11:37	20.58 ± 0.07	18.95 ± 0.02	0.98	2.6	7	−0.00008
10	10:31:12.6	–14:11:10	22.97 ± 0.45	20.40 ± 0.05	1.00	2.0	0	···

[a]Star/galaxy classifier calculated by SExtractor. Values near unity indicate a stellar-like point-spread function.

[b]This binary flag has the following code: 1: Survey target; 2: Spectrum taken; 4: Redshift measured.

Note. — [The complete version of this table is in the electronic edition of the Journal. The printed edition contains only a sample.]

Table 12. PG1116+215: Object Summary

ID	RA	DEC	B (mag)	R (mag)	S/G[a]	Area ($\square''$)	flg[b]	z
1	11:18:30.2	+21:17:08	18.76 ± 0.05	10.10 ± 0.03	0.98	125.2	0	···
2	11:18:29.2	+21:14:00	17.34 ± 0.01	15.64 ± 0.01	0.07	8.0	7	0.06038
3	11:18:25.4	+21:08:33	20.25 ± 0.05	19.17 ± 0.02	0.59	5.4	1	···
4	11:18:25.1	+21:18:15	23.88 ± 1.14	21.55 ± 0.14	0.22	14.2	0	···
5	11:18:25.9	+21:18:06	21.21 ± 0.18	19.83 ± 0.06	0.03	15.4	0	···
6	11:18:25.3	+21:16:13	23.11 ± 0.57	20.92 ± 0.10	0.08	12.8	0	···
7	11:18:24.9	+21:16:10	22.87 ± 0.59	20.75 ± 0.09	0.03	16.2	0	···
8	11:18:25.9	+21:16:25	20.53 ± 0.10	18.95 ± 0.03	0.03	12.2	0	···
9	11:18:26.9	+21:27:28	16.91 ± 0.01	15.06 ± 0.01	1.00	3.2	0	···
10	11:18:26.0	+21:27:25	21.56 ± 0.21	18.46 ± 0.01	0.99	4.5	1	···

[a]Star/galaxy classifier calculated by SExtractor. Values near unity indicate a stellar-like point-spread function.

[b]This binary flag has the following code: 1: Survey target; 2: Spectrum taken; 4: Redshift measured.

Note. — [The complete version of this table is in the electronic edition of the Journal. The printed edition contains only a sample.]

Table 13. PG1211+143: Object Summary

ID	RA	DEC	B (mag)	R (mag)	S/G[a]	Area ($\square''$)	flg[b]	z
1	12:14:00.7	+14:13:16	12.30 ± 0.09	10.94 ± 0.07	0.99	28.4	0	···
2	12:13:51.9	+14:13:23	16.04 ± 0.09	14.81 ± 0.07	0.03	35.2	0	···
3	12:13:58.3	+14:13:05	14.94 ± 0.09	13.93 ± 0.07	1.00	5.9	0	···
4	12:14:35.3	+14:13:44	25.76 ± 2.12	22.05 ± 0.12	0.98	2.5	0	···
5	12:14:29.6	+14:14:05	19.90 ± 0.10	17.77 ± 0.07	0.07	6.9	7	0.15545
6	12:13:42.4	+14:14:13	21.00 ± 0.11	19.93 ± 0.08	0.12	6.9	0	···
7	12:14:45.0	+14:13:57	21.25 ± 0.12	19.80 ± 0.07	0.13	4.8	0	···
8	12:14:28.2	+14:14:05	20.27 ± 0.10	18.88 ± 0.07	0.13	7.1	1	···
9	12:14:40.8	+14:14:01	19.92 ± 0.10	18.00 ± 0.07	0.78	7.2	1	···
10	12:14:40.9	+14:14:06	23.36 ± 0.32	21.58 ± 0.11	0.82	4.4	0	···

[a]Star/galaxy classifier calculated by SExtractor. Values near unity indicate a stellar-like point-spread function.

[b]This binary flag has the following code: 1: Survey target; 2: Spectrum taken; 4: Redshift measured.

Note. — [The complete version of this table is in the electronic edition of the Journal. The printed edition contains only a sample.]

Table 14. PG1216+069: Object Summary

ID	RA	DEC	B (mag)	R (mag)	S/G[a]	Area ($\square''$)	flg[b]	z
1	12:18:32.1	+06:32:29	28.60 ± 23.69	23.06 ± 0.41	1.00	1.6	0	···
2	12:18:38.6	+06:42:29	15.83 ± 0.00	14.86 ± 0.00	0.05	33.1	7	0.00667
3	12:18:35.1	+06:29:41	19.17 ± 0.05	18.07 ± 0.02	0.03	20.7	0	···
4	12:18:33.7	+06:28:08	24.86 ± 1.37	22.17 ± 0.14	0.96	3.1	0	···
5	12:18:33.7	+06:29:06	22.62 ± 0.25	20.61 ± 0.05	1.00	2.6	0	···
6	12:18:33.2	+06:40:52	19.86 ± 0.13	16.77 ± 0.02	0.03	57.2	0	···
7	12:18:33.6	+06:46:39	14.59 ± 0.00	13.99 ± 0.00	1.00	3.4	0	···
8	12:18:33.0	+06:34:06	20.03 ± 0.04	18.67 ± 0.02	0.99	3.4	0	···
9	12:18:33.4	+06:38:45	24.76 ± 1.82	21.16 ± 0.10	0.12	5.6	0	···
10	12:18:33.1	+06:40:30	22.14 ± 0.37	18.97 ± 0.04	0.03	16.6	0	···

[a]Star/galaxy classifier calculated by SExtractor. Values near unity indicate a stellar-like point-spread function.

[b]This binary flag has the following code: 1: Survey target; 2: Spectrum taken; 4: Redshift measured.

Note. — [The complete version of this table is in the electronic edition of the Journal. The printed edition contains only a sample.]

Table 15. 3C273: Object Summary

ID	RA	DEC	B (mag)	R (mag)	S/G[a]	Area ($\square''$)	flg[b]	z
1	12:28:23.7	+02:09:17	26.82 ± 5.73	23.58 ± 0.25	1.00	3.5	0	···
2	12:28:22.2	+01:55:30	23.45 ± 0.35	21.95 ± 0.07	1.00	2.1	0	···
3	12:28:22.2	+01:55:01	22.74 ± 0.23	21.31 ± 0.05	1.00	2.1	0	···
4	12:28:22.1	+01:54:39	23.44 ± 0.35	22.18 ± 0.08	0.98	1.7	0	···
5	12:28:21.8	+01:51:53	23.13 ± 0.31	21.53 ± 0.05	1.00	1.9	0	···
6	12:28:23.7	+02:09:08	24.55 ± 1.24	22.21 ± 0.11	0.98	3.4	0	···
7	12:28:23.0	+02:02:25	24.95 ± 1.82	22.59 ± 0.16	0.15	2.9	0	···
8	12:28:23.1	+02:02:11	28.23 ± 14.61	23.70 ± 0.32	0.98	1.3	0	···
9	12:28:23.8	+02:08:12	25.41 ± 1.28	24.00 ± 0.35	0.98	1.5	0	···
10	12:28:23.5	+02:05:35	24.12 ± 0.86	22.17 ± 0.13	0.90	5.6	0	···

[a]Star/galaxy classifier calculated by SExtractor. Values near unity indicate a stellar-like point-spread function.

[b]This binary flag has the following code: 1: Survey target; 2: Spectrum taken; 4: Redshift measured.

Note. — [The complete version of this table is in the electronic edition of the Journal. The printed edition contains only a sample.]

Table 16. Q1230+095: Object Summary

ID	RA	DEC	B (mag)	R (mag)	S/G[a]	Area ($\square''$)	flg[b]	z
1	12:33:53.8	+09:31:53	11.39 ± 0.01	9.17 ± 0.01	0.69	217.9	0	···
2	12:32:44.9	+09:39:38	11.28 ± 0.00	10.81 ± 0.00	0.72	46.6	0	···
3	12:32:44.6	+09:22:05	17.48 ± 0.01	16.13 ± 0.01	0.01	8.5	7	0.11526
4	12:32:42.9	+09:20:40	19.51 ± 0.06	18.59 ± 0.03	0.03	12.2	1	···
5	12:32:44.0	+09:30:56	17.58 ± 0.01	16.02 ± 0.01	1.00	2.8	0	···
6	12:32:43.0	+09:24:56	18.57 ± 0.02	16.88 ± 0.01	1.00	2.6	0	···
7	12:32:42.9	+09:27:53	22.81 ± 0.45	20.24 ± 0.05	0.57	2.5	0	···
8	12:32:43.6	+09:35:56	21.20 ± 0.13	19.57 ± 0.04	0.18	2.9	0	···
9	12:32:41.8	+09:20:56	18.48 ± 0.02	16.35 ± 0.01	1.00	4.6	0	···
10	12:32:43.6	+09:36:08	22.53 ± 0.37	20.08 ± 0.05	0.40	3.0	0	···

[a]Star/galaxy classifier calculated by SExtractor. Values near unity indicate a stellar-like point-spread function.

[b]This binary flag has the following code: 1: Survey target; 2: Spectrum taken; 4: Redshift measured.

Note. — [The complete version of this table is in the electronic edition of the Journal. The printed edition contains only a sample.]

Table 17. PKS1302-102: Object Summary

ID	RA	DEC	B (mag)	R (mag)	S/G[a]	Area ($\square''$)	flg[b]	z
1	13:05:43.7	–10:30:07	10.28 ± 0.00	8.93 ± 0.01	0.69	334.3	0	···
2	13:04:57.9	–10:25:47	13.20 ± 0.00	12.36 ± 0.00	1.00	13.8	0	···
3	13:04:57.8	–10:26:05	17.48 ± 0.02	15.15 ± 0.01	1.00	3.2	0	···
4	13:04:56.0	–10:29:18	20.06 ± 0.11	18.11 ± 0.02	0.09	6.8	7	0.27252
5	13:04:54.6	–10:39:58	18.85 ± 0.04	17.89 ± 0.01	0.13	4.6	7	0.04576
6	13:04:54.9	–10:33:57	17.45 ± 0.01	15.92 ± 0.01	1.00	2.3	0	···
7	13:04:56.1	–10:25:29	23.12 ± 0.78	20.75 ± 0.08	0.98	1.9	0	···
8	13:04:55.0	–10:32:28	21.53 ± 0.25	19.65 ± 0.04	0.13	3.7	0	···
9	13:04:56.0	–10:21:04	20.36 ± 0.11	18.71 ± 0.02	0.15	3.6	1	···
10	13:04:55.1	–10:29:17	19.09 ± 0.03	18.13 ± 0.01	0.98	3.4	0	···

[a]Star/galaxy classifier calculated by SExtractor. Values near unity indicate a stellar-like point-spread function.

[b]This binary flag has the following code: 1: Survey target; 2: Spectrum taken; 4: Redshift measured.

Note. — [The complete version of this table is in the electronic edition of the Journal. The printed edition contains only a sample.]

Table 18. PG1307+085: Object Summary

ID	RA	DEC	B (mag)	R (mag)	S/G[a]	Area ($\square''$)	flg[b]	z
1	13:09:49.7	+08:11:05	11.72 ± 0.00	10.34 ± 0.01	0.69	84.1	0	···
2	13:09:08.0	+08:09:16	13.90 ± 0.00	13.12 ± 0.00	1.00	6.7	0	···
3	13:09:07.3	+08:09:35	20.00 ± 0.09	14.10 ± 0.02	1.00	4.8	0	···
4	13:09:09.7	+08:27:13	22.33 ± 0.33	20.41 ± 0.06	0.13	3.3	0	···
5	13:09:09.5	+08:27:09	21.29 ± 0.16	20.35 ± 0.07	0.15	5.2	0	···
6	13:09:07.9	+08:11:41	17.33 ± 0.01	16.59 ± 0.01	1.00	2.3	0	···
7	13:09:09.1	+08:23:48	17.21 ± 0.01	16.48 ± 0.01	1.00	2.3	0	···
8	13:09:09.6	+08:28:56	17.98 ± 0.01	16.94 ± 0.01	1.00	2.2	0	···
9	13:09:07.6	+08:09:48	23.62 ± 1.08	20.83 ± 0.10	0.20	5.1	0	···
10	13:09:09.5	+08:27:53	24.44 ± 1.45	20.89 ± 0.07	0.99	1.8	0	···

[a]Star/galaxy classifier calculated by SExtractor. Values near unity indicate a stellar-like point-spread function.

[b]This binary flag has the following code: 1: Survey target; 2: Spectrum taken; 4: Redshift measured.

Note. — [The complete version of this table is in the electronic edition of the Journal. The printed edition contains only a sample.]

Table 19. MRK1383: Object Summary

ID	RA	DEC	B (mag)	R (mag)	S/G[a]	Area ($\square''$)	flg[b]	z
1	14:29:00.6	+01:26:39	10.44 ± 0.00	9.62 ± 0.00	0.69	140.4	0	···
2	14:28:57.4	+01:24:05	11.17 ± 0.00	10.52 ± 0.00	0.73	60.6	0	···
3	14:28:29.6	+01:07:36	12.80 ± 0.01	11.16 ± 0.01	0.87	34.0	0	···
4	14:28:21.9	+01:06:47	18.66 ± 0.04	17.19 ± 0.01	0.01	6.3	1	···
5	14:28:21.3	+01:06:46	23.57 ± 0.82	21.66 ± 0.13	0.98	2.4	0	···
6	14:28:24.2	+01:27:37	20.25 ± 0.09	18.02 ± 0.01	1.00	2.4	0	···
7	14:28:24.2	+01:27:51	22.63 ± 0.54	20.90 ± 0.10	0.12	2.9	0	···
8	14:28:23.2	+01:18:37	22.68 ± 0.57	19.94 ± 0.05	0.99	2.5	0	···
9	14:28:23.7	+01:26:27	22.09 ± 0.30	20.53 ± 0.07	0.93	2.5	0	···
10	14:28:24.0	+01:28:01	22.26 ± 0.37	19.38 ± 0.03	0.98	2.1	0	···

[a]Star/galaxy classifier calculated by SExtractor. Values near unity indicate a stellar-like point-spread function.

[b]This binary flag has the following code: 1: Survey target; 2: Spectrum taken; 4: Redshift measured.

Note. — [The complete version of this table is in the electronic edition of the Journal. The printed edition contains only a sample.]

Table 20. Q1553+113: Object Summary

ID	RA	DEC	B (mag)	R (mag)	S/G[a]	Area ($\square''$)	flg[b]	z
1	15:55:06.9	+11:14:54	12.14 ± 0.00	11.18 ± 0.00	0.96	30.4	0	···
2	15:55:00.4	+10:59:45	18.57 ± 0.05	17.24 ± 0.02	0.17	23.0	0	···
3	15:55:02.2	+10:59:33	17.53 ± 0.02	16.71 ± 0.01	0.03	22.3	0	···
4	15:55:00.7	+11:04:26	16.22 ± 0.01	14.89 ± 0.01	0.02	15.4	7	0.04052
5	15:54:57.8	+11:01:35	22.80 ± 0.67	19.64 ± 0.04	0.20	3.0	1	···
6	15:54:58.5	+11:19:32	17.09 ± 0.01	15.82 ± 0.01	1.00	2.5	0	···
7	15:54:58.2	+11:17:38	16.57 ± 0.01	15.40 ± 0.01	1.00	2.6	0	···
8	15:54:58.1	+11:21:23	21.30 ± 0.15	19.22 ± 0.02	0.99	2.4	0	···
9	15:54:57.6	+11:21:27	22.22 ± 0.39	20.12 ± 0.06	0.12	3.8	0	···
10	15:54:56.3	+11:05:18	22.28 ± 0.29	20.62 ± 0.06	0.98	2.1	0	···

[a]Star/galaxy classifier calculated by SExtractor. Values near unity indicate a stellar-like point-spread function.

[b]This binary flag has the following code: 1: Survey target; 2: Spectrum taken; 4: Redshift measured.

Note. — [The complete version of this table is in the electronic edition of the Journal. The printed edition contains only a sample.]

Table 21. PKS2005-489: Object Summary

ID	RA	DEC	B (mag)	R (mag)	S/G[a]	Area ($\square''$)	flg[b]	z
1	20:09:57.0	–48:39:37	24.07 ± 0.55	22.75 ± 0.14	0.98	3.0	0	···
2	20:10:27.4	–48:39:42	25.30 ± 9.99	23.33 ± 0.22	0.97	1.7	0	···
3	20:10:18.0	–48:39:41	25.25 ± 9.99	23.47 ± 0.26	0.97	3.7	0	···
4	20:10:11.1	–48:39:40	25.20 ± 2.48	20.77 ± 0.07	0.99	2.5	0	···
5	20:10:17.0	–48:39:44	24.47 ± 0.97	22.50 ± 0.14	0.98	3.9	0	···
6	20:09:45.5	–48:39:37	21.46 ± 0.13	20.35 ± 0.07	0.98	2.6	0	···
7	20:09:10.9	–48:39:36	26.00 ± 2.54	23.67 ± 0.24	0.96	1.7	0	···
8	20:09:19.3	–48:39:37	24.66 ± 0.93	23.31 ± 0.22	0.97	2.6	0	···
9	20:09:23.9	–48:39:32	22.53 ± 0.33	20.48 ± 0.07	0.82	3.7	0	···
10	20:10:22.2	–48:39:49	23.53 ± 0.46	22.03 ± 0.11	1.00	2.5	0	···

[a]Star/galaxy classifier calculated by SExtractor. Values near unity indicate a stellar-like point-spread function.

[b]This binary flag has the following code: 1: Survey target; 2: Spectrum taken; 4: Redshift measured.

Note. — [The complete version of this table is in the electronic edition of the Journal. The printed edition contains only a sample.]

Table 22. FJ2155-092: Object Summary

ID	RA	DEC	B (mag)	R (mag)	S/G[a]	Area ($\square''$)	flg[b]	z
1	21:54:16.5	–09:20:36	13.37 ± 0.09	11.93 ± 0.06	1.00	19.4	0	···
2	21:54:15.7	–09:29:17	16.32 ± 0.09	14.94 ± 0.06	0.68	9.7	0	···
3	21:54:13.4	–09:14:10	15.51 ± 0.09	14.55 ± 0.06	1.00	3.2	0	···
4	21:54:12.0	–09:23:15	13.41 ± 0.09	12.65 ± 0.06	1.00	10.3	0	···
5	21:54:12.0	–09:12:53	20.31 ± 0.15	18.05 ± 0.07	0.22	3.8	0	···
6	21:54:11.6	–09:12:54	24.50 ± 2.61	21.14 ± 0.14	0.13	4.8	0	···
7	21:54:11.4	–09:20:01	20.78 ± 0.14	19.03 ± 0.07	0.99	2.3	0	···
8	21:54:11.1	–09:18:56	20.04 ± 0.14	17.71 ± 0.07	0.22	4.1	0	···
9	21:54:11.0	–09:19:03	21.20 ± 0.19	18.50 ± 0.07	0.99	2.5	0	···
10	21:54:11.5	–09:15:46	19.16 ± 0.10	17.82 ± 0.06	1.00	2.5	0	···

[a]Star/galaxy classifier calculated by SExtractor. Values near unity indicate a stellar-like point-spread function.

[b]This binary flag has the following code: 1: Survey target; 2: Spectrum taken; 4: Redshift measured.

Note. — [The complete version of this table is in the electronic edition of the Journal. The printed edition contains only a sample.]

Table 23. PKS2155-304: Object Summary

ID	RA	DEC	B (mag)	R (mag)	S/G[a]	Area ($\square''$)	flg[b]	z
1	21:59:04.0	–30:09:30	9.80 ± 0.08	9.27 ± 0.06	0.69	265.2	0	···
2	21:58:12.6	–30:17:46	12.89 ± 0.08	12.00 ± 0.06	0.99	21.0	0	···
3	21:58:11.4	–30:19:08	15.88 ± 0.09	14.82 ± 0.06	0.03	22.0	7	0.04528
4	21:58:08.2	–30:11:58	13.55 ± 0.09	12.33 ± 0.06	1.00	15.6	0	···
5	21:58:02.3	–30:15:35	15.22 ± 0.08	14.49 ± 0.06	1.00	3.1	0	···
6	21:58:03.0	–30:06:04	19.50 ± 0.12	17.12 ± 0.06	0.04	6.3	0	···
7	21:58:00.3	–30:19:49	20.61 ± 0.14	18.30 ± 0.06	0.89	3.7	0	···
8	21:58:01.8	–30:02:37	21.55 ± 0.20	19.17 ± 0.07	0.48	4.0	0	···
9	21:58:00.8	–30:07:21	21.61 ± 0.18	19.21 ± 0.07	1.00	2.4	0	···
10	21:57:59.4	–30:21:38	19.98 ± 0.09	18.80 ± 0.06	0.98	2.1	0	···

[a]Star/galaxy classifier calculated by SExtractor. Values near unity indicate a stellar-like point-spread function.

[b]This binary flag has the following code: 1: Survey target; 2: Spectrum taken; 4: Redshift measured.

Note. — [The complete version of this table is in the electronic edition of the Journal. The printed edition contains only a sample.]

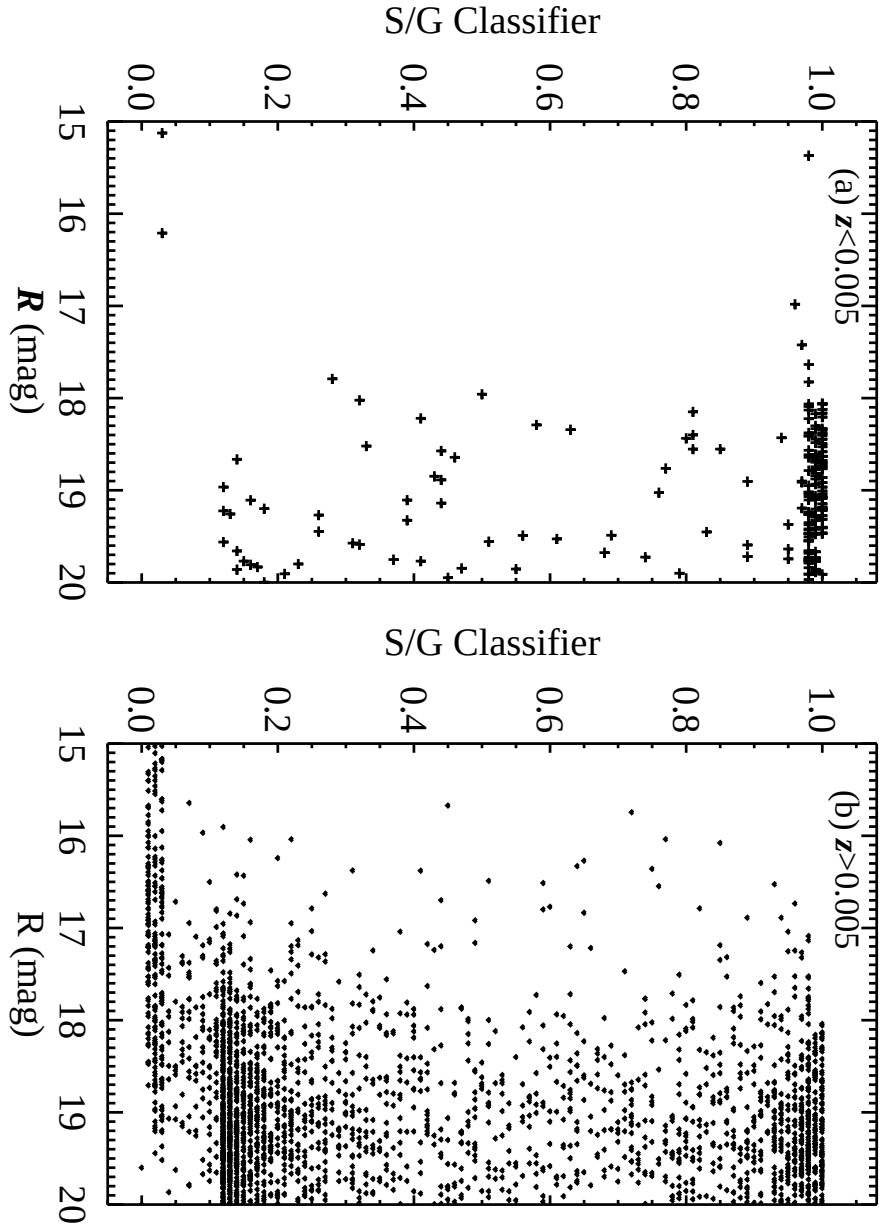

Fig. 1.— SExtractor S/G classifier as a function of the objects apparent R-band magnitude and having spectroscopic redshifts (a) $z < 0.005$ (predominantly Galactic stars) and (b) $z > 0.005$ (exclusively galaxies).

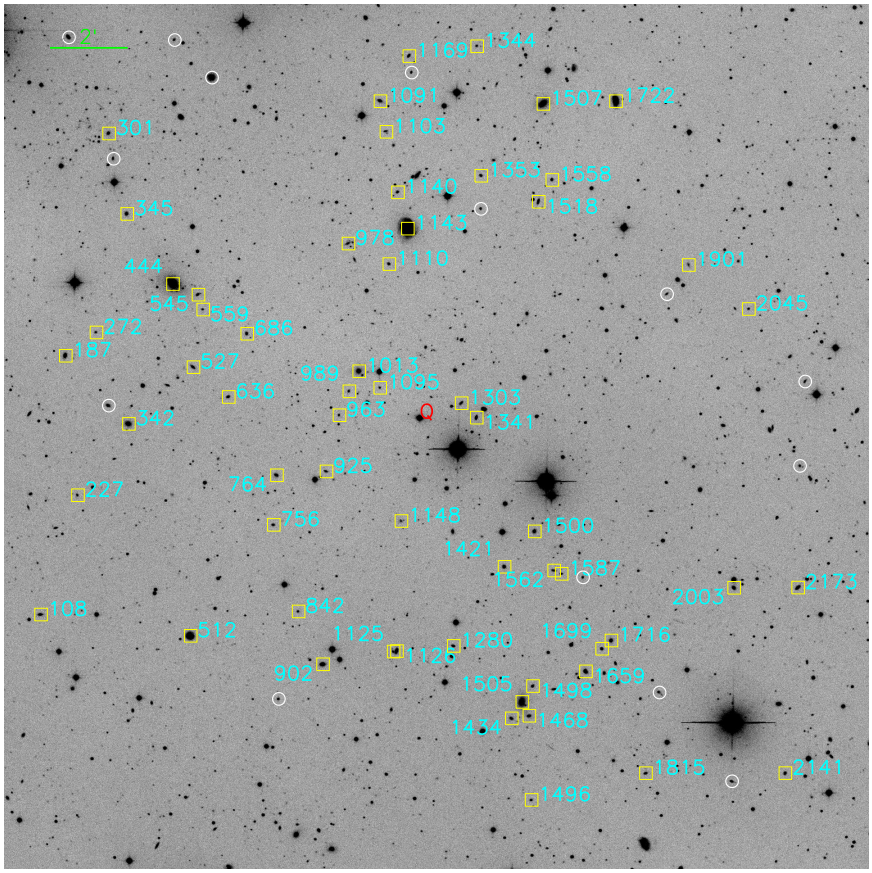

Fig. 2.— R-band image of the field surrounding Q0026+1259 ($z_{\rm em} = 0.142$; marked with a red "Q"). All galaxies with $z < (z_{\rm em}+0.01)$ are labelled with their redshifts. Unless otherwise indicated, labels are placed to the right and just above the galaxy. Objects circled in pink were targeted (i.e. $R < 19.5$ mag and the imaging indicated it was not a point source) but no redshift was determined either because no mask included it or a secure redshift could not be determined from the spectrum.

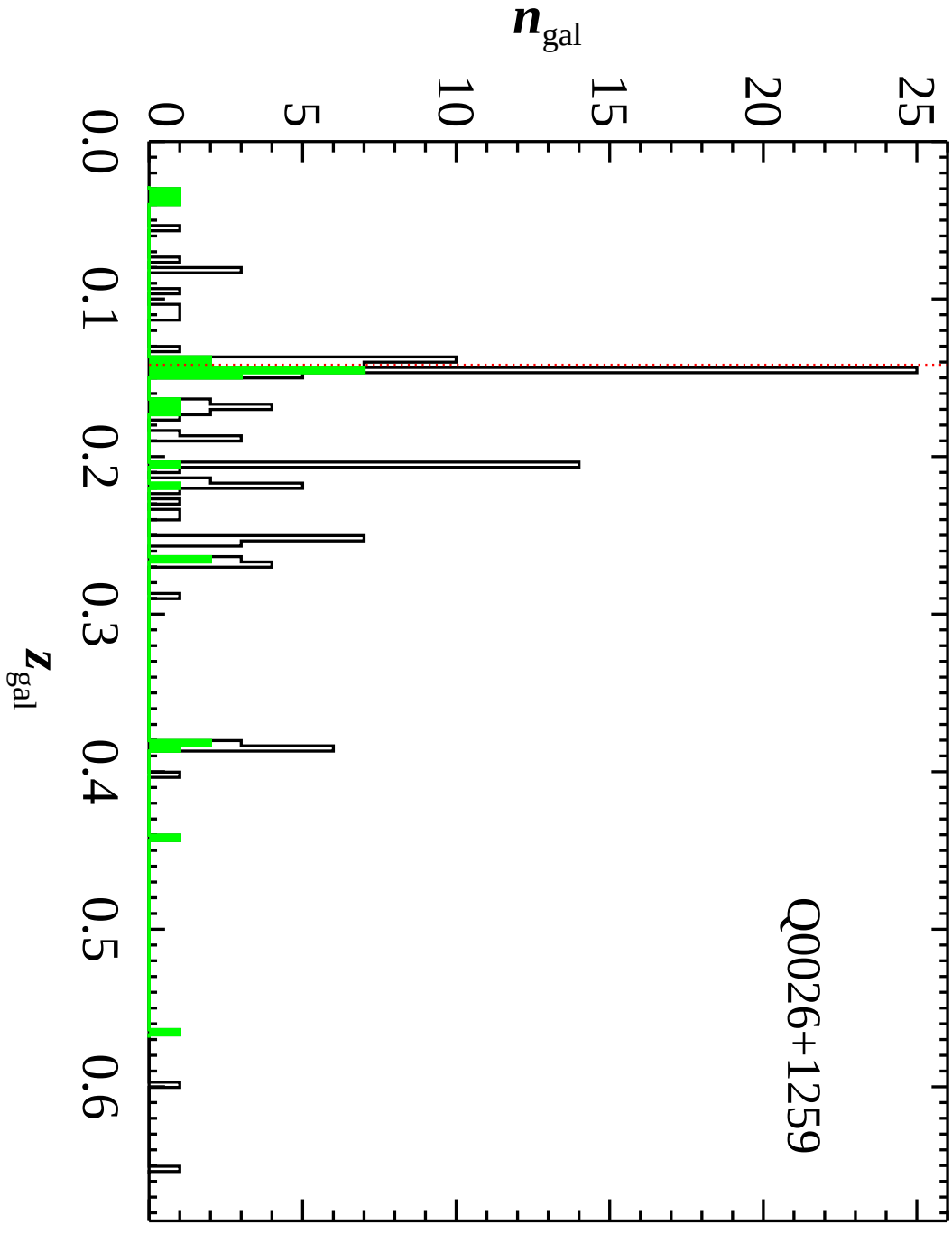

Fig. 3.— Histogram of galaxy redshifts for the field surrounding Q0026+1259 ($z_{em} = 0.142$), binned in intervals of $\Delta z = 0.00333$. The solid (green) histogram shows the distribution for galaxies within $5'$ of the quasar while the open (black) histogram is for all galaxies surveyed in the field. The dotted (red) vertical line indicates the quasar emission-line redshift (z_{em}).

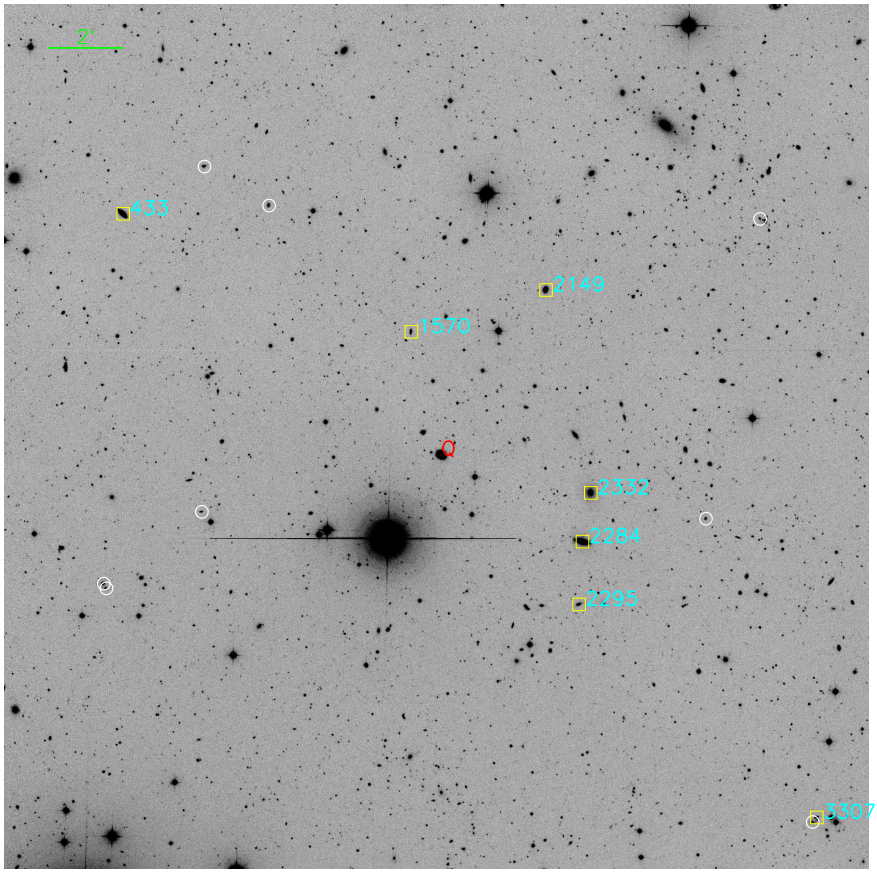

Fig. 4.— Same as for Figure 2 but for the field surrounding Ton S 180 ($z_{\rm em} = 0.062$).

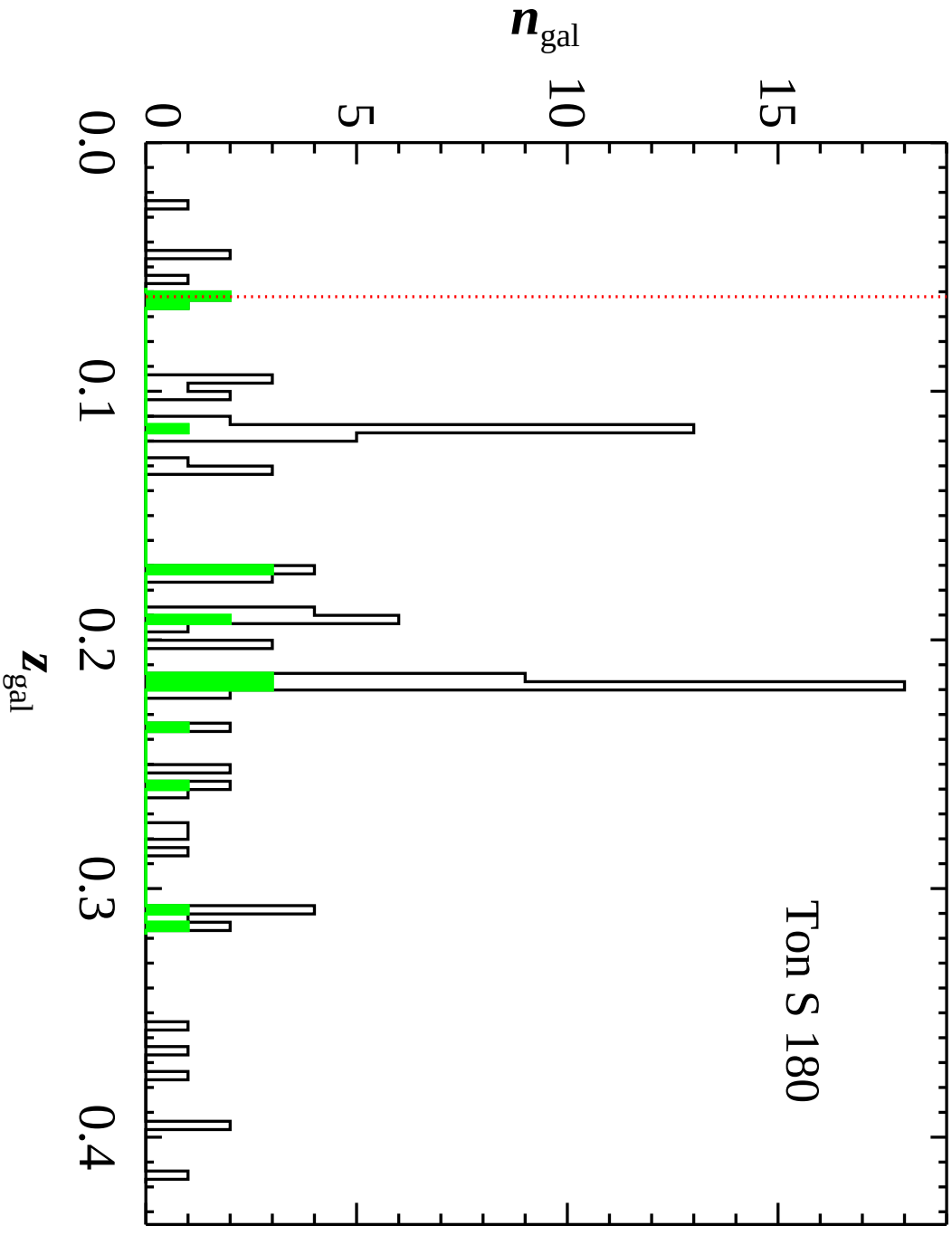

Fig. 5.— Same as for Figure 3 but for the field surrounding Ton S 180 ($z_{em} = 0.062$).

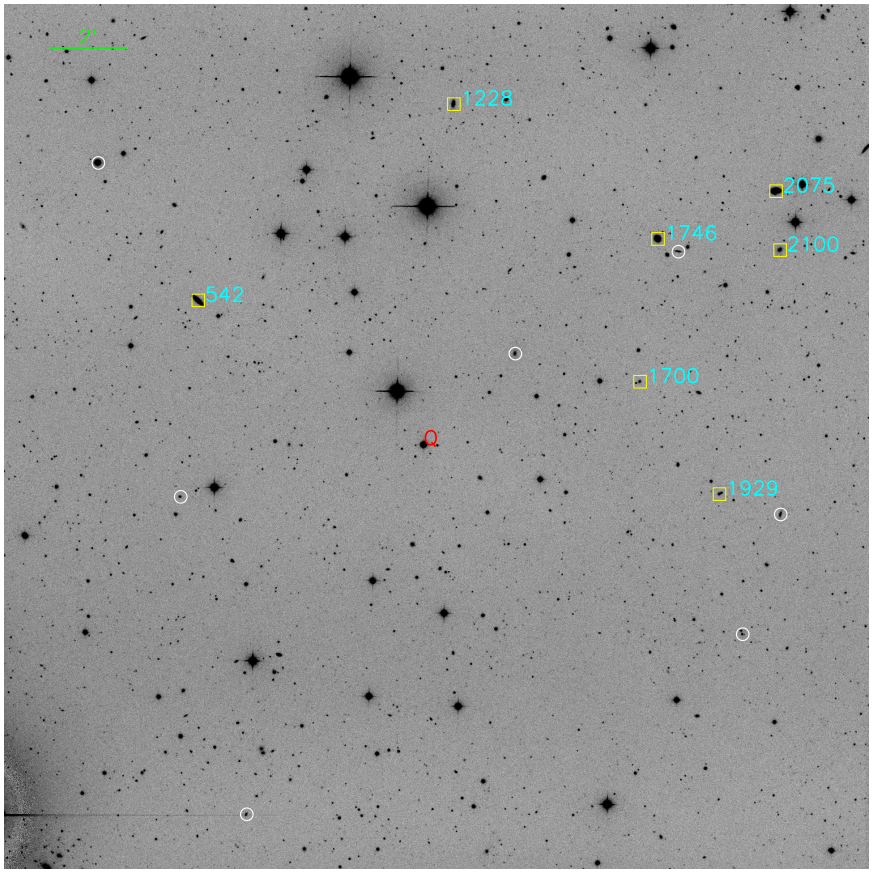

Fig. 6.— Same as for Figure 2 but for the field surrounding Ton S 210 ($z_{\rm em} = 0.116$).

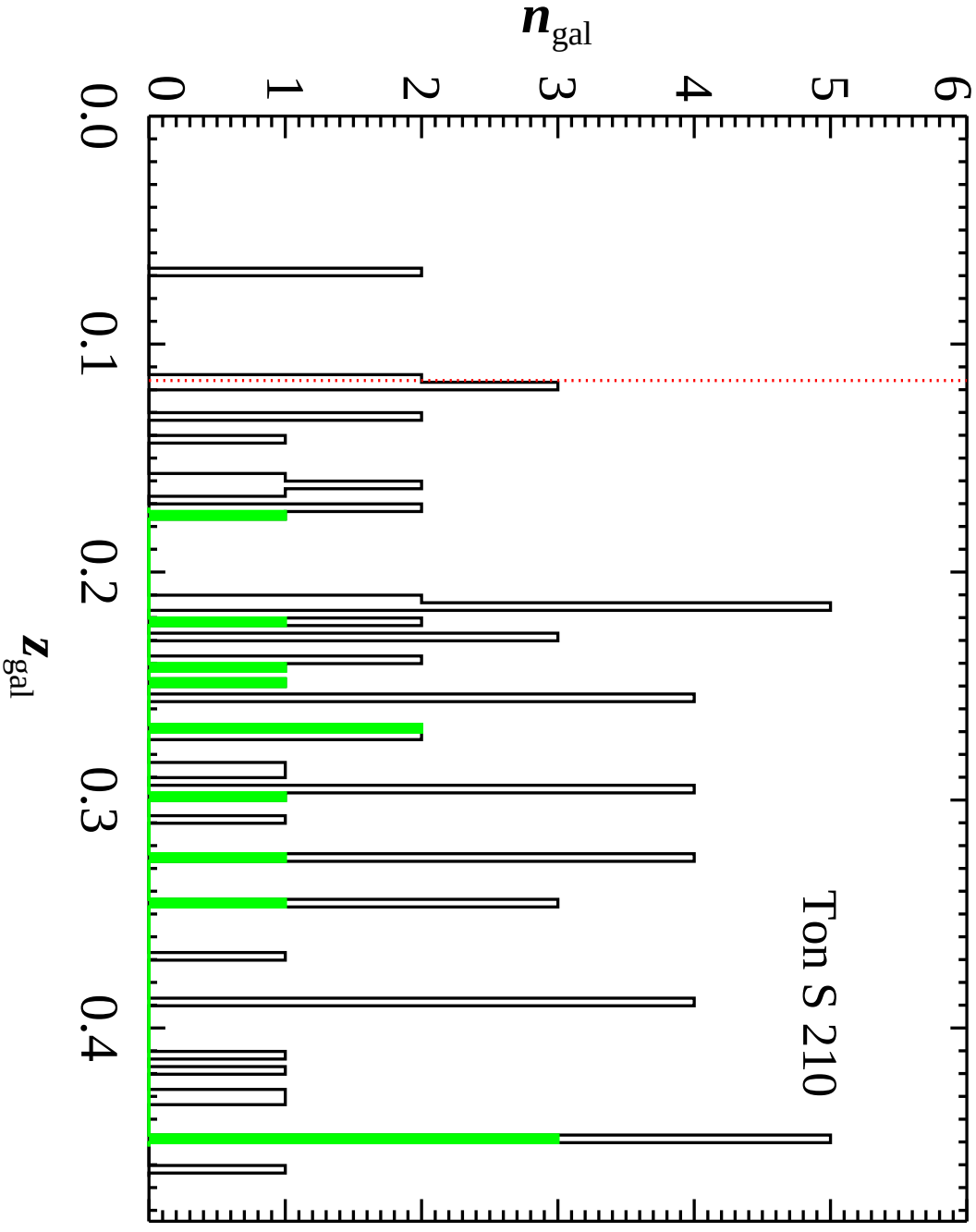

Fig. 7.— Same as for Figure 3 but for the field surrounding Ton S 210 ($z_{em} = 0.116$).

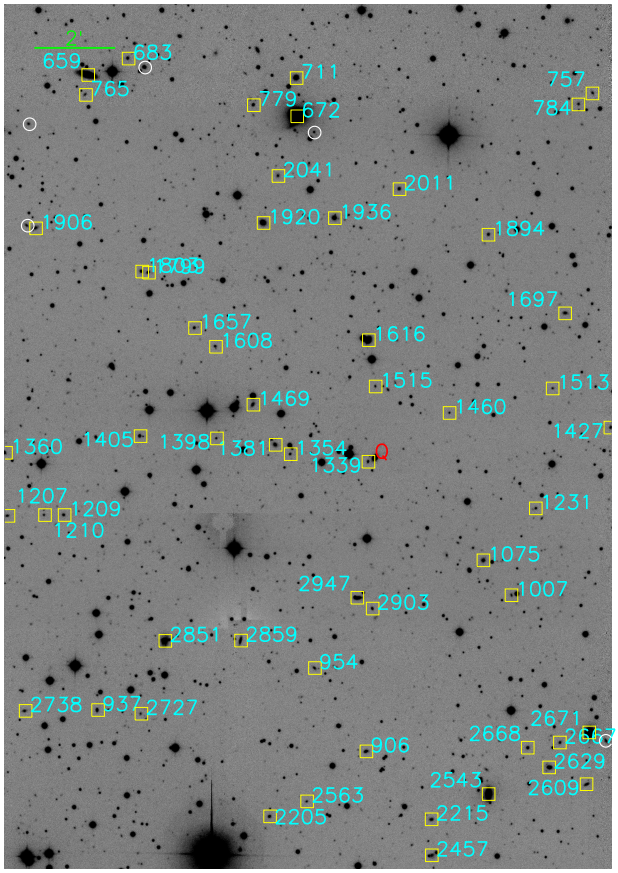

Fig. 8.— Same as for Figure 2 but for the field surrounding PKS0312–770 ($z_{\rm em} = 0.223$).

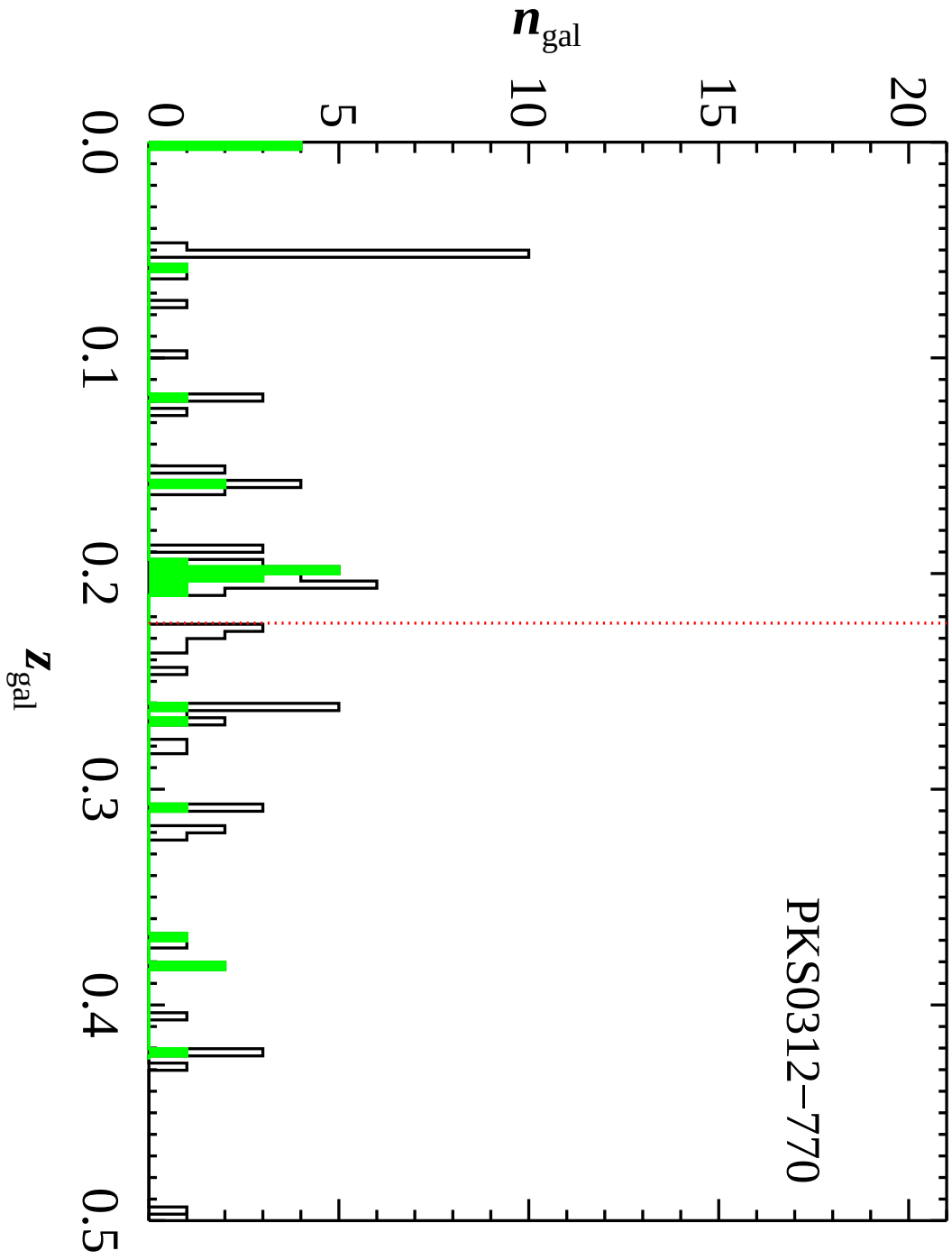

Fig. 9.— Same as for Figure 3 but for the field surrounding PKS0312–770 ($z_{\rm em} = 0.223$).

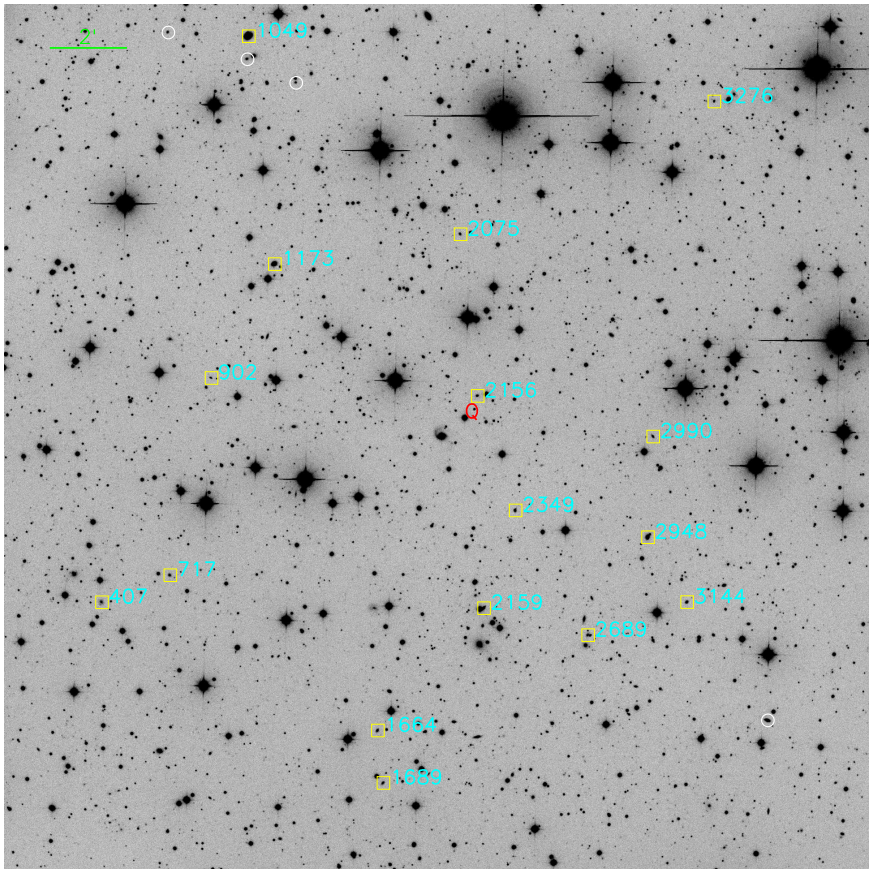

Fig. 10.— Same as for Figure 2 but for the field surrounding PKS0558–504 ($z_{\rm em} = 0.137$).

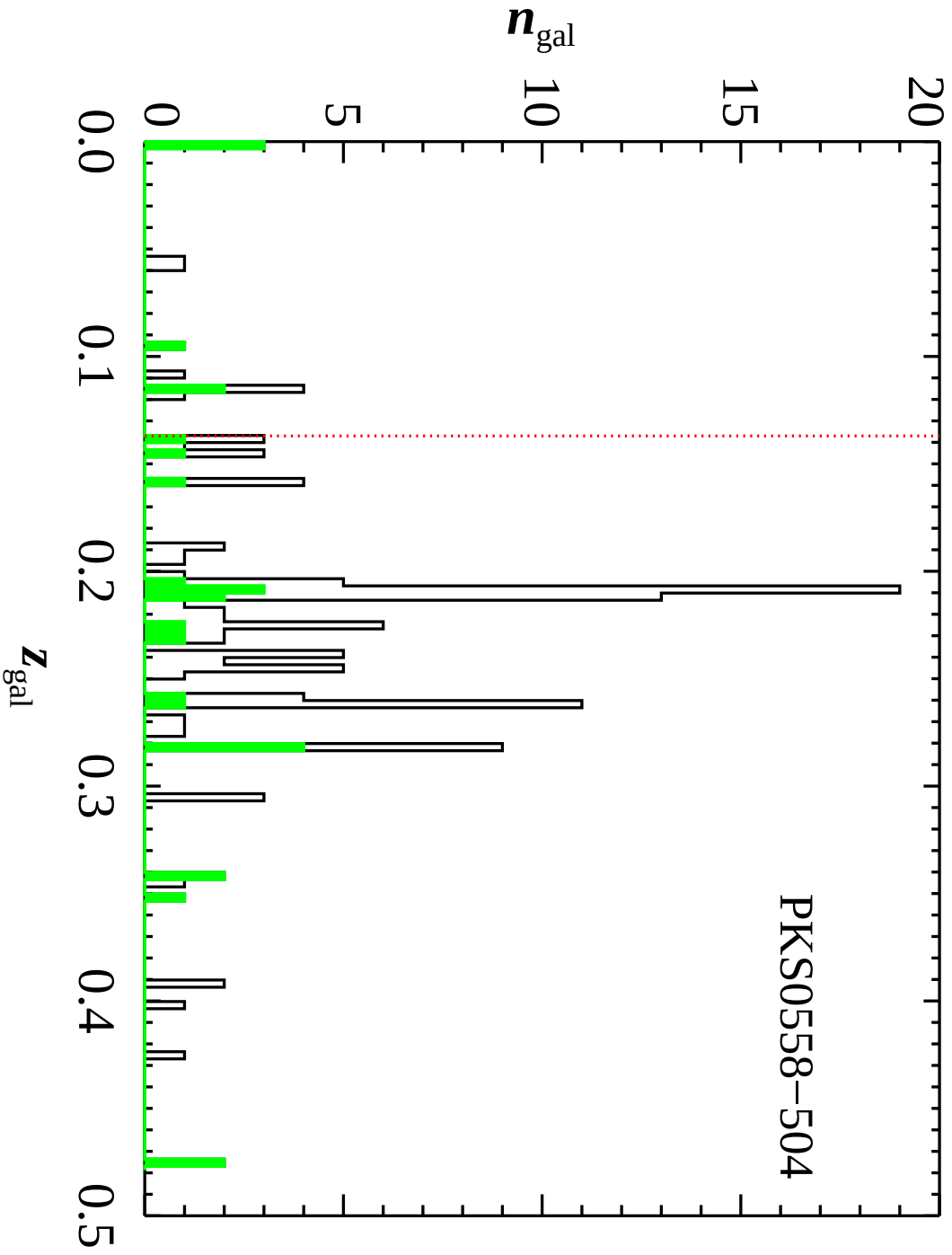

Fig. 11.— Same as for Figure 3 but for the field surrounding PKS0558–504 ($z_{em} = 0.137$).

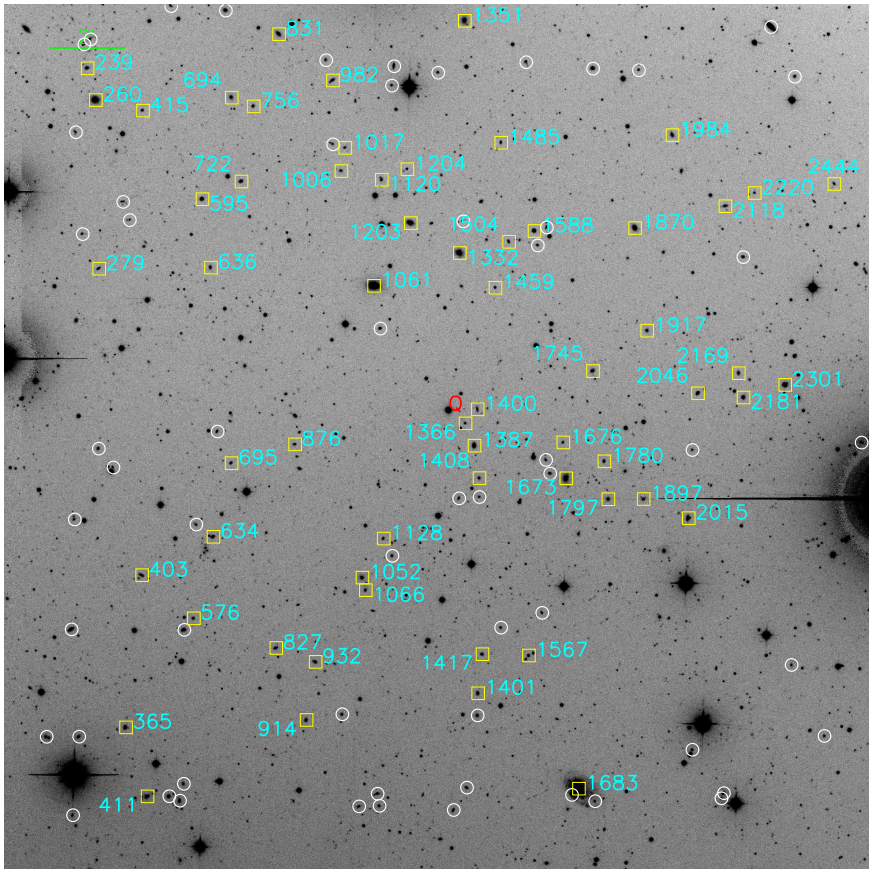

Fig. 12.— Same as for Figure 2 but for the field surrounding PG1004+130 ($z_{\rm em} = 0.240$).

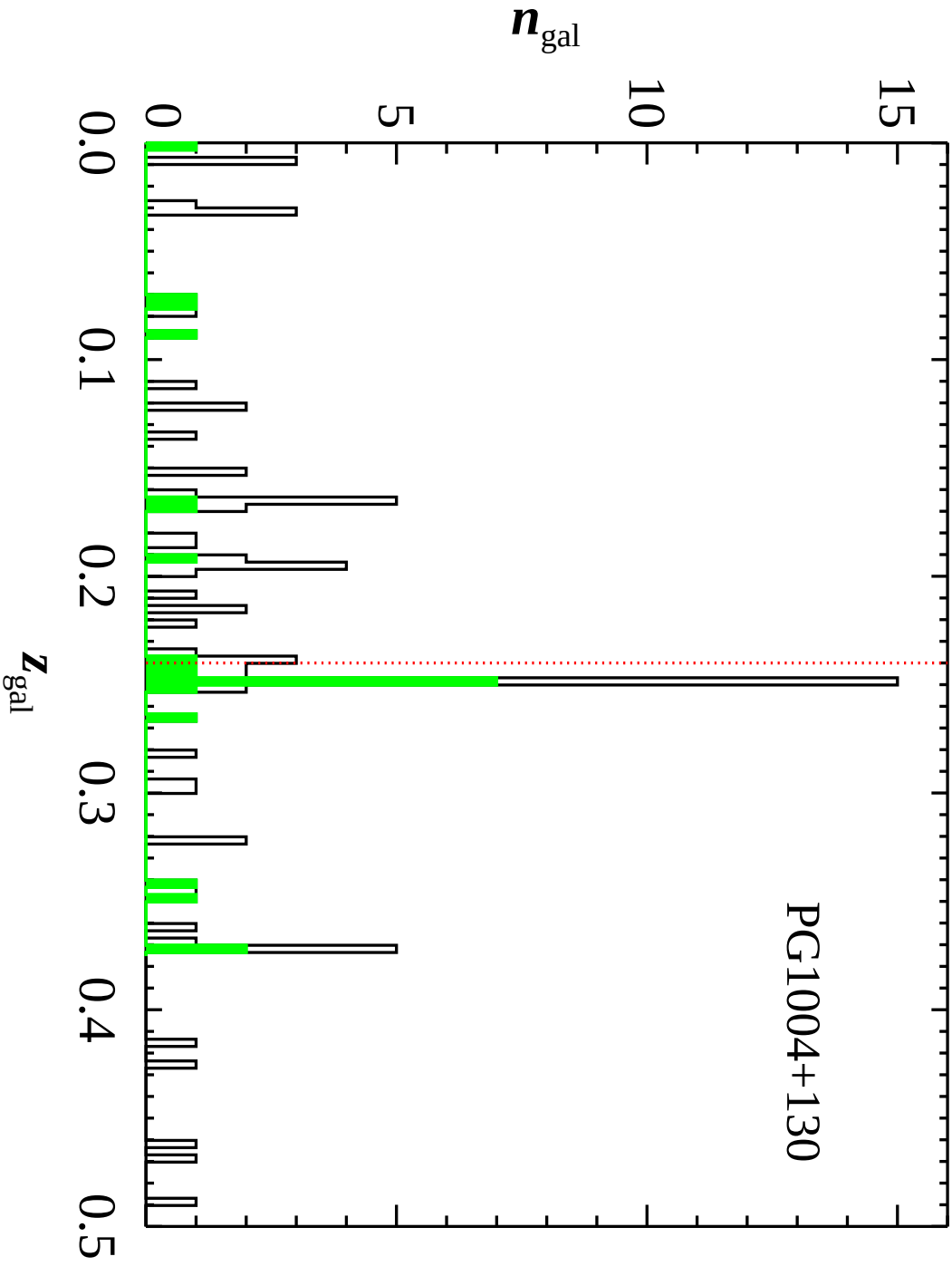

Fig. 13.— Same as for Figure 3 but for the field surrounding PG1004+130 ($z_{em} = 0.240$).

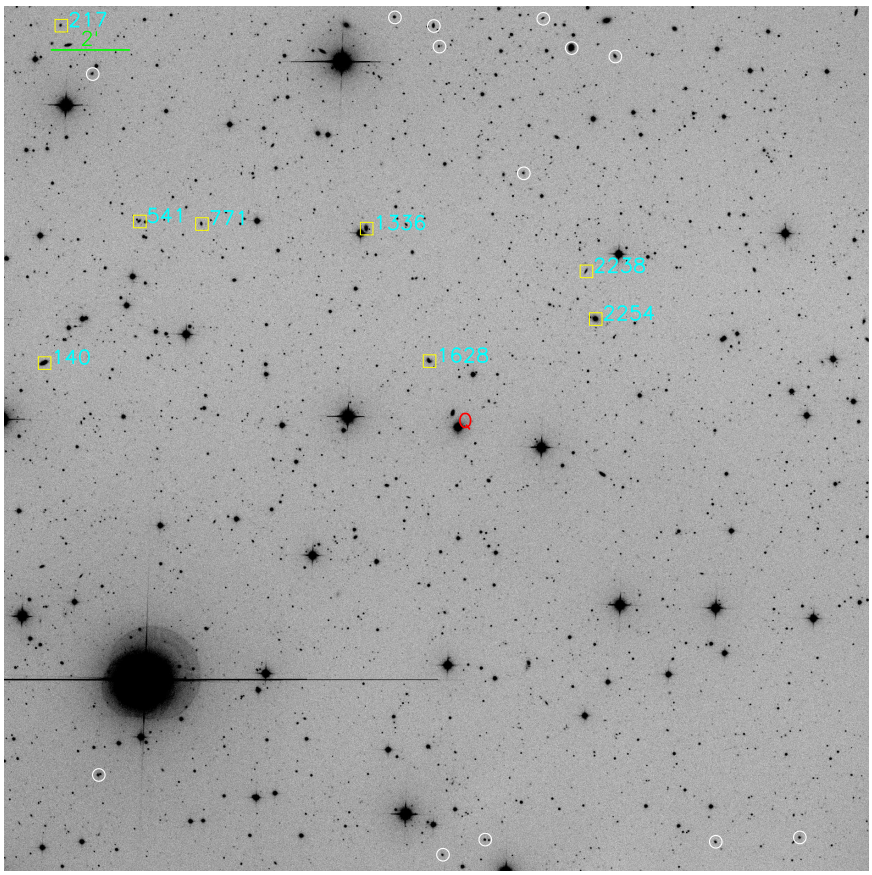

Fig. 14.— Same as for Figure 2 but for the field surrounding HE1029–140 ($z_{\rm em} = 0.086$).

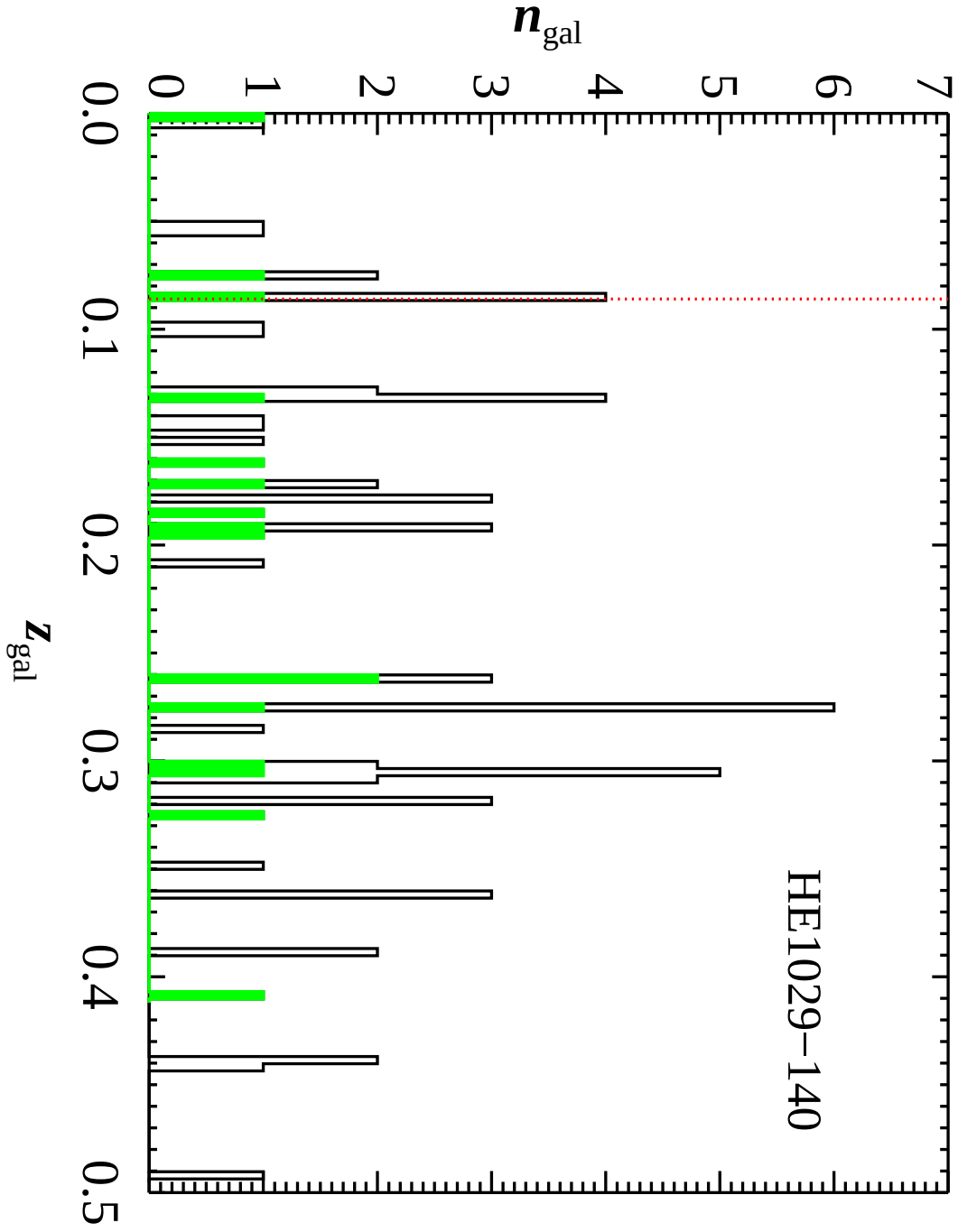

Fig. 15.— Same as for Figure 3 but for the field surrounding HE1029–140 ($z_{em} = 0.086$).

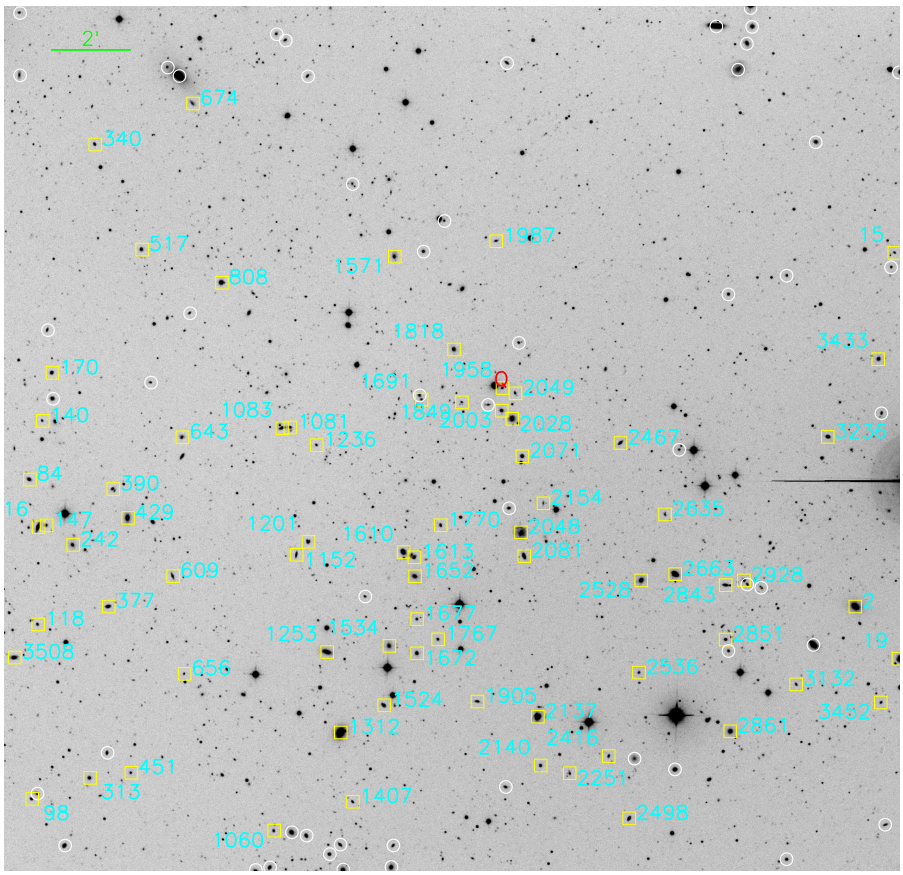

Fig. 16.— Same as for Figure 2 but for the field surrounding PG1116+215 ($z_{\rm em} = 0.177$).

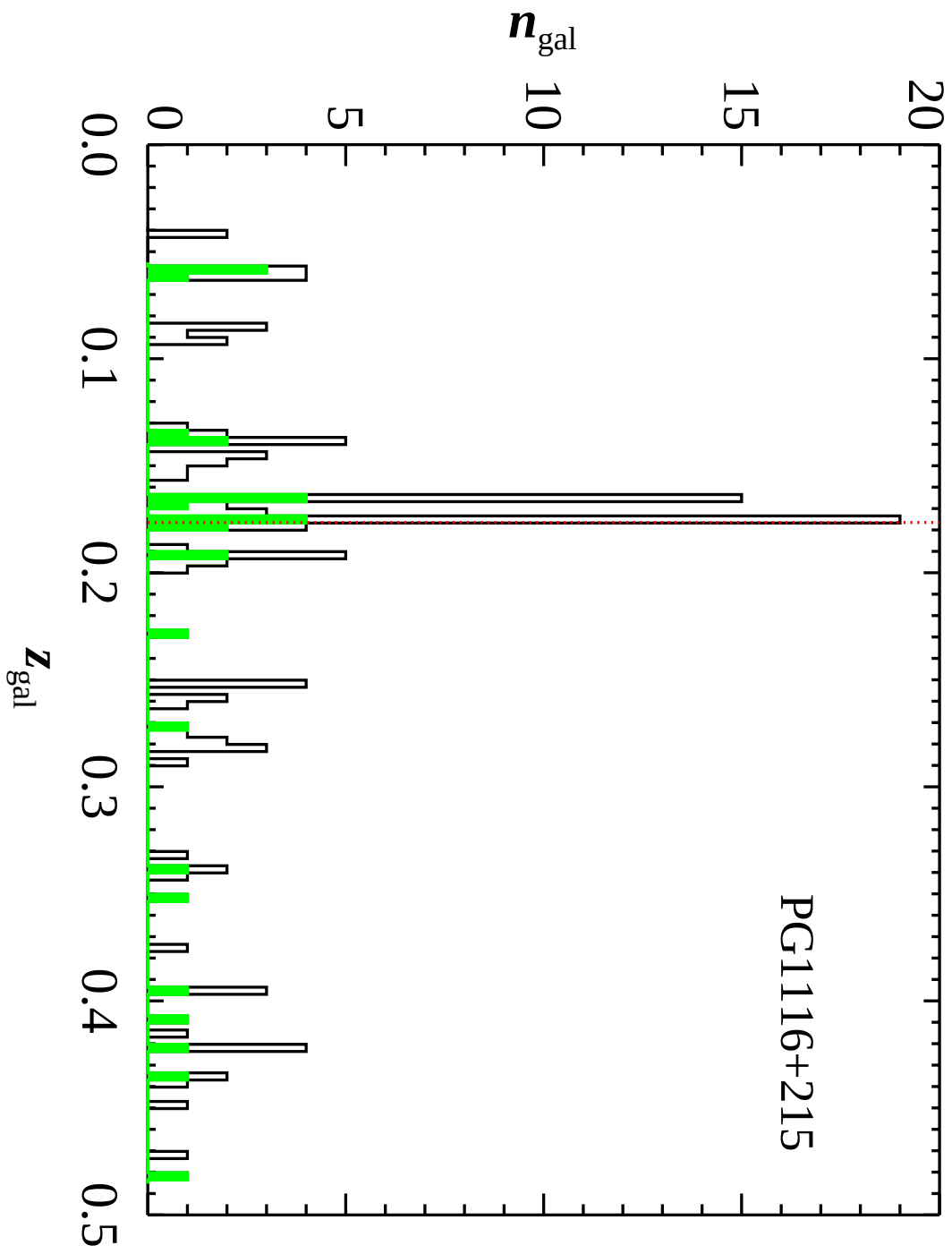

Fig. 17.— Same as for Figure 3 but for the field surrounding PG1116+215 ($z_{\rm em} = 0.177$).

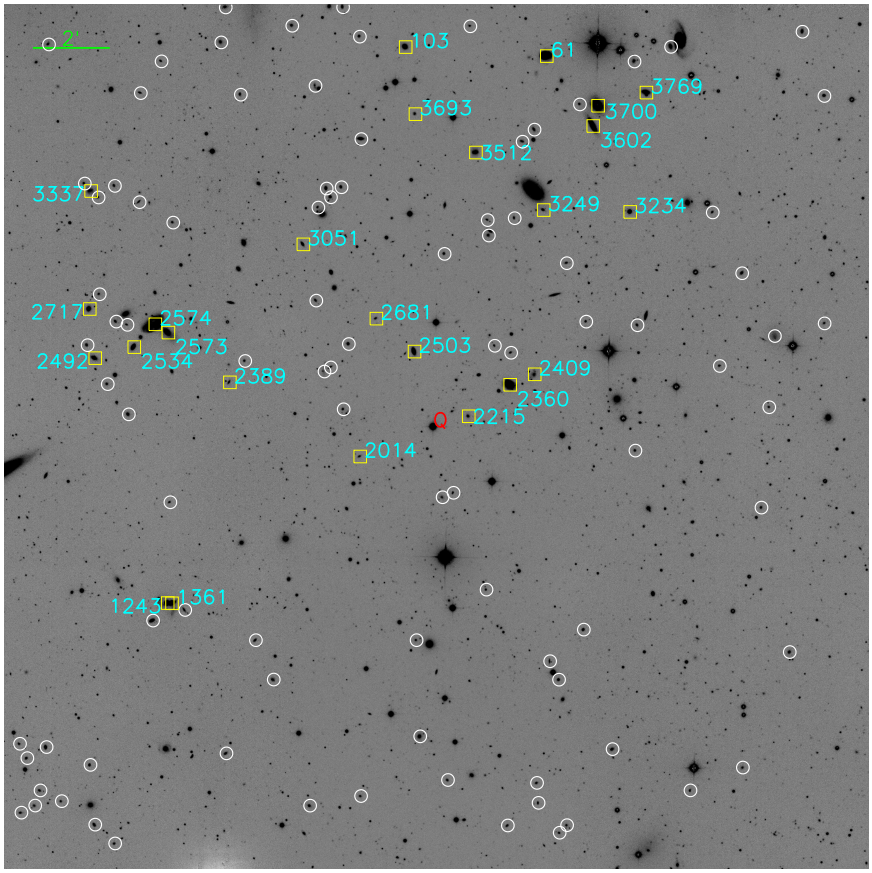

Fig. 18.— Same as for Figure 2 but for the field surrounding PG1211+143 ($z_{\rm em} = 0.809$).

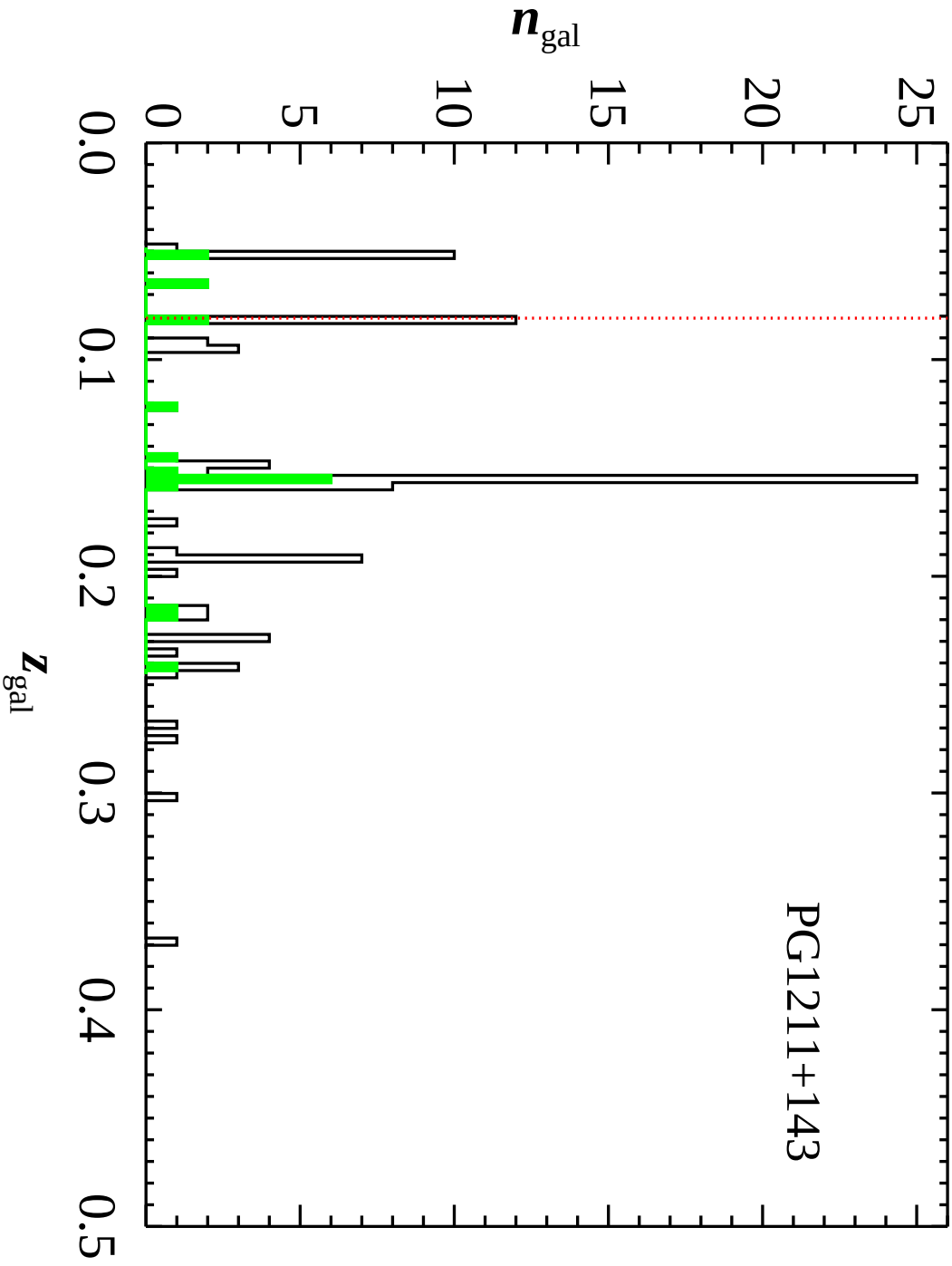

Fig. 19.— Same as for Figure 3 but for the field surrounding PG1211+143 ($z_{em} = 0.809$).

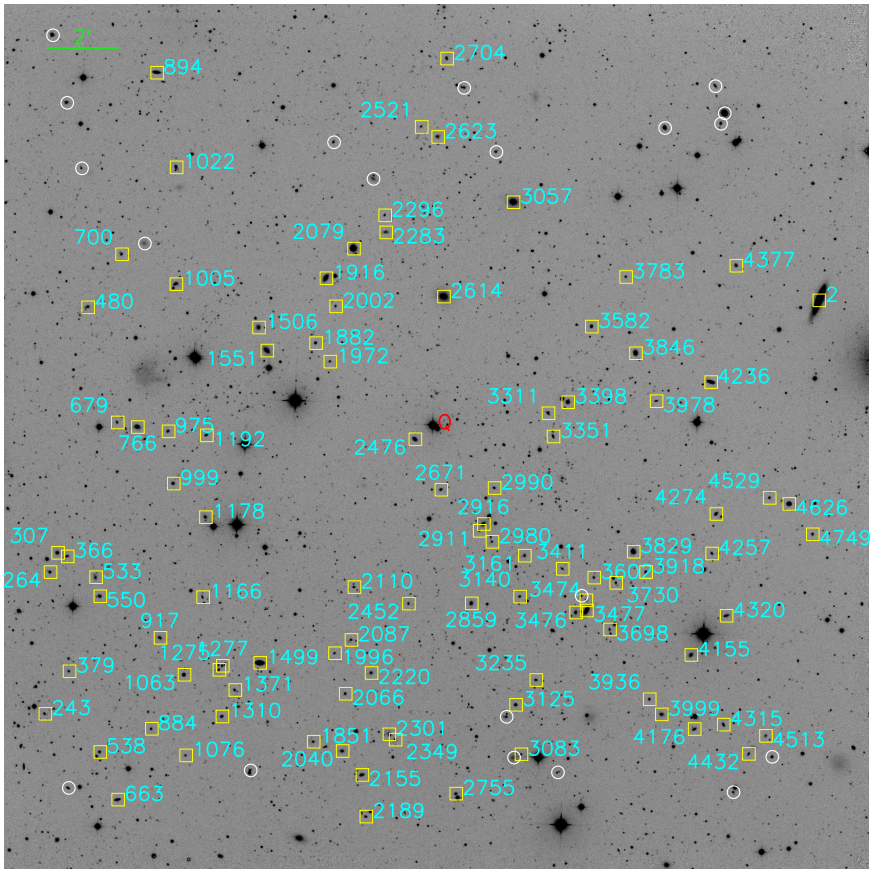

Fig. 20.— Same as for Figure 2 but for the field surrounding PG1216+069 ($z_{\rm em} = 0.331$).

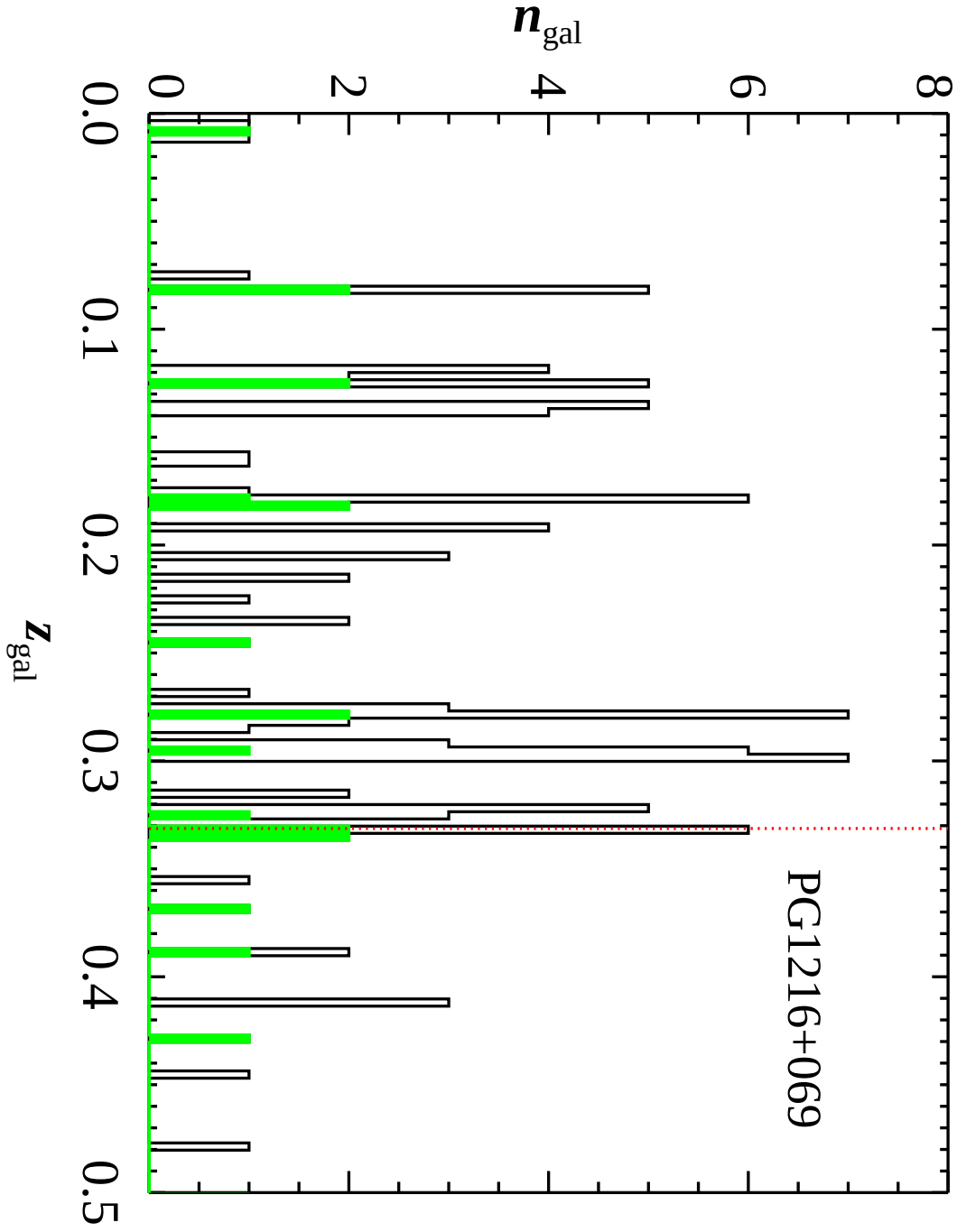

Fig. 21.— Same as for Figure 3 but for the field surrounding PG1216+069 ($z_{em} = 0.331$).

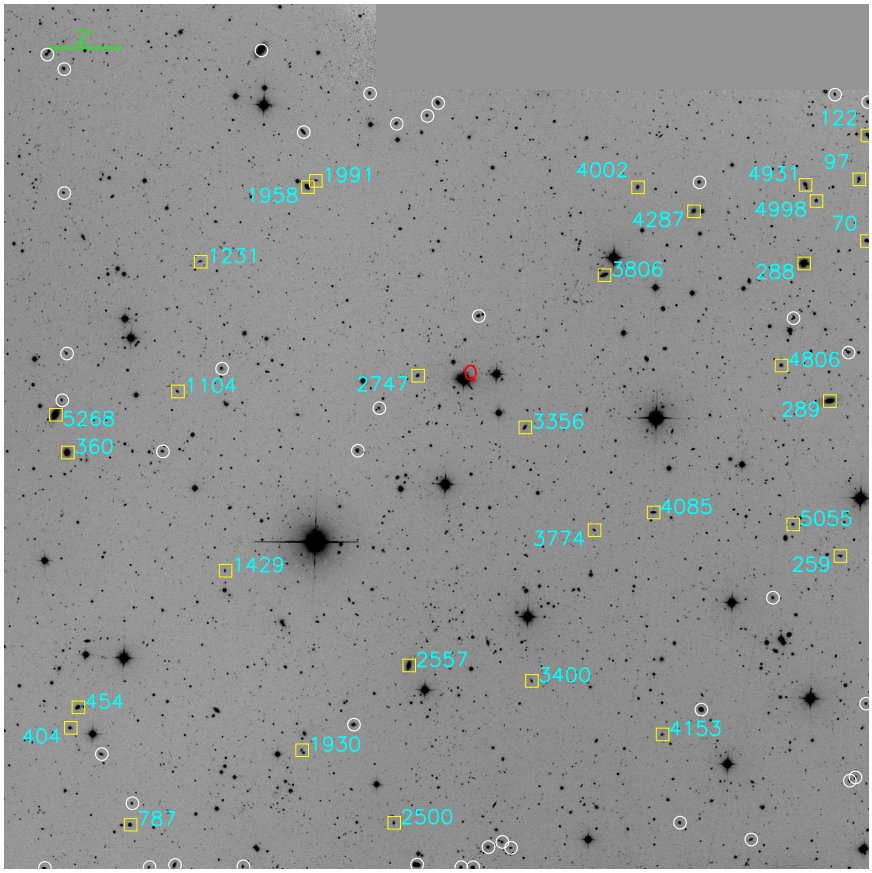

Fig. 22.— Same as for Figure 2 but for the field surrounding 3C273 ($z_{\rm em} = 0.158$).

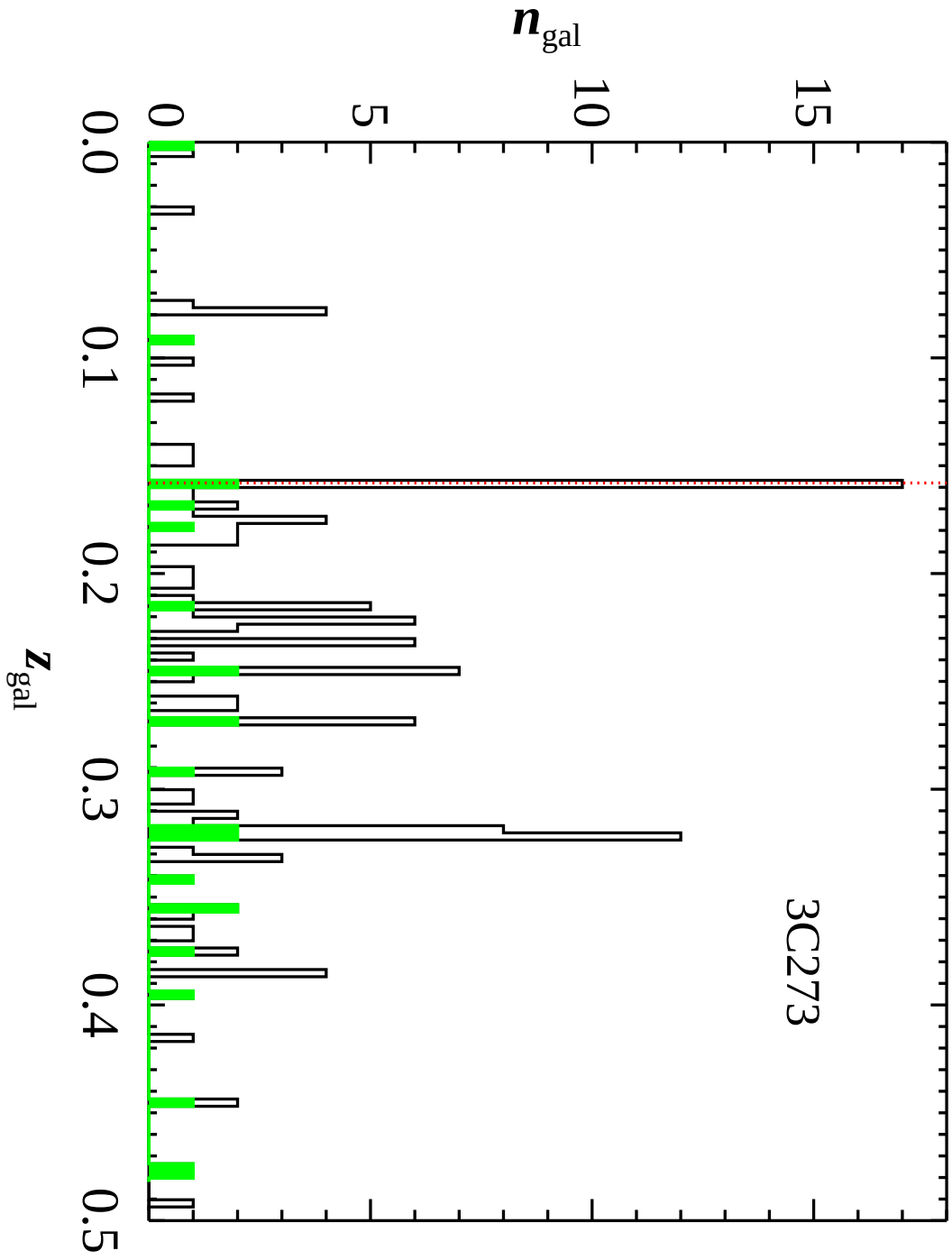

Fig. 23.— Same as for Figure 3 but for the field surrounding 3C273 ($z_{em} = 0.158$).

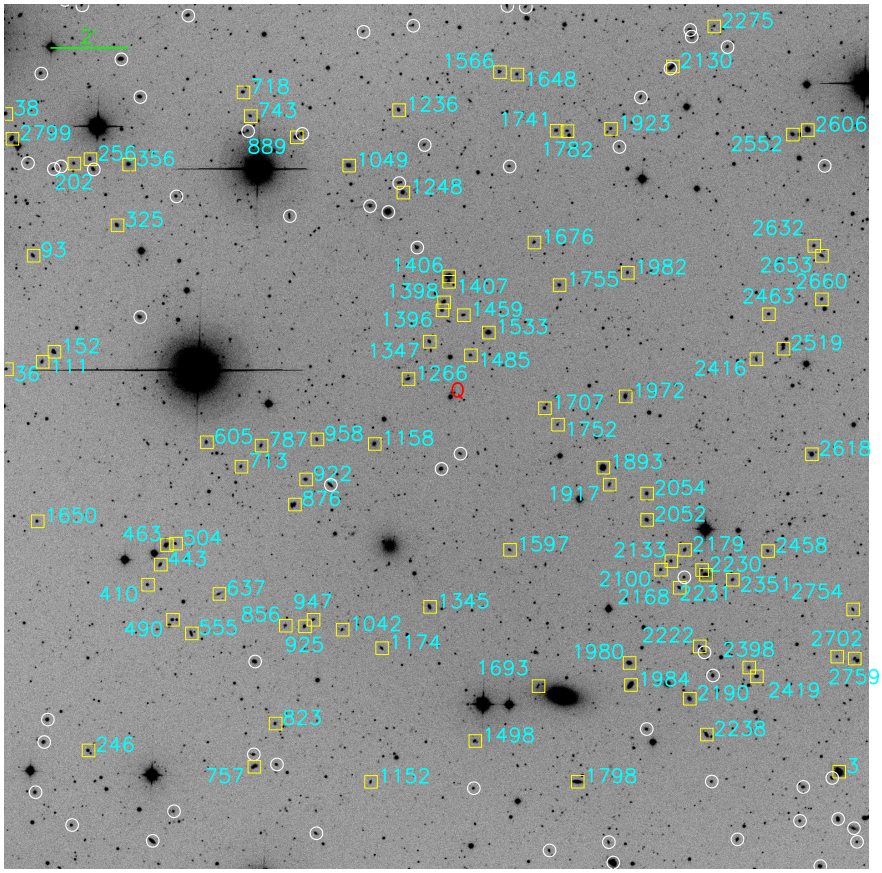

Fig. 24.— Same as for Figure 2 but for the field surrounding Q1230+095 ($z_{\rm em} = 0.415$).

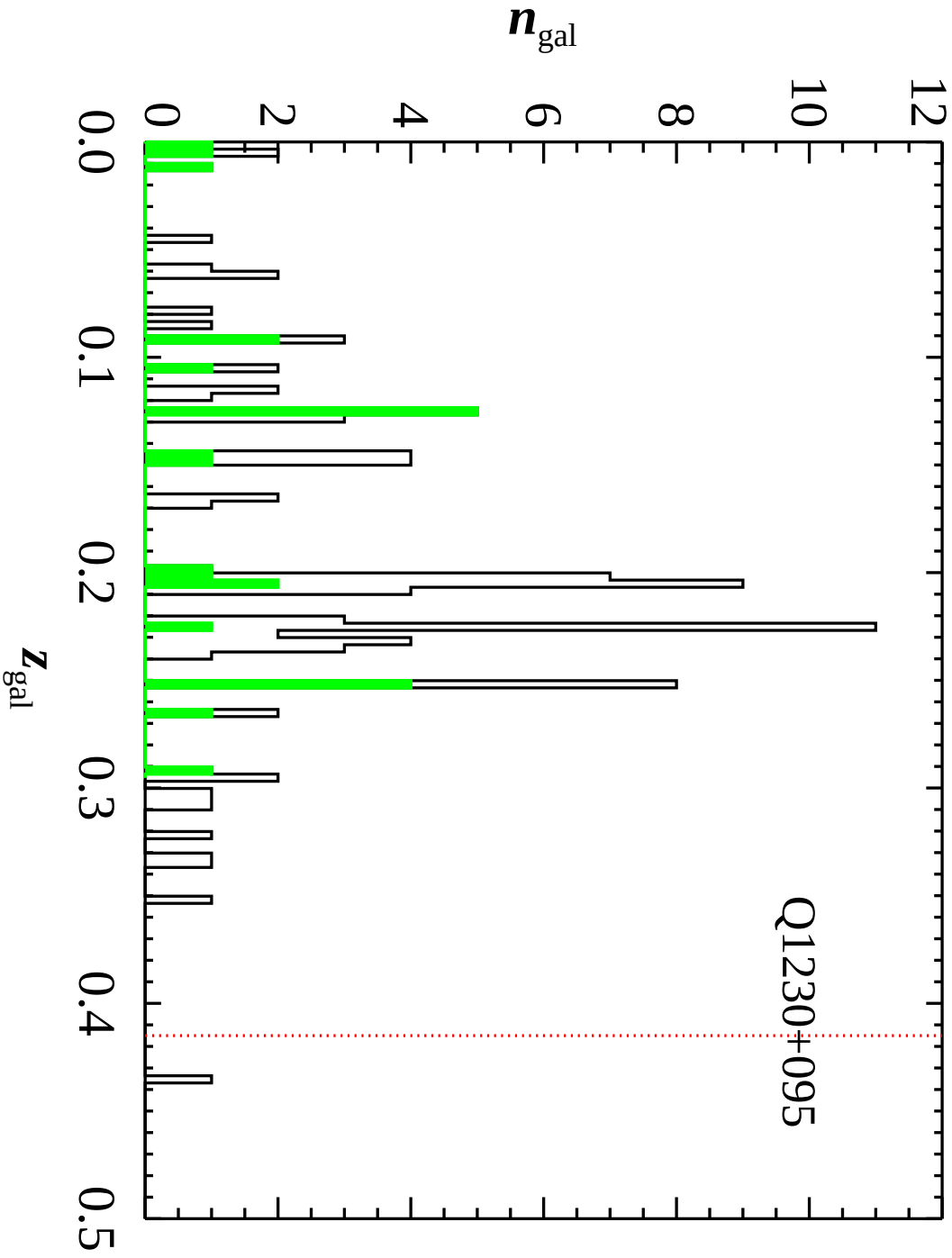

Fig. 25.— Same as for Figure 3 but for the field surrounding Q1230+095 ($z_{em} = 0.415$).

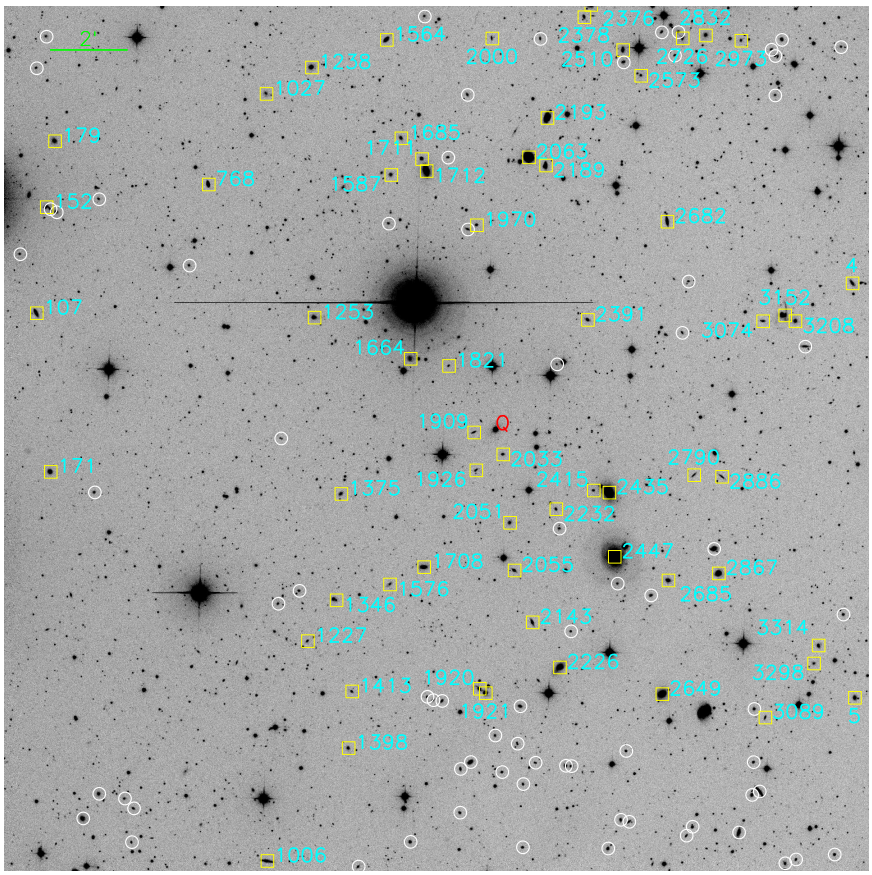

Fig. 26.— Same as for Figure 2 but for the field surrounding PKS1302–102 ($z_{\rm em} = 0.286$).

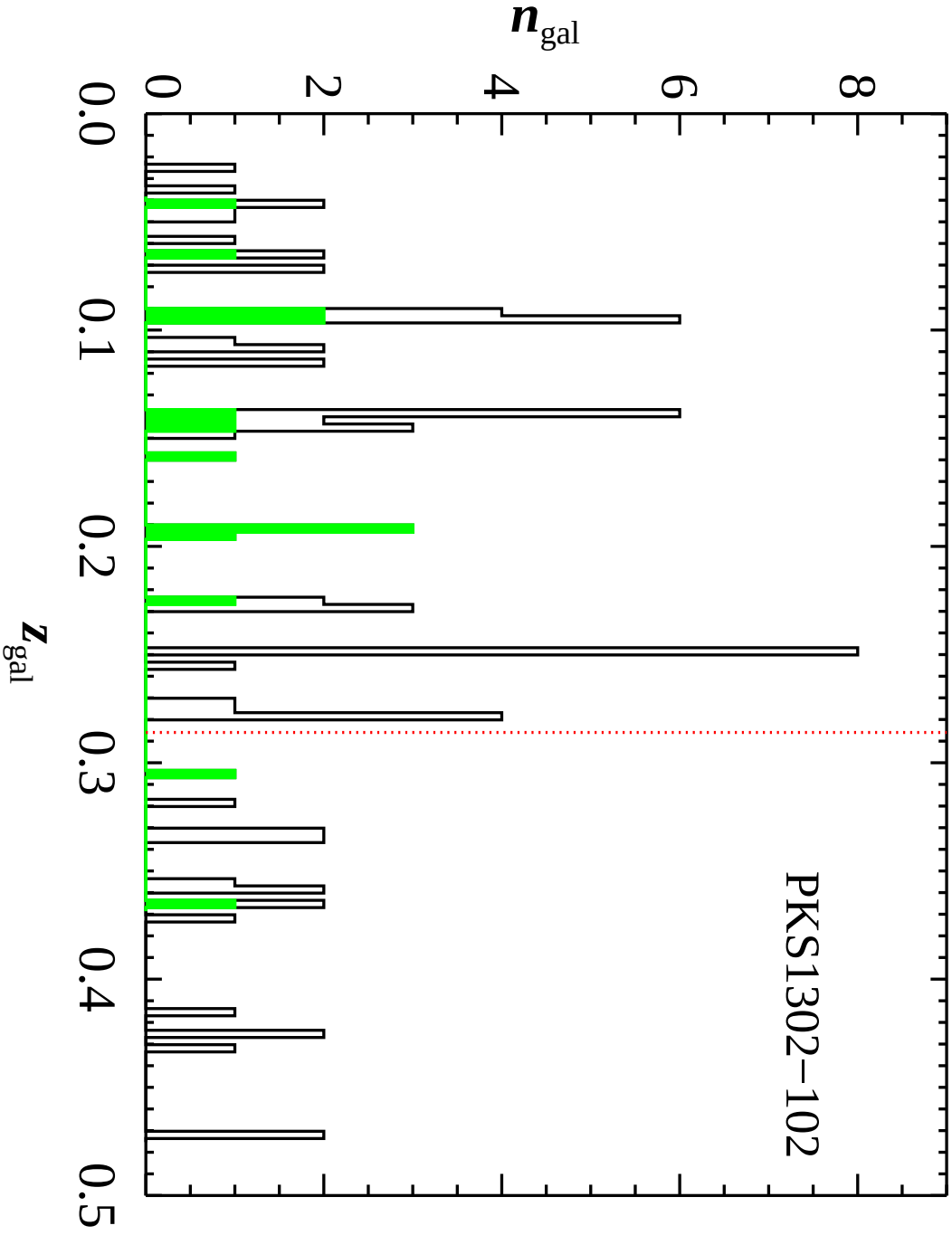

Fig. 27.— Same as for Figure 3 but for the field surrounding PKS1302–102 ($z_{\rm em} = 0.286$).

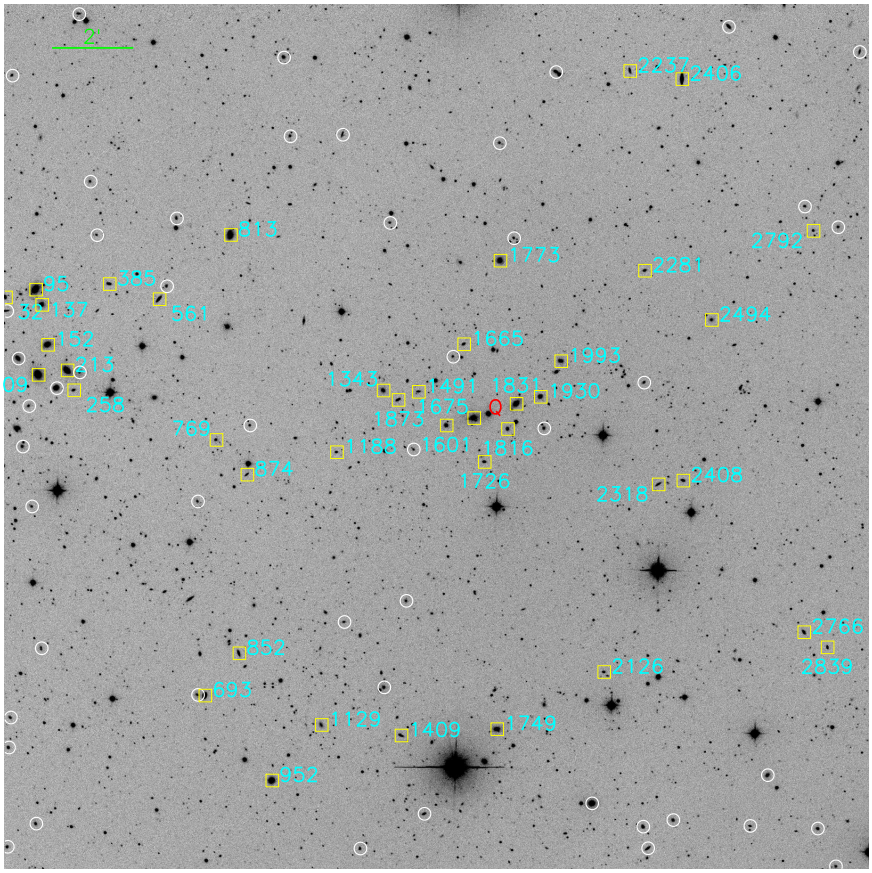

Fig. 28.— Same as for Figure 2 but for the field surrounding PG1307+085 ($z_{\rm em} = 0.155$).

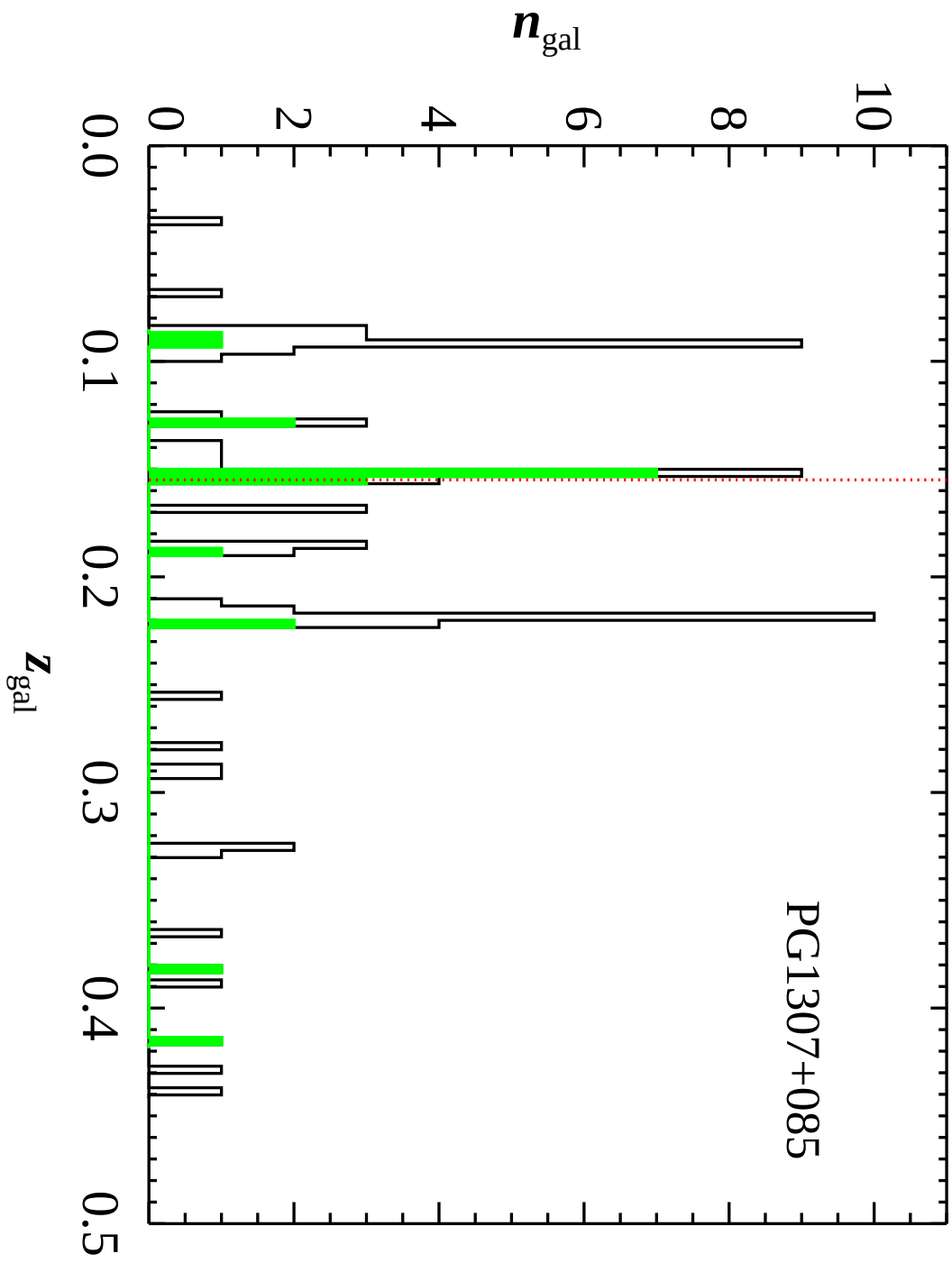

Fig. 29.— Same as for Figure 3 but for the field surrounding PG1307+085 ($z_{em} = 0.155$).

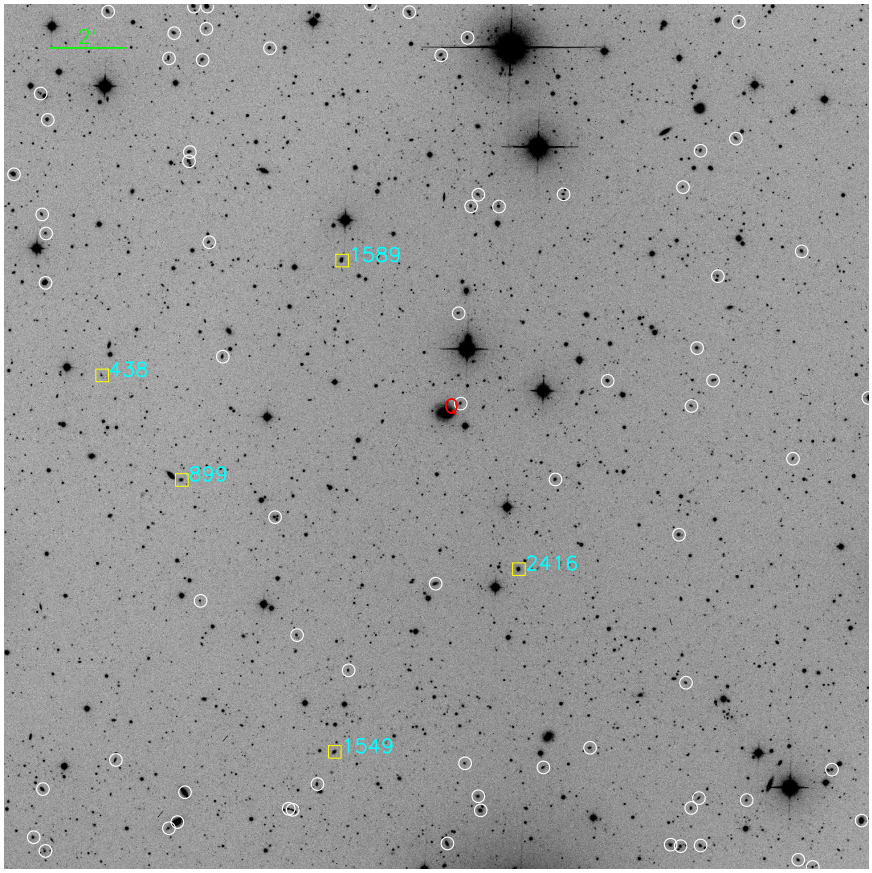

Fig. 30.— Same as for Figure 2 but for the field surrounding MRK1383 ($z_{\rm em} = 0.086$).

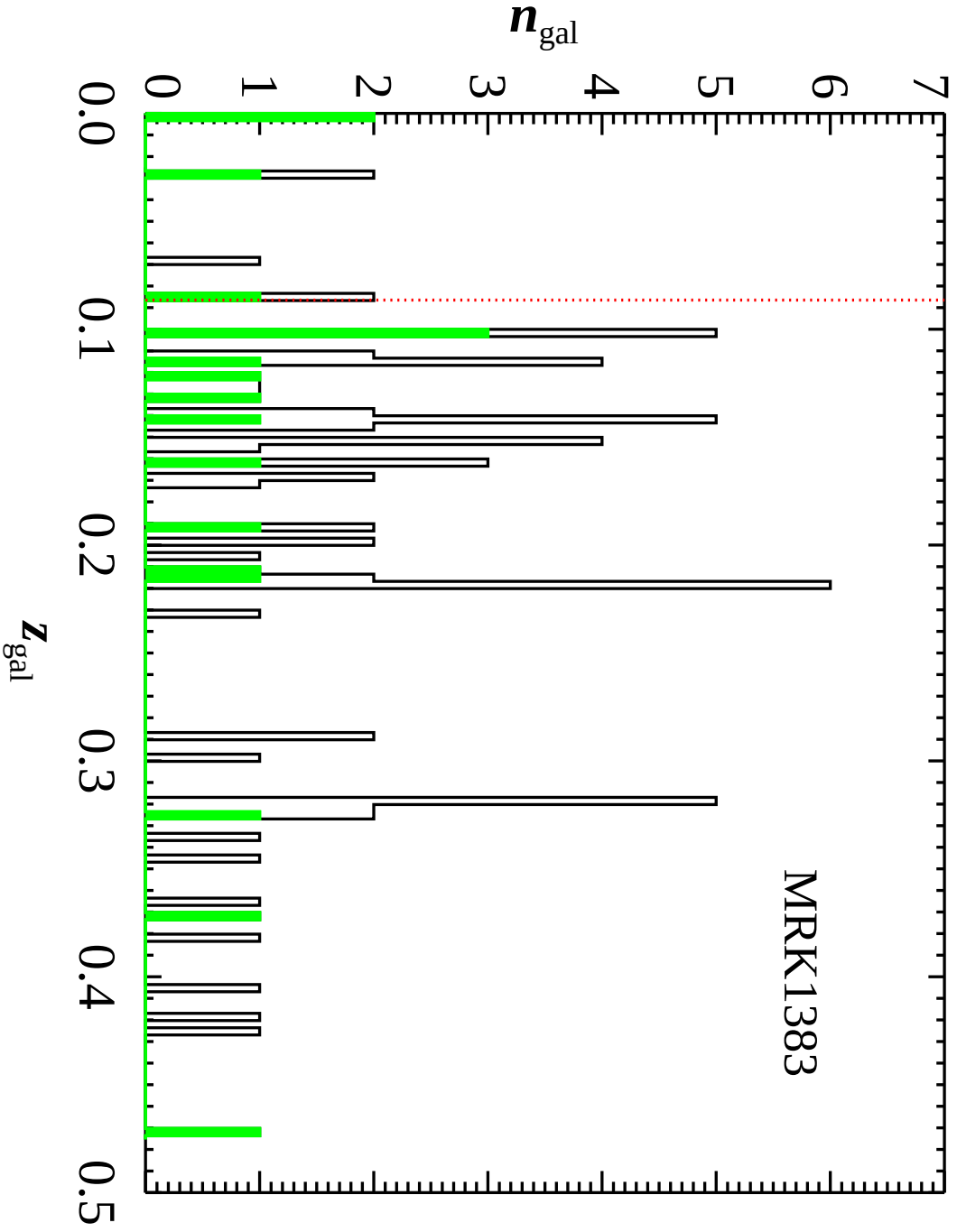

Fig. 31.— Same as for Figure 3 but for the field surrounding MRK1383 ($z_{em} = 0.086$).

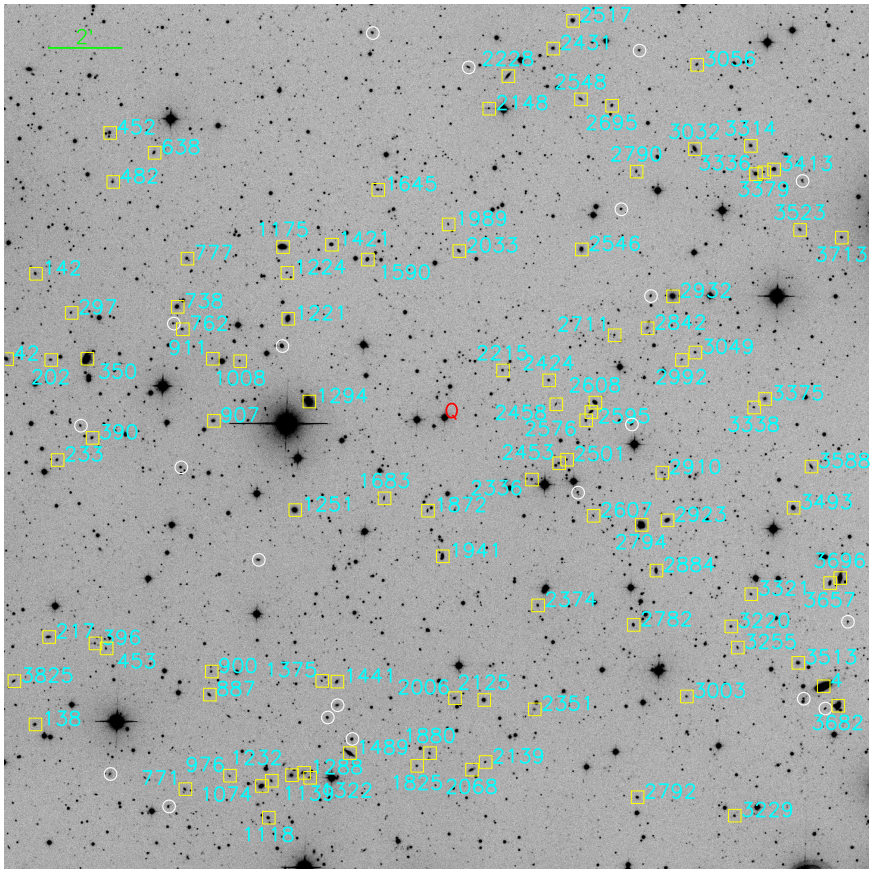

Fig. 32.— Same as for Figure 2 but for the field surrounding Q1553+113 ($z_{\rm em} = 0.360$).

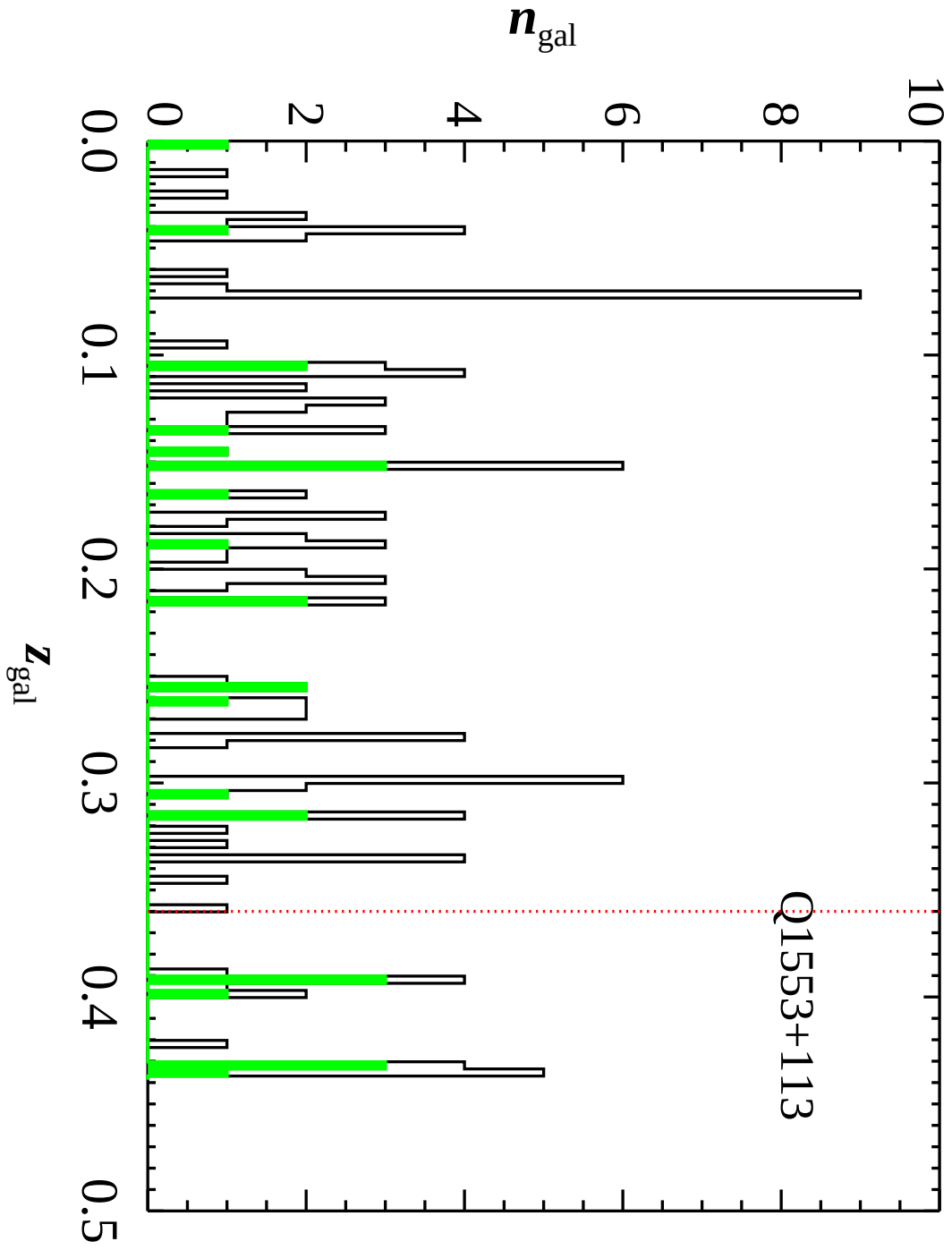

Fig. 33.— Same as for Figure 3 but for the field surrounding Q1553+113 ($z_{em} = 0.360$).

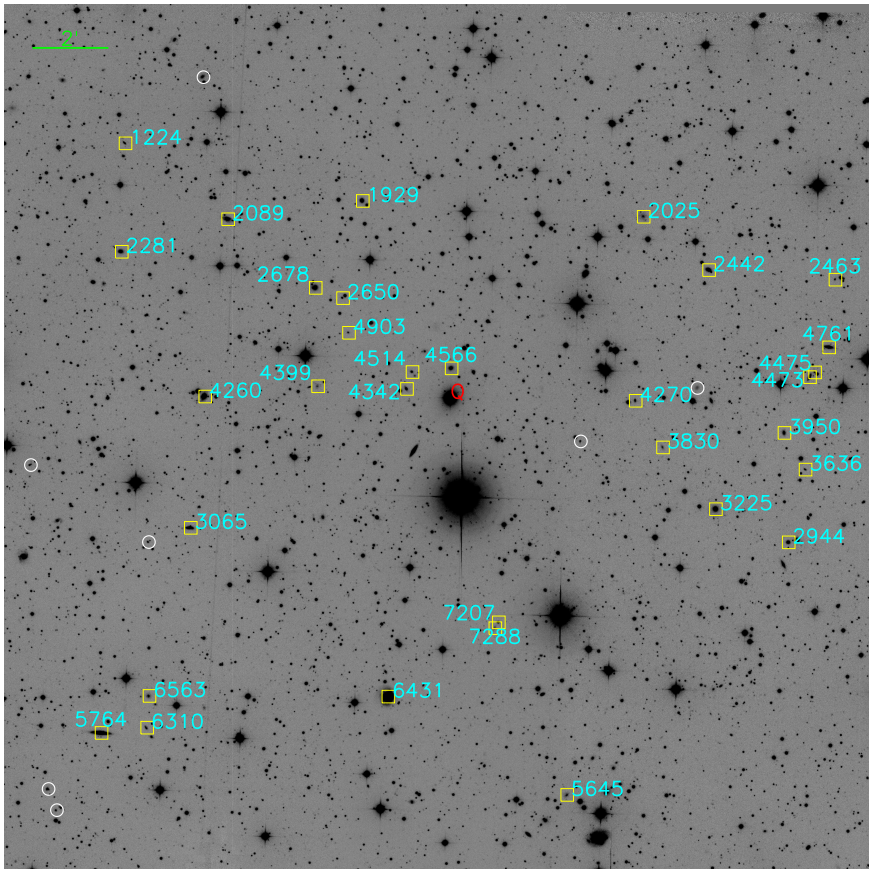

Fig. 34.— Same as for Figure 2 but for the field surrounding PKS2005–489 ($z_{\rm em} = 0.071$).

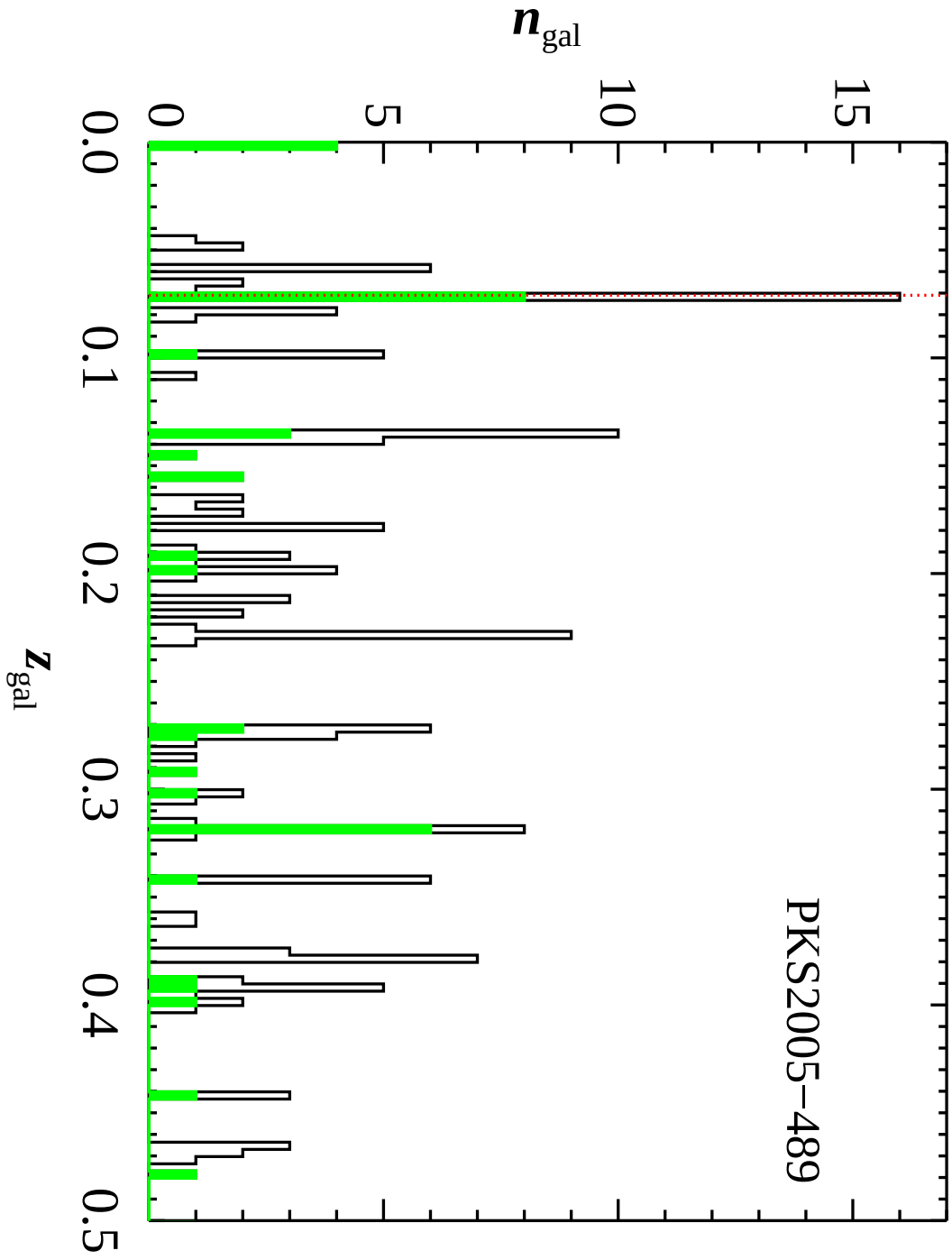

Fig. 35.— Same as for Figure 3 but for the field surrounding PKS2005–489 ($z_{em} = 0.071$).

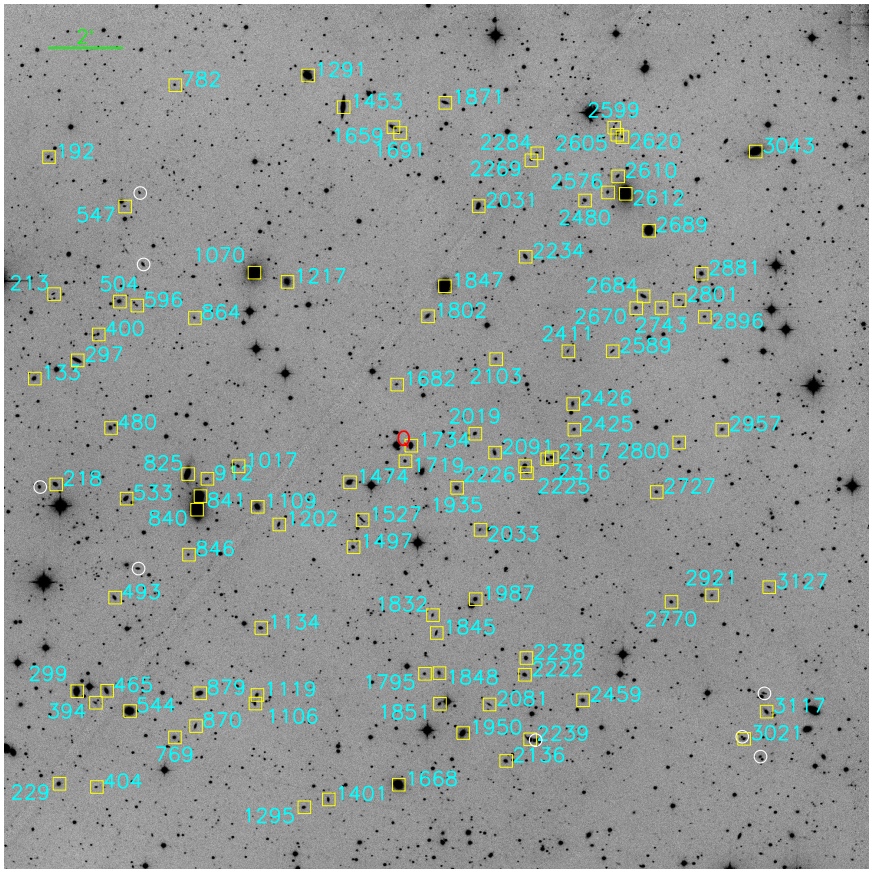

Fig. 36.— Same as for Figure 2 but for the field surrounding FJ2155–092 ($z_{\rm em} = 0.170$).

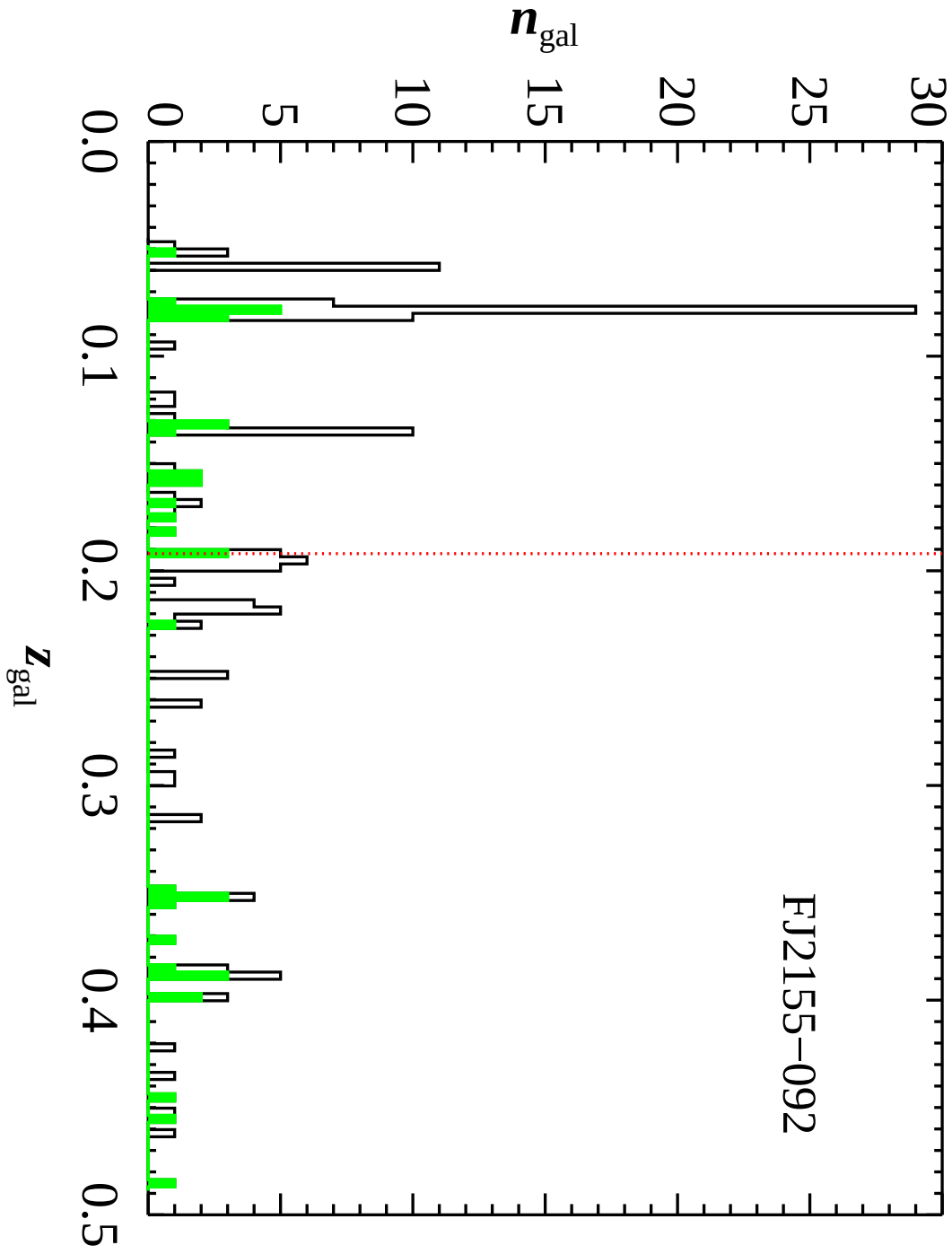

Fig. 37.— Same as for Figure 3 but for the field surrounding FJ2155–092 ($z_{em} = 0.170$).

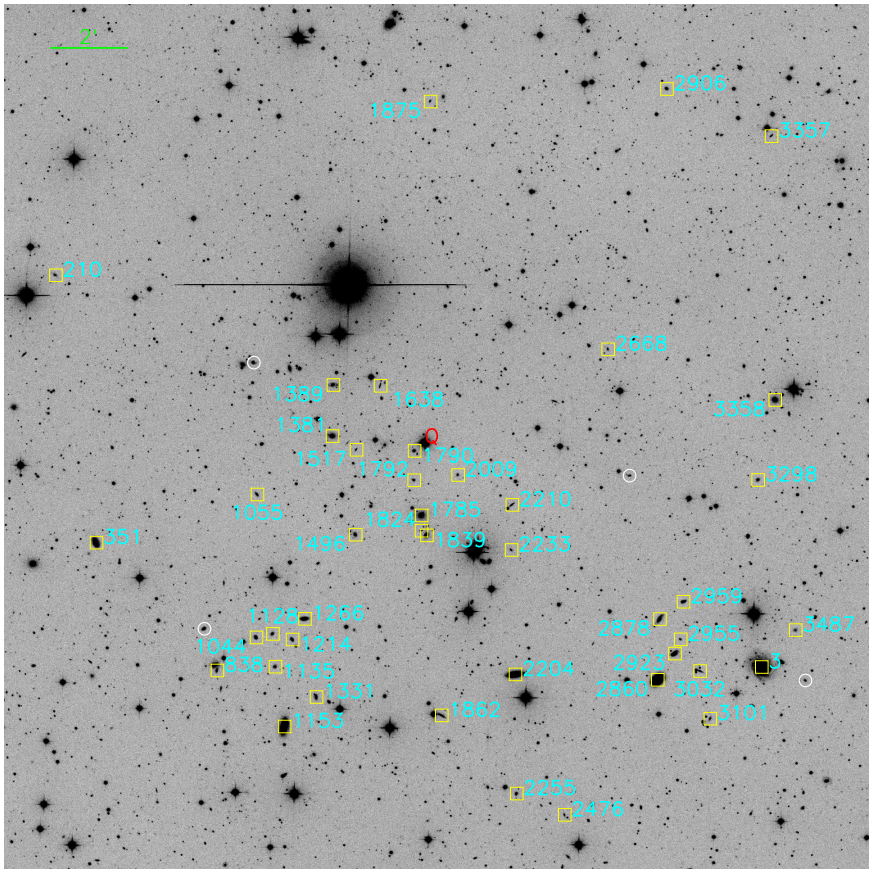

Fig. 38.— Same as for Figure 2 but for the field surrounding PKS2155–304 ($z_{\rm em} = 0.116$).

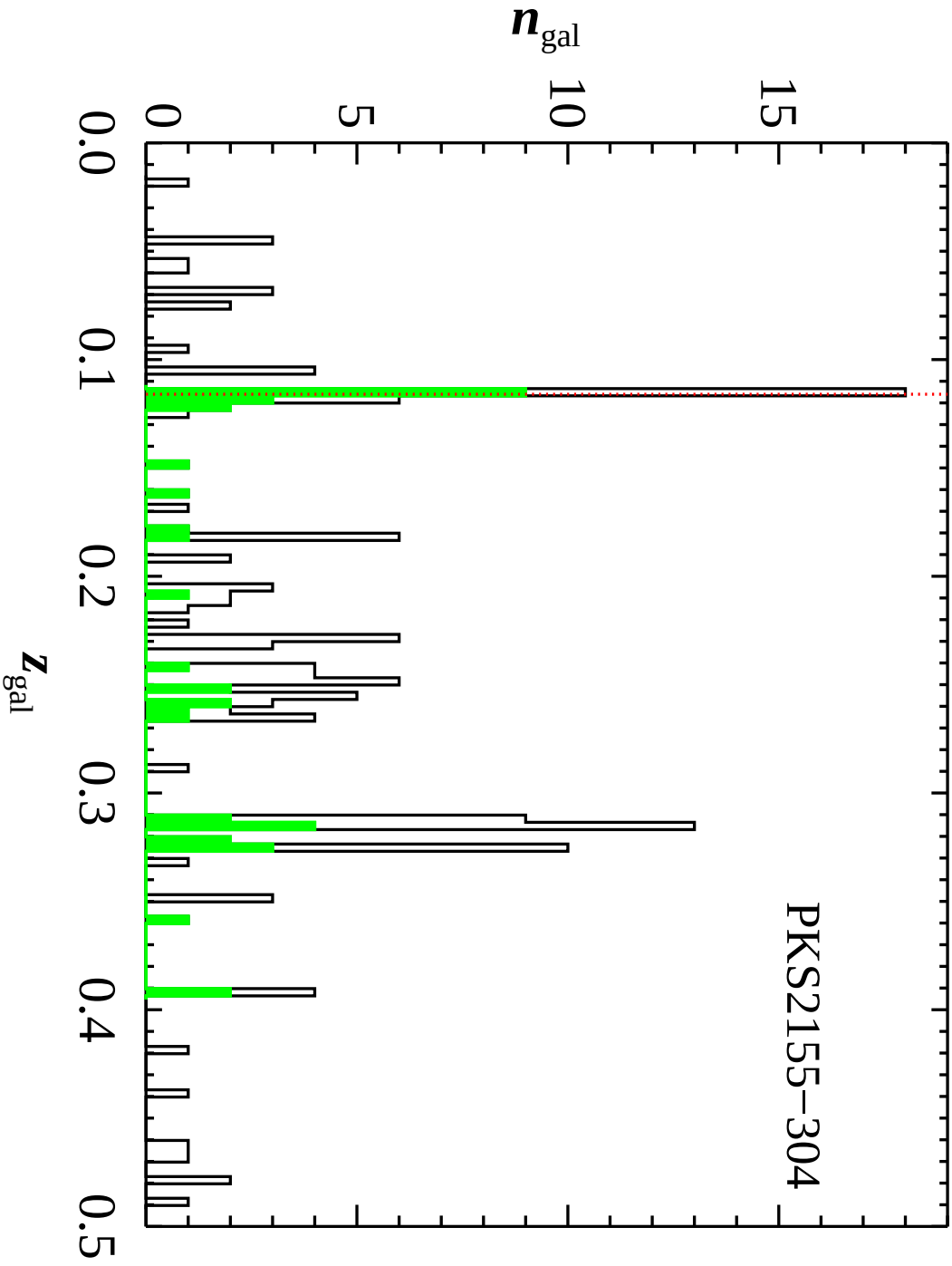

Fig. 39.— Same as for Figure 3 but for the field surrounding PKS2155–304 ($z_{em} = 0.116$).

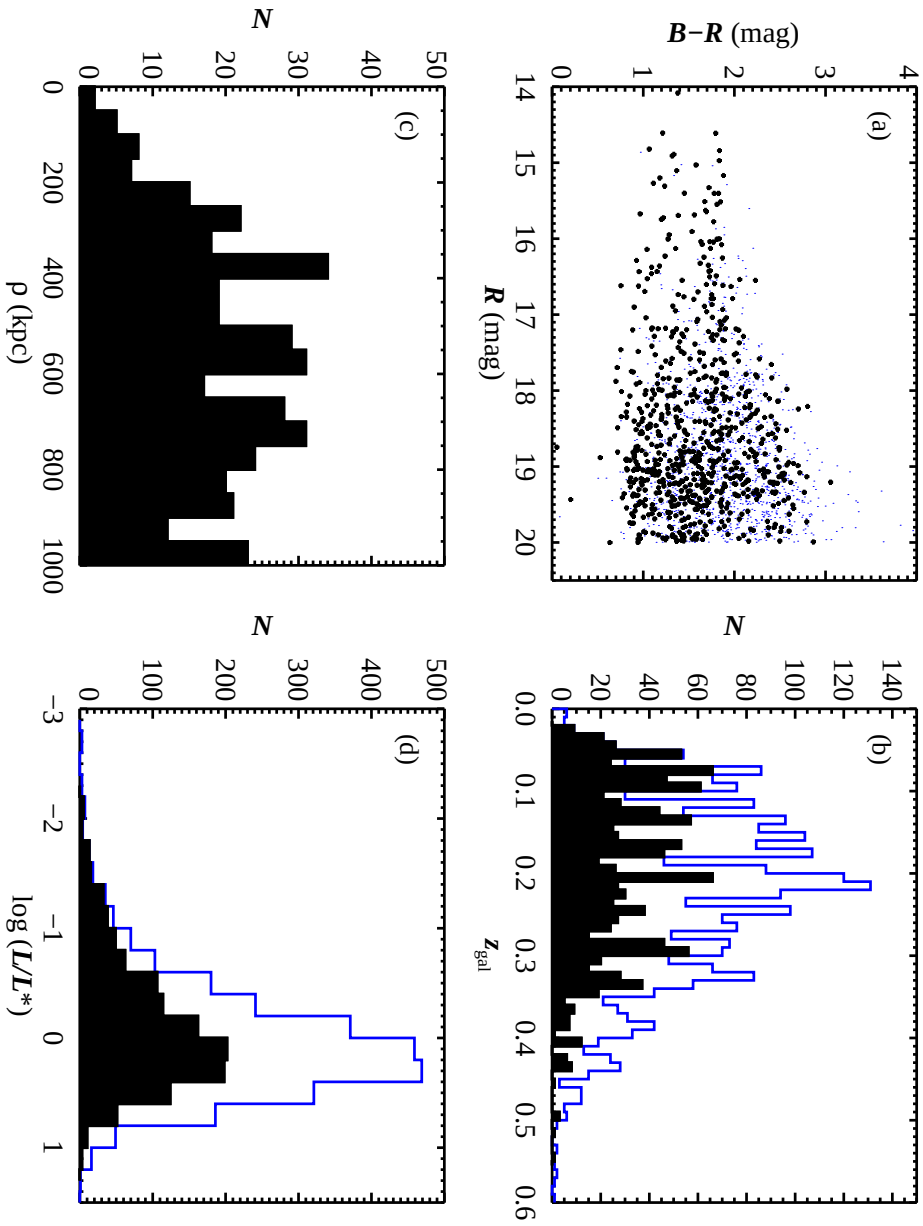

Fig. 40.— (a) Color-magnitude diagram of all galaxies with redshifts $z > 0.005$ (blue dots) in LCO/WFCCD survey and galaxies with $0.02 < z < (z_{\rm em} - 0.01)$ (black symbols). (b) Histogram of the galaxy redshifts for sources detected in our survey. The open (blue) histogram shows all sources with $z > 0.005$, while the solid black histogram is restricted to $0.02 < z < (z_{\rm em} - 0.01)$ and therefore represents the sample that may be used to study associations with the low z IGM. (c) Distribution of impact parameters ρ for the galaxies in our survey with $0.02 < z < (z_{\rm em} - 0.01)$. The incidence of objects does not increase as $N \propto \rho$ for $\rho \gtrsim 400\,$kpc because of the (nearly) fixed angular extent of the survey. (d) Luminosity distribution for the galaxies in our LCO/WFCCD survey restricted to the sample of sources with $z > 0.005$ (blue, open histogram) and $0.02 < z < (z_{\rm em} - 0.01)$ (black, solid histogram).

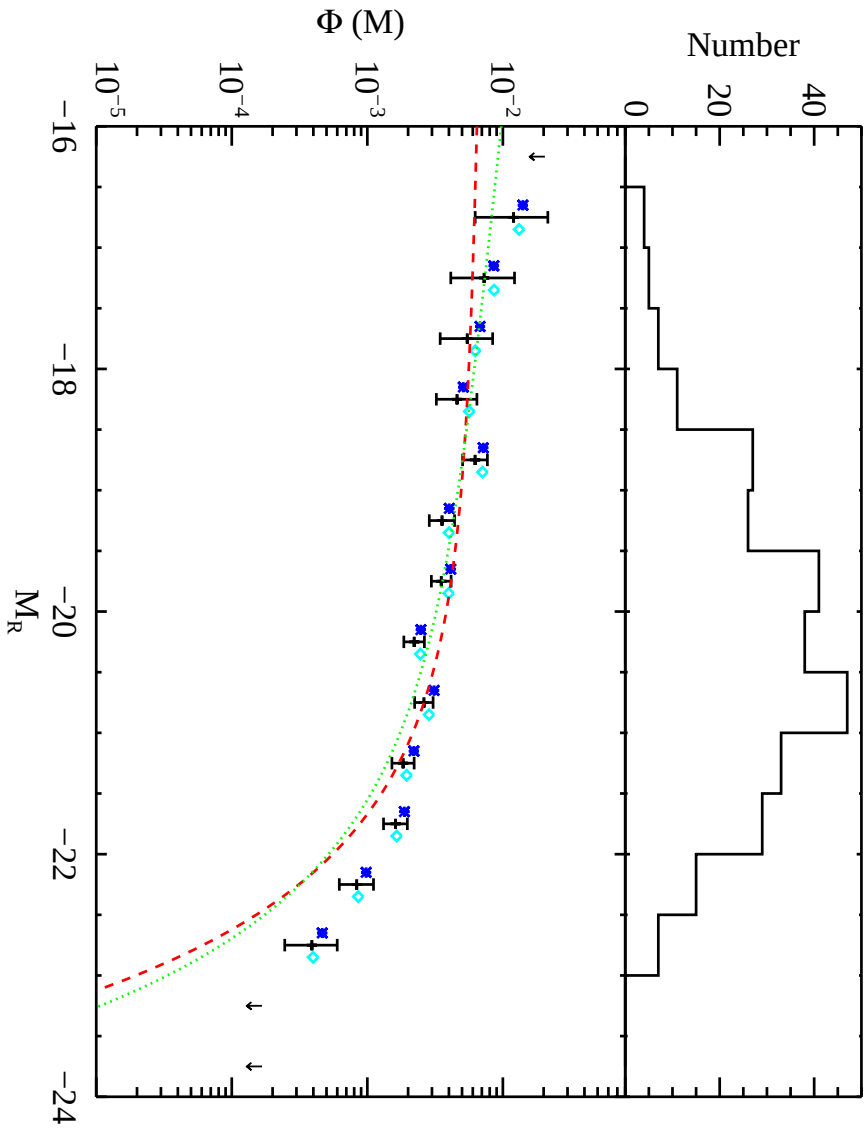

Fig. 41.— Luminosity function estimated from the 17 fields of the LCO/WFCCD survey that have greater than 70% completeness to 10′ from the quasar to $R \leq 19.5$ mag. Black points with error bars show the results without a correction for incompleteness and assume Poisson uncertainties based on the number of galaxies detected (upper panel). The blue stars and cyan diamonds show the estimated $\Phi(M)$ values after adopting magnitude-independent and dependent completeness corrections respectively (see the text for a full description). The dashed (red) and dotted (green) curves show the luminosity functions derived from the SDSS by Blanton et al. (2003) and Montero-Dorta & Prada (2009) respectively, corrected to our assumed cosmology ($h = 0.72$). The offset at high luminosity may be the result of an Eddington bias in our estimation of $\Phi(M)$ and/or a modest offset between our R-band photometry and the SDSS r-band measurements.

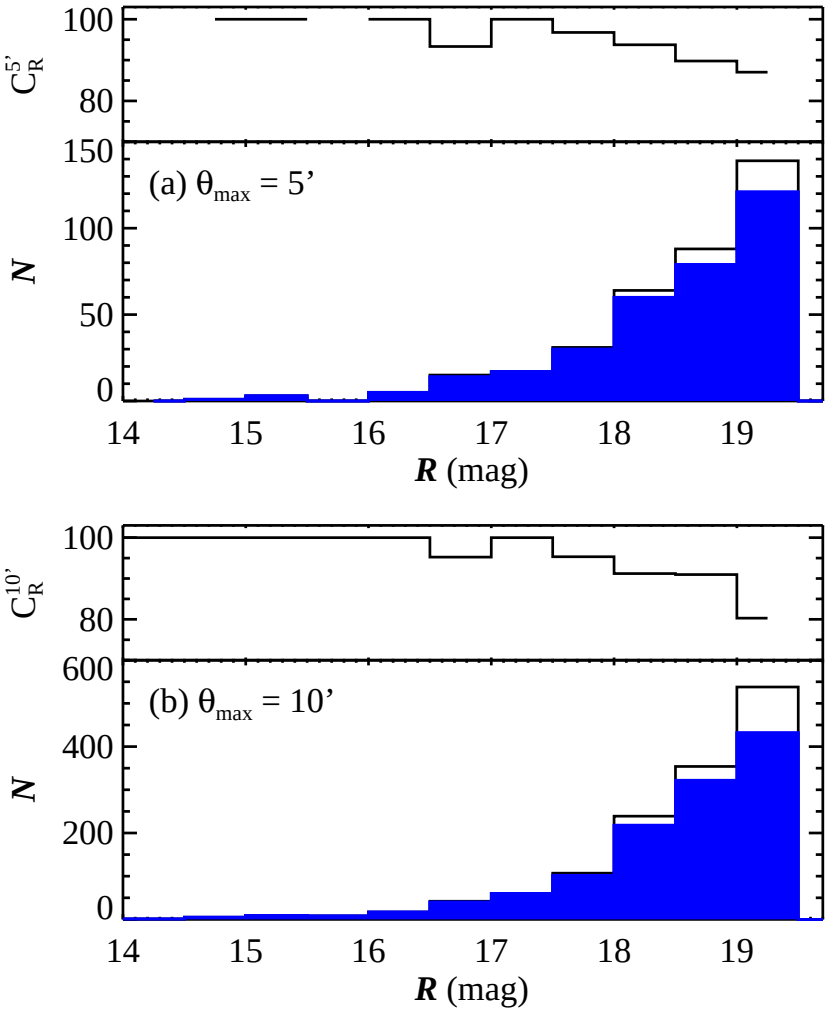

Fig. 42.— The lower plots of each panel show histograms of the targeted (open, black) and observed (solid, blue) galaxies in the 17 fields used to estimate the luminosity function (Figure 41). These histograms are shown for (a) $\theta_{\rm max} = 5'$ and (b) $\theta_{\rm max} = 10'$. In the upper plot of each panel, we show the completeness percentile C_R as a function of apparent magnitude. These values are used in the magnitude-dependent completeness correction of the luminosity function.